OPTIMIZATION OF A NEW LINEAR FM DETECTOR
USING DIGITAL SIGNAL PROCESSING TECHNIQUES

EDWARD J. A. KRATT III

THESIS FOR DOCTOR OF ENGINEERING SCIENCE DEGREE
ELECTRICAL ENGINEERING DEPARTMENT
NEW JERSEY INSTITUTE OF TECHNOLOGY
MAY 26, 1983
JACOB KLAPPER, Advisor

ABSTRACT

This dissertation describes and synthesizes a new member of the family of FM detectors introduced earlier by Klapper and Kratt. A salient property of these detectors is low delay with excellent sensitivity. The emphasis in the new detector is on the ease of digital implementation. In addition, the new detector is also extremely linear. In congruence with the other Klapper-Kratt detectors, it makes use of zero group delay elements, balance at RF, quasi-synchronous detection and carrier cancellation. The performance of the detector is mathematically analyzed under the conditions of a modulated input wave, sinewave interference, and noise. The results indicate improved performance over other members of the family in terms of linearity, threshold, and ease of digital implementation. Realization of the detector using FIR digital signal processing methods is discussed, including linearity optimization. Substantial algorithm simplification was achieved. High center frequencies with low sampling frequencies are obtainable due to the frequency foldover effect. Narrowband predetection filtering can be included in the detector provided a wider predetection filter is present. Results of a working model are shown.

OPTIMIZATION OF A NEW LINEAR FM DETECTOR

USING DIGITAL SIGNAL PROCESSING TECHNIQUES

BY

EDWARD J. A. KRATT III

A DISSERTATION

PRESENTED IN PARTIAL FULFILLMENT OF

THE REQUIREMENTS FOR THE DEGREE

OF

DOCTOR OF ENGINEERING SCIENCE IN ELECTRICAL ENGINEERING

AT

NEW JERSEY INSTITUTE OF TECHNOLOGY

Newark, New Jersey

1982

(degree granted May 1983)

VITA

Name: Edward John Andrew Kratt III

Degree and date to be conferred: D.Engr.Sc., 1983

Secondary education: Butler High School, June 1960

Collegiate Institutions	Date	Degree	Date of Degree
Lehigh University	1960-1964	BSEE	June 8, 1964
NCE	1967-1973	MSEE	June 1, 1973
NJIT	1973-1983	D.Engr.Sc.	May 26, 1983

Major: Electrical Engineering

Position held: Chief Engr., RFL Industries, Boonton, N.J. 07005

APPROVAL OF DISSERTATION

OPTIMIZATION OF A NEW LINEAR FM DETECTOR

USING DIGITAL SIGNAL PROCESSING TECHNIQUES

BY

EDWARD J. A. KRATT III

FOR

DEPARTMENT OF ELECTRICAL ENGINEERING

NEW JERSEY INSTITUTE OF TECHNOLOGY

BY

FACULTY COMMITTEE

APPROVED: ______________________________ CHAIRMAN

____

____

____

NEWARK, NEW JERSEY

OCTOBER 1982

(May 1983)

ACKNOWLEDGEMENTS

The author gratefully acknowledges the guidance and assistance of the chairman of his doctoral committee, Dr. Jacob Klapper. He also expresses his appreciation to the other members of his committee, Dr. Joseph Frank, Dr. Solomon Rosenstark, and Dr. Michael Baltrush, for their assistance.

The author also acknowledges the encouragement and understandings of his family, and the support of colleages, who have all helped make this work possible.

TABLE OF CONTENTS

TABLE OF CONTENTS (contd)

LIST OF FIGURES

LIST OF FIGURES

LIST OF TABLES

CHAPTER I

INTRODUCTION

1.1 Background

The FM detector described in this paper is one of a family of FM detectors (Ref. 1) that originally resulted from the need to discriminate a frequency modulated signal with extremely low delay and excellent sensitivity.

Up to that time, all FM detectors used low-pass filters to remove the undesired carrier frequency components and their harmonics generated in the detection process, and usually a tuned circuit for the FM to AM conversion. These circuits would normally not be low delay circuits. Components such as integrators, differentiators, summers, and multipliers, on the other hand, are low delay (zero group delay) elements. However, even previous FM detectors using integrators and differentiators still incorporated low-pass filters in their output circuitry (Refs. 2, 3, and 4).

The solution to this problem utilized an integrator, differentiator and summer to perform the FM to AM conversion. A synchronous demodulator was used to detect the amplitude modulation. This circuitry has theoretically zero delay, and the only undesirable product produced is the second harmonic of the carrier frequency, which was eliminated by adding an additional integrator and multiplier to generate a cancelling signal. The resulting detector is shown in Figure 1-1.

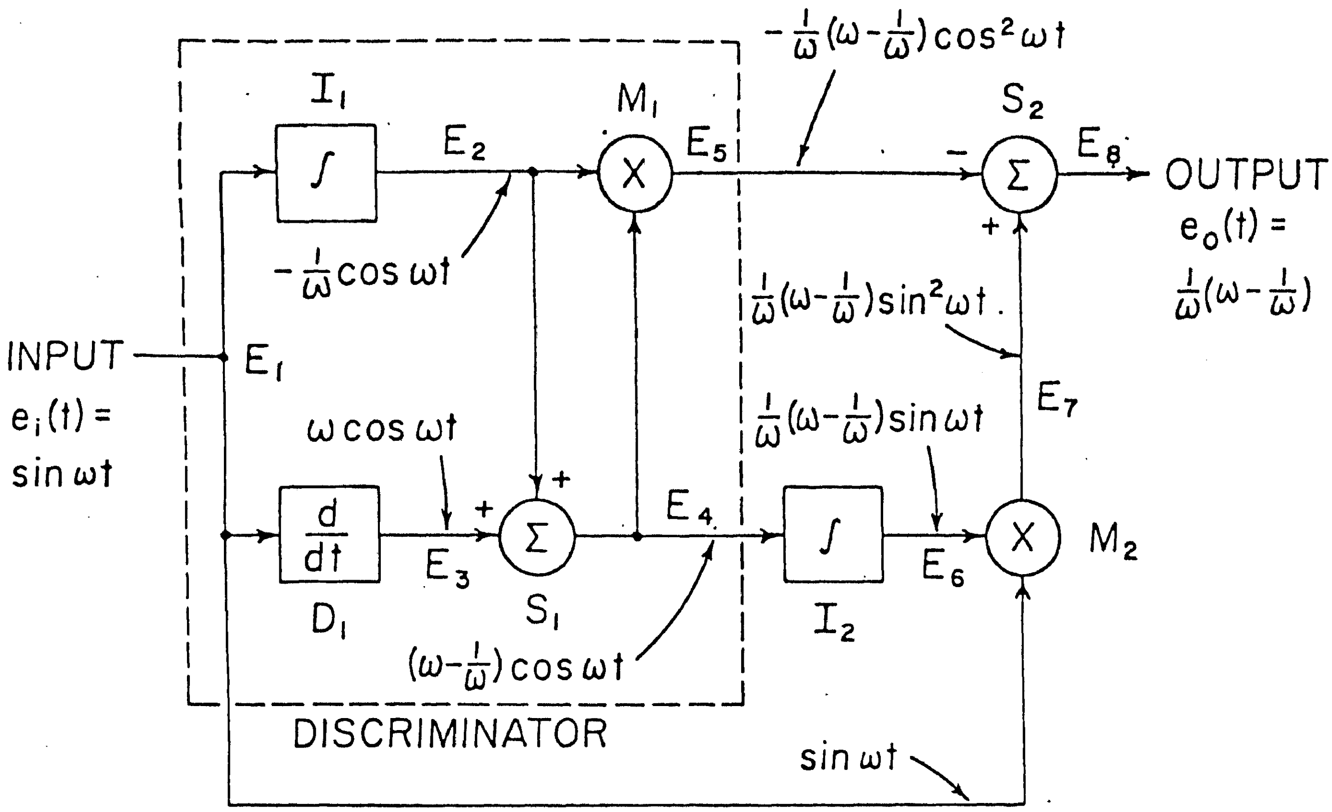

Figure 1-1. Block Diagram of the Original Detector

Slight variations of this circuit are possible by using the differentiator output or the difference between the integrator and differentiator outputs for the reference signal in the synchronous detector.

Although the detector performs well under narrow-band conditions, there are some problems when used under wide-band conditions. First, the non- linearity of the output causes distortion products that are no longer negligible, as indicated in Figure 1-2. Secondly, an integrator problem exists if the input frequency to the detector is changed instantaneously. This situation as shown in Figure 1-3, causes a dc component to appear at the integrator output due to the effective initial condition of the integrator at the time of the frequency change. This dc component at the input of the multiplier causes a considerable component of the fundamental carrier frequency to appear at the output.

A form of the detector that does not require integrators in the discrimination section and therefore is not subject to the initial condition problem is shown in Figure 1-4. An integrator is still needed in the carrier cancellation section, and the output is still non-linear. Another basic form of the detector is shown in Figure 1-5. However, all these forms required integrators and produced outputs that were not ideally linear.

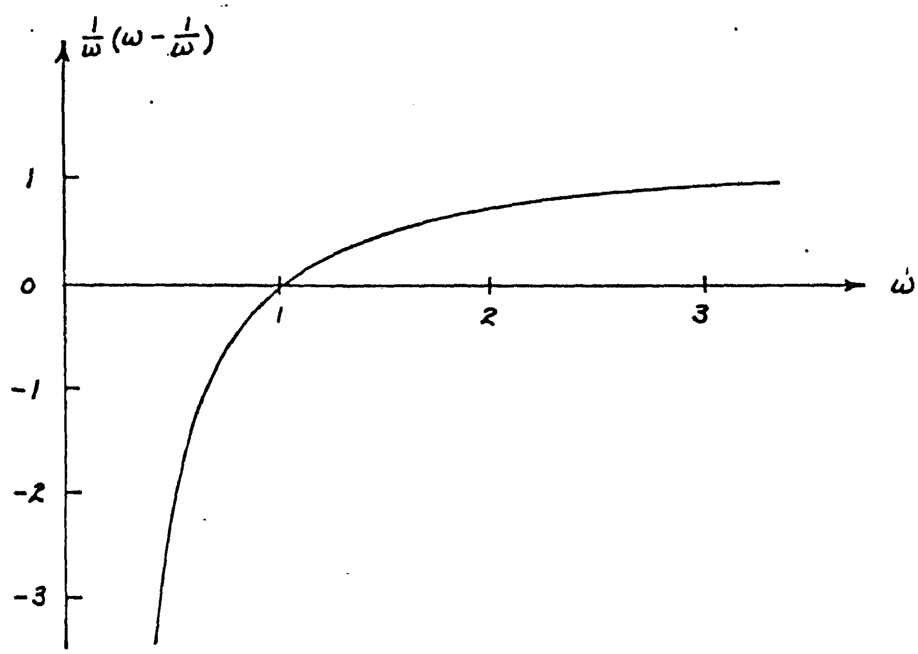

Figure 1-2. Output Characteristic of the Original Detector

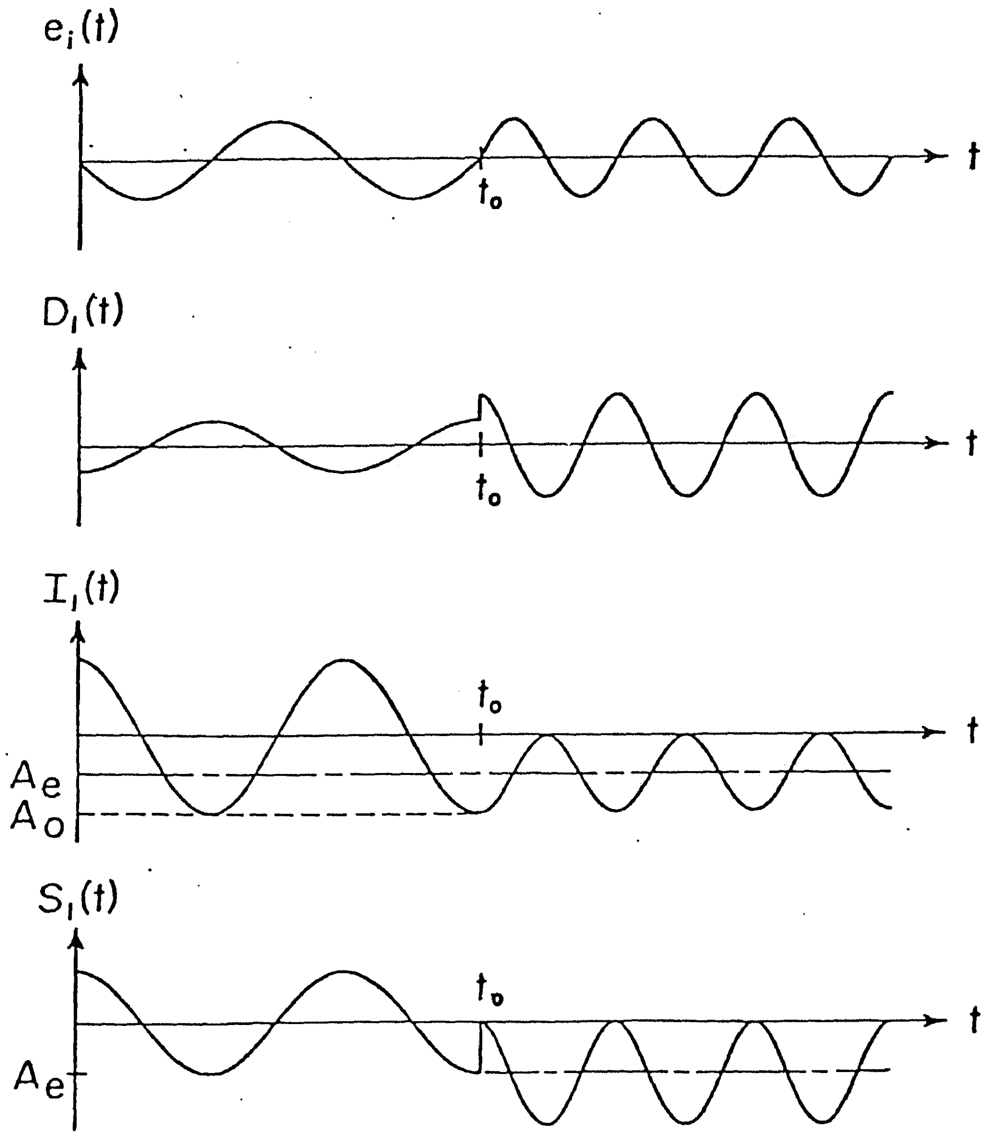

Figure 1-3. Integrator Problem under Wide-Band Conditions

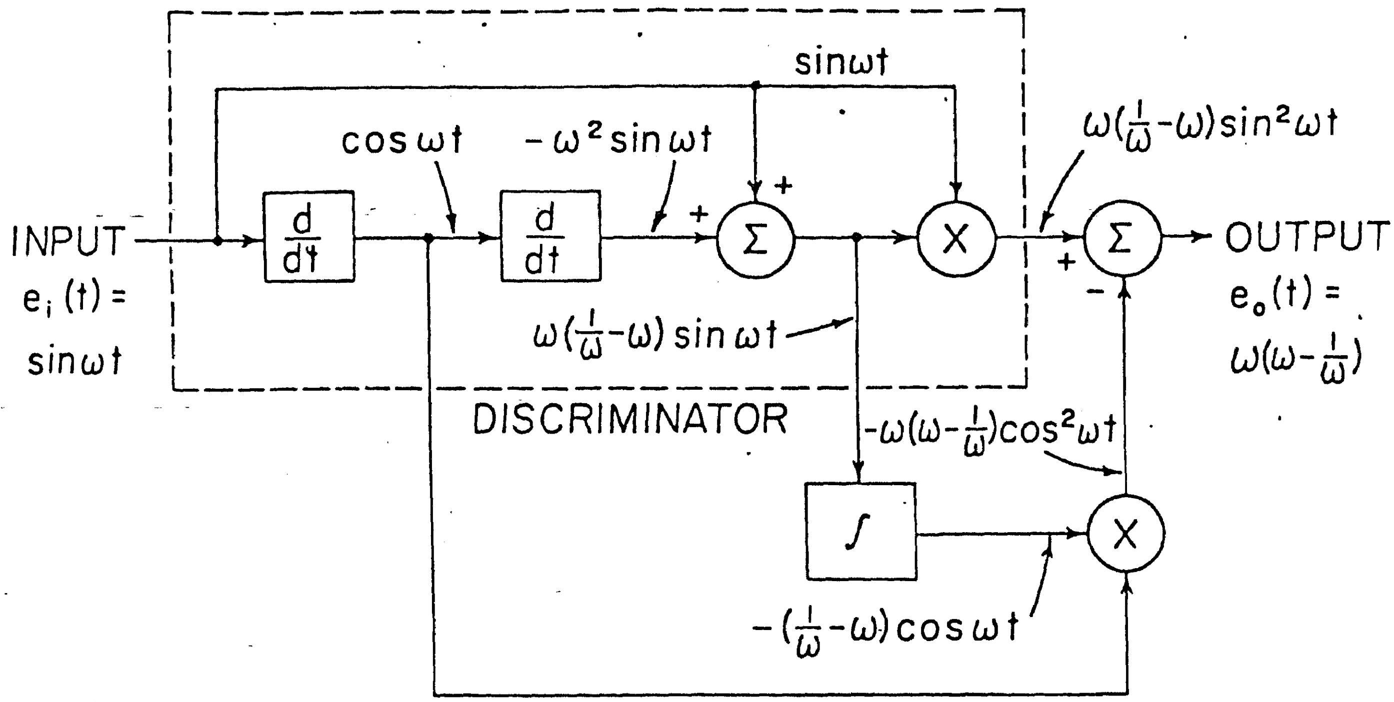

Figure 1-4. Block Diagram of Another Form of the Detector

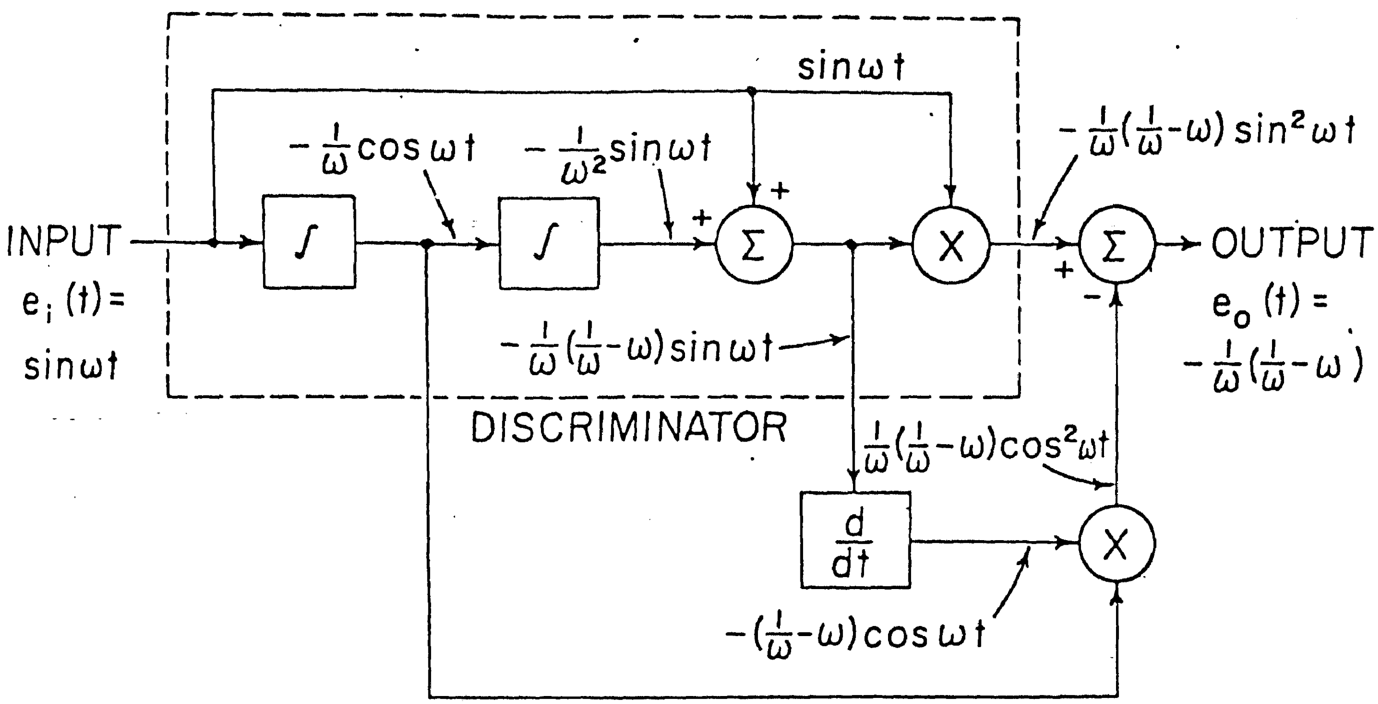

Figure 1-5. Block Diagram of a Third Form of the Detector

1.2 Investigation of an Improved Detector

At present, all work done with this family of detectors assumed analog realization, using operational amplifiers and analog multipliers. With the recent advancement of the digital signal processing technology, however, digital implementation of systems is becoming quite attractive. Therefore, an investigation was made to utilize the advantages of digital signal processing techniques to develop a new version of detector that had optimal wide-band performance.

Research into digital realizations of the basic functional blocks showed that differentiators could be readily realized, but integrators still had problems. However, realization of the Hilbert transformer was found to be comparable to that of the differentiator with good accuracy, even though an accurate Hilbert transform analog realization is usually rather complex. The Hilbert transformer is another zero delay element with a 90 degree phase shift for all frequencies. By replacing the integrators in the detector of Figure 1-1 with Hilbert transformers, the resulting detector was found to have theoretically perfect linearity and excellent wide-band potential.

REFERENCES - Chapter I

1. J. Klapper and E. Kratt, "A New Family of Low-Delay FM Detectors," IEEE Transactions on Communications, Vol. COM-27, No. 2, Feb. 1979.

2. K. K. Clarke and D. T. Hess, "Communications Circuits: Analysis and Design," Addison-Wesley, 1971.

3. J. Park, "An FM Detector for Low S/N," IEEE Transactions on Communication Technology, Vol. COM-18, No. 2, April 1970.

4. E. T. Patronis, "A Frequency Modulation Detector using Operational Amplifiers," Audio Mag., Feb. 1970.

CHAPTER II

FUNCTIONAL DESCRIPTION

2.1 Introduction

A block diagram of one form of the new detector is given in Figure 2-1. It is comprised of a differentiator, two Hilbert transformers, two summers, and two multipliers -- all compatible with FIR discrete time signal processing techniques. The detector may be divided into two basic functions: 1) wide-band quasi-coherent discriminator, and 2) low-delay carrier supression.

2.2 Wide-Band Quasi-Coherent FM Discriminator

This function is performed by the portion of the detector in the dashed box. The input signal is fed simultaneously into differentiator D1 and Hilbert transformer H1. The output of the differentiator leads the input wave by 90 degrees, and its amplitude varies directly with frequency. For simplicity, the time constant is selected to give unity gain at some radian frequency ω_o. The output of the Hilbert transformer, on the other hand, also leads the input wave by 90 degrees, but its amplitude is constant with frequency and has a gain of unity. The result is that the outputs of D1 and H1 are always in phase, and their difference vanishes at ω_o. Thus a balance is achieved at the carrier frequency. Above and below ω_o the output of the summer S1 has an increasing amplitude proportional to the frequency difference. There is, however,

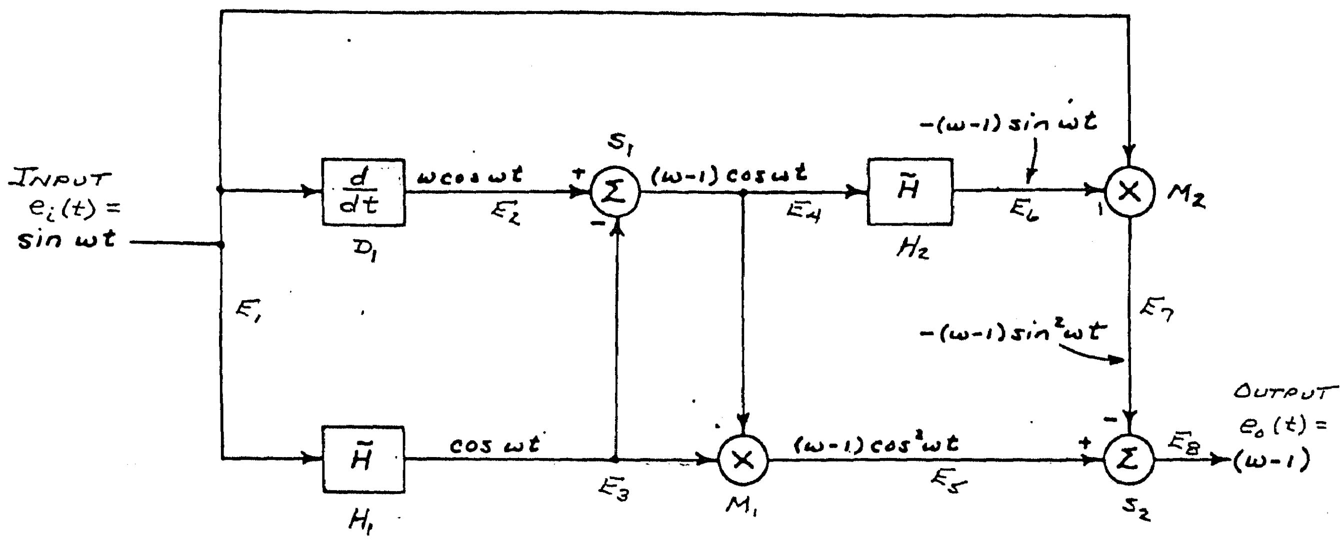

Figure 2-1. Block Diagram of the New Detector

a phase reversal when going through ω_o, because below ω_o the Hilbert transformer output dominates, while above ω_o the differentiator output dominates. The wave thus lends itself to coherent detection.

The coherent detection is performed by the multiplier M1. One input of M1 receives the output of S1, while the other input receives the output of the Hilbert transformer H1. The output of M1 is a wave containing the demodulated output and a carrier of twice the frequency and modulation index.

On a steady-state frequency-offset basis, the pertinent wave equations at each stage are shown in Figure 2-1. An input of sin t is assumed, where the frequency is normalized with respect to the center frequency (i.e. $\omega_o = 1$). The output of the discriminator thus consists of a dc component and a second harmonic component, both of which are proportional to $(\omega - 1)$. The output thus exhibits perfect arithmetic symmetry about the center frequency, a property which the other discriminators in the same family can only approximate.

As with the other discriminators, however, all of the components in Figure 2-1 are still capable of very wide-band operation and are instantaneous (introduce no group delay).

2.3 Cancellation of RF

The output of M1 is proportional to $\cos^2 \omega t$. Observe in Figure 2-1 that the Hilbert transformer H2 and multiplier M2 receive inputs that are in quadrature with the corresponding components in the discriminator portion and generate a wave proportional to $\sin^2 \omega t$ with the same proportionality factor. The outputs of the two multipliers are combined in summer S2. Since $\cos^2 \omega t + \sin^2 \omega t = 1$, the RF is fully cancelled instantaneously, introducing no delay. As is shown later, this characteristic also holds for a modulated input wave because of the perfect linearity of the detector. The cancellation is not perfect for the previous versions due to their nonlinear characteristics.

CHAPTER III

THEORETICAL PERFORMANCE

3.1 Modulated Input Wave

Consider a narrow-band FM wave, as in the case of a sine wave modulation of a small modulation index or the case in which a time-modulated FM wave was passed through a narrow-band filter which attenuated all sidebands except the first pair. The input to the detector may then be considered as an FM wave comprised of three components -- the center frequency and a pair of sidebands. It may be written as

$$e_i(t) = A[\cos \omega_o t - k/2 \cos(\omega_o - \omega_m)t + k/2 \cos(\omega_o + \omega_m)t] \tag{3-1}$$

where A and k are constants related to the amplitude of the wave and the modulation index ($k = \Delta\omega/\omega_m$), while ω_o and ω_m are the center and modulation frequencies, respectively.

It can be shown (see Appendix I) that the output of the detector is then given by

$$e_o(t) = (A^2 kR/2) \cos \omega_m t = \frac{A^2}{2}\left(\frac{\Delta\omega}{\omega_o}\right) \cos \omega_m t \tag{3-2}$$

where R is the ratio of the modulating frequency to the center frequency ($R = \omega_m/\omega_o$). Thus the output consists only of a undistorted baseband.

The outputs of two other versions of the detector as computed in Ref. 1 and Ref. 2 are shown in Table 3-1. In addition to the undistorted baseband, these outputs also

TABLE 3-1

Modulated Input Wave

DETECTOR	$e_o(t)$	NORMALIZED RMS DISTORTION	ASSUMPTIONS
INTEGRATOR-DIFFERENTIATOR	$A^2 kR \Big[2\cos\omega_m t + kR\cos 2\omega_m t + \frac{R}{4}(2+3R)\cos(2\omega_o - \omega_m)t - \frac{R}{4}(2-3R)\cos(2\omega_o + \omega_m)t - \frac{3}{2}kR(1-\cos 2\omega_o t)\Big]$	$\frac{\left[26(Rk)^2 + 2R^2\right]^{1/2}}{4}$	$R \ll 1$
DUAL DIFFERENTIATOR	$\frac{A^2 kR}{2} \Big[-4\cos\omega_m t - kR\cos 2\omega_m t + R\cos(2\omega_o - \omega_m)t - R\cos(2\omega_o + \omega_m)t - kR(1 - 2\cos 2\omega_o t)\Big]$	$\frac{\left[7(Rk)^2 + 2R^2\right]^{1/2}}{4}$	$R \ll 1$
DIFFERENTIATOR-HILBERT TRANSF.	$\frac{A^2 kR}{2}\cos\omega_m t$	0	NONE

contain a low-level signal of twice the baseband frequency, a low-level component of first order sidebands about twice the center frequency, and low-level components of dc and twice the center frequency. These results also assume that the modulating frequency is much smaller than the carrier frequency ($R \ll 1$). These terms result from the non-linearity characteristics of these other forms.

Expressions for the amount of rms distortion d at the various detector outputs are also shown in Table 3-1. These were obtained by taking the ratio of the distortion terms to the desired signal on an rms basis. The value of d for the new detector is zero, since there are no distortion terms. The values of d for the other two detectors are in the order of several percent for $k = 0.1$ and $R = 0.1$, and vary proportionally with R. Thus, the distortion terms may be neglected for small values of R.

Removing the restriction of narrow-band operation, consideration will now be given to the performance of the detector with wide-band modulated input signals, where the input frequency to the detector could theoretically change instantaneously.

Referring back to Figure 2-1, no dc components should be present at the inputs of the multipliers if the detector is to perform as previously described. If this condition is violated, a considerable component of the fundamental carrier frequency will appear at the output. By investigating the sources for the multipliers, no components theoretically produce any dc components under these conditions. The detector should therefore perform equally as well under wide-band conditions.

As shown in Ref. 1, this does not hold for other versions of the detector that use integrators, since dc components are generated as a result of the effective initial conditions of the integrators at the time of a rapid frequency change. This was one of the original purposes for generating a version of the detector without using integrators.

3.2 Sine Wave Interference

Consider the case where the input wave consists of a desired carrier of a frequency ω_d and an interference carrier of a frequency ω_i, such as

$$e_i(t) = A \cos \omega_d t + B \cos \omega_i t \qquad (3\text{-}3)$$

where $\omega_d = \omega_o + \Delta\omega_d$ and $\omega_i = \omega_o + \Delta\omega_i$.

It can be shown (see Appendix II) that the baseband output of the detector shown in Figure 2-1 is then given by

$$e_o(t) = A^2 \frac{\Delta\omega_d}{\omega_o} + B^2 \frac{\Delta\omega_i}{\omega_o} + AB\left(\frac{\Delta\omega_d}{\omega_o} + \frac{\Delta\omega_i}{\omega_o}\right) \cos(\omega_d - \omega_i)t \qquad (3\text{-}4)$$

For the case where $\Delta\omega_d = 0$, the normalized output of the detector reduces to

$$e_o(t) = (\Delta\omega_i/\omega_o)(B/A)^2 + (\Delta\omega_i/\omega_o)(B/A) \cos \Delta\omega_i t \qquad (3\text{-}5)$$

and the rms value of the normalized output is given by

$$\langle e_o(t)\rangle = \{[(\Delta\omega_i/\omega_o)(B/A)]^2 + (1/2)[(\Delta\omega_i/\omega_o)(B/A)]^2\}^{1/2} \quad (3\text{-}6)$$

Curves of $\langle e_o(t)\rangle$ for various values of B/A and $\Delta\omega_i/\omega_o$ are shown in Figure 3-1. Since the output is symmetric about $\Delta\omega_i/\omega_o = 0$, only positive values of $\Delta\omega_i/\omega_o$ are graphed.

Corrington (Ref. 3) has derived the equivalent output of a conventional wide-band limiter-discriminator for $\Delta\omega_d = 0$ as

$$e_{oc}(t) = \frac{(\Delta\omega_i/\omega_o)(\cos\Delta\omega_i t + B/A)}{2\cos\Delta\omega_i t + A/B + B/A} \quad (3\text{-}7)$$

The equivalent rms output for A/B < 1 is given by

$$\langle e_{oc}(t)\rangle = \frac{(\frac{\Delta\omega_i}{\omega_o})^2 (B/A)^2}{2[1 - (B/A)^2]} \quad (3\text{-}8)$$

Curves of $\langle e_{oc}(t)\rangle$ for various values of B/A and $\Delta\omega_i/\omega_o$ are also shown in Figure 3-1. In comparing these curves with those of the detector of Figure 2-1, one observes that the two curves are almost identical for small values of B/A. However, as B/A approaches 1, the output of the ideal limiter-discriminator approaches infinity, while the output of the new detector remains finite. This may also be observed by comparing Equation 3-5 and Equation 3-7. Therefore, as the interference increases, the detector of Figure 2-1 has a much better output purity both in terms of rms and peak-to-peak values, and this improvement increases without bound.

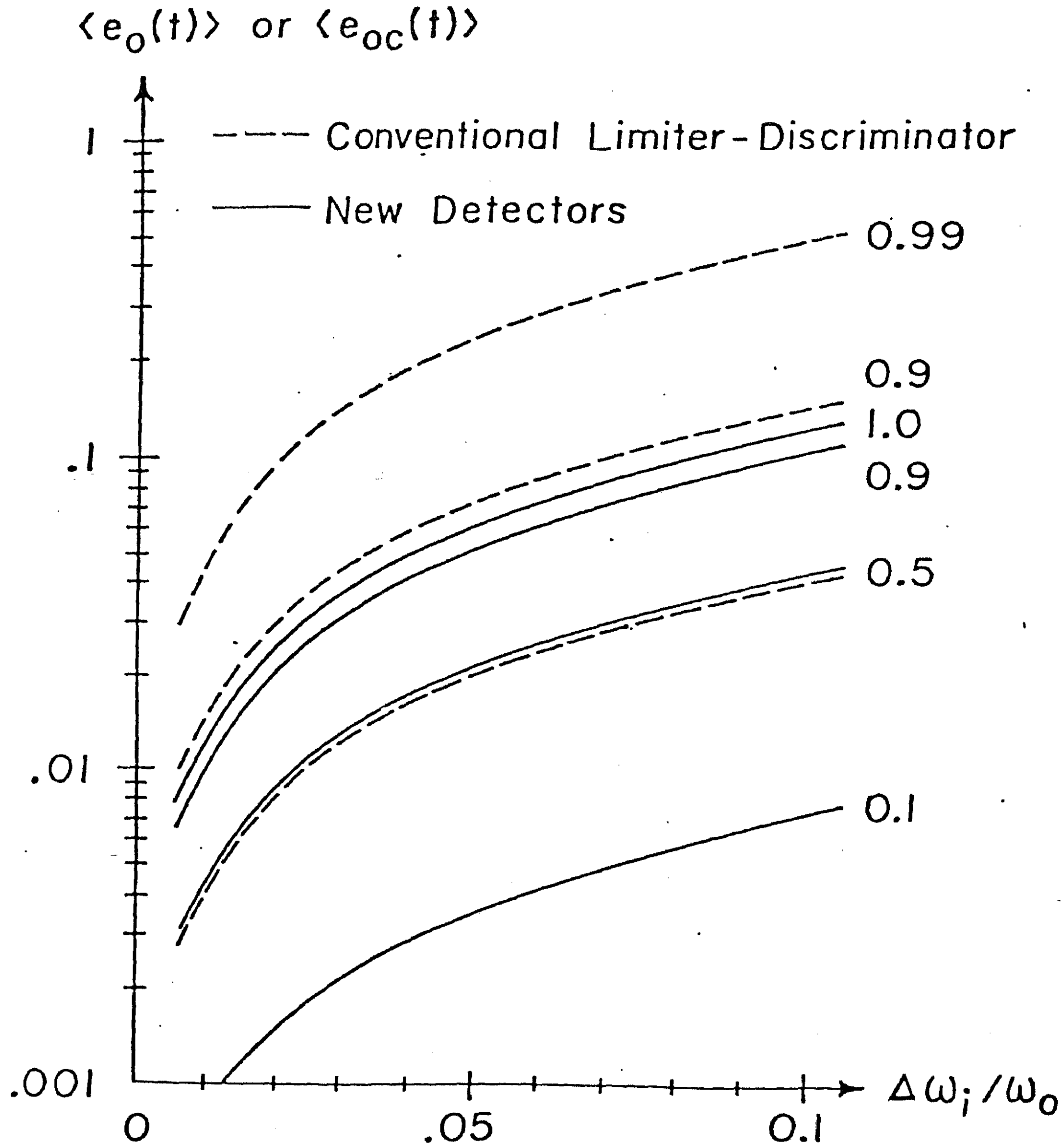

Figure 3-1. $\langle e_o(t) \rangle$ vs. $\Delta\omega_i/\omega_o$ for Various Values of B/A

In comparison, similar results for the detectors of Figure 1-1 and Figure 1-4 as given by Ref. 1 and Ref. 2, respectively, are shown in Table 3-2. The expressions for <e (t)> are identical to Equation 3-6 if the frequency deviations are small compared to the carrier frequency ($\Delta\omega_i/\omega_o$ << 1 and $\Delta\omega_d/\omega_o$ << 1). These assumptions were not needed in the derivation of Equation 3-6, which therefore describes the detector of Figure 2-1 also under wide-band sinusoidal interference conditions.

3.3 Noise Performance

Consideration will now be given to the performance of the detector of Figure 2-1 in the presence of narrow-band noise. The complete detector, including the pre-detection and post-detection filters, is shown in Figure 3-2. The definition of output SNR used in this derivation is taken to be the ratio of mean output signal power to mean output noise power, where the signal power is measured in the absence of noise and the noise power in the absence of signal (i.e. the carrier is unmodulated). This definition is valid for high SNR, where the mean signal and noise powers may be assumed to add linearly, and the signal power measured in the absence of noise does not differ substantially from that measured with noise present. Signal suppression occurs as the values of CNR drop below 0 dB (Ref. 4).

The noise is assumed to be of a bandwidth no wider than twice the carrier center frequency, and therefore may be

TABLE 3-2

Sine Wave Interference

DETECTOR	NORMALIZED $e_o(t)$*	$\langle e_o(t) \rangle$*	ASSUMPTIONS
INTEGRATOR - DIFFERENTIATOR	$\frac{\omega_r}{\omega_o}\left(\frac{B}{A}\right)^2 + \frac{\omega_r}{\omega_o}\frac{B}{A}\cos\omega_r t$	$\left\{\left[\frac{\omega_r}{\omega_o}\left(\frac{B}{A}\right)^2\right]^2 + \frac{1}{2}\left[\frac{\omega_r}{\omega_o}\frac{B}{A}\right]^2\right\}^{1/2}$	$\frac{\omega_r}{\omega_o} \ll 1$ $\frac{\omega_c}{\omega_o} \ll 1$
DUAL DIFFERENTIATOR	$-\frac{\omega_r}{\omega_o}\left(\frac{B}{A}\right)^2 - \frac{\omega_r}{\omega_o}\frac{B}{A}\cos\omega_r t$		
DIFFERENTIATOR - HILBERT TRANSF.	$\frac{\omega_r}{\omega_o}\left(\frac{B}{A}\right)^2 + \frac{\omega_r}{\omega_o}\frac{B}{A}\cos\omega_r t$		NONE
LIMITER - DISCRIMINATOR (CORRINGTON)	$\dfrac{\frac{\omega_r}{\omega_o}\left(\cos\omega_r t + \frac{B}{A}\right)}{2\cos\omega_r t + \frac{A}{B} + \frac{B}{A}}$	$\left[\dfrac{\left(\frac{\omega_r}{\omega_o}\right)^2\left(\frac{B}{A}\right)^2}{2\left[1-\left(\frac{B}{A}\right)^2\right]}\right]^{1/2}$	

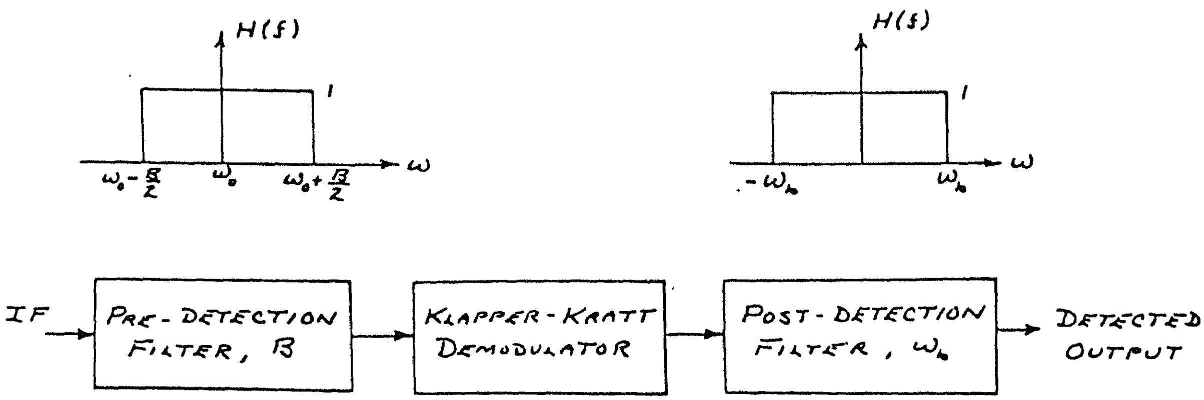

Figure 3-2. Complete Detector for Noise Calculations

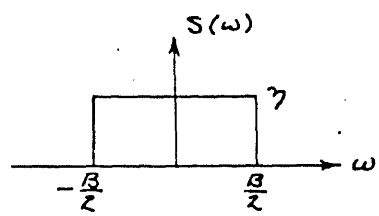

Figure 3-3. PSD of x(t) and y(t)

represented by

$$n(t) = x(t) \cos \omega_o t - y(t) \sin \omega_o t \qquad (3\text{-}9)$$

which consists of a carrier at the center frequency ω_o, modulated by two random variables, $x(t)$ and $y(t)$. The noise is also assumed to have a zero mean and a Gaussian distribution. The random variables $x(t)$ and $y(t)$ thus have the following properties: a) Lowpass, rectangular power spectral density of bandwidth B/2 and amplitude n as shown in Figure 3-3, b) Equal variances for $n(t)$, $x(t)$, and $y(t)$, and c) $x(t)$ and $y(t)$ are independent.

Therefore, consider an input signal given by

$$e_i(t) = A \cos \omega_o t + x(t) \cos \omega_o t - y(t) \sin \omega_o t \qquad (3\text{-}10)$$

which consists of an unmodulated carrier with added narrow-band noise. It may be shown (see Appendix III) that the baseband output of the detector is then given by

$$e_o(t) = 1/\omega_o \{ \dot{x}(t) [A - y(t)] + \dot{y}(t)\, x(t) \} \qquad (3\text{-}11)$$

The output power spectral density may then be obtained by taking the Fourier Transform of the autocorrelation function of $e_o(t)$. By integrating this result over the post-discrimination bandwidth and dividing by 2π, the detector output noise power is shown to be given by

$$\text{NOISE POWER} = \frac{A^2 \eta\, \omega_b^3}{3\pi\, \omega_o^2} + \frac{\eta^2}{\pi^2 \omega_o^2}\left[\frac{B^3 \omega_b}{12} - \frac{B^2 \omega_b^2}{8} + \frac{B\, \omega_b^3}{6} - \frac{\omega_b^4}{12}\right] \qquad (3\text{-}12)$$

Next, the output signal power may be obtained using a modulated input signal given by

$$e_i(t) = A\cos(\omega_o t + \beta \sin \omega_m t) \tag{3-13}$$

where A is the carrier amplitude, β is the modulation index, and ω_m is the modulation frequency. The corresponding output power is then shown to be given by

$$\text{SIGNAL POWER} = \frac{A^4 \beta^2 \omega_m^2}{8\,\omega_o^2} \tag{3-14}$$

The output SNR is obtained by taking the ratio of the output signal power to the noise power. In terms of the CNR at the input, the SNR is given by

$$\text{SNR} = \frac{\frac{3}{2}(CNR)\,B\,\beta^2 \omega_m^2/\omega_b^3}{1 + \frac{1}{CNR}\left[\frac{X^2}{4} - \frac{3X}{8} + \frac{1}{2} - \frac{1}{4X}\right]} \tag{3-15}$$

where $x = B/\omega_b$. The only assumptions made were that $\omega_b < B/2$ and that the signal and noise terms are additive.

For the special case of high CNR, the denominator in Equation 3-15 becomes unity. Letting $\omega_m = \omega_b$ for optimum performance, and using the relationship $CNR = (CNR)_{AM}\,(2\omega_b/B)$, then the SNR for high CNR conditions is given by

$$\text{SNR}_{HIGH\ CNR} = 3\,\beta^2 (CNR)_{AM} \tag{3-16}$$

which is identical to the expression for a limiter-discriminator well above threshold (Ref. 5). The performance of the detector is therefore identical to a limiter-discriminator well above threshold, but without using a limiter.

As indicated in Figure 3-4, the threshold point for an FM system is usually defined as the point where the SNR has dropped 1 dB more than that predicted by the linear improvement region. Referring to Equation 3-15, this occurs where the denominator increases an amount above unity equivalent to 1 dB. The result may be written as

$$(CNR_{AM})_{Th} = 1.931 \, [\, x^3/2 - 3x^2/8 + x/2 - 1/4 \,] \qquad (3\text{-}17)$$

In comparison, the SNR relationship for the detector of Figure 1-4 is given by Tarbell (Ref. 6) as

$$SNR = \frac{\frac{3}{2}\,(CNR)\,B\,\beta^2\,\omega_m^2/\omega_b^3}{1 + \frac{1}{CNR}\left[\frac{X^2}{2} - \frac{3X}{4} + \frac{1}{2} - \frac{1}{8X}\right]} \qquad (3\text{-}18)$$

The corresponding equation for the threshold CNR is

$$(CNR_{AM})_{Th} = 1.931 \, [\, X^3/2 - 3X^2/4 + X/2 + 1/8 \,] \qquad (3\text{-}19)$$

The results of Equation 3-16 and Equation 3-18 are shown in Figure 3-5 for various values of $B/2\omega_b$, along with data for a conventional limiter-discriminator (Ref. 7) for comparison. The new detector has a 3 dB improvement in threshold performance over the detector of Figure 1-4, but still no improvement over the limiter-discriminator.

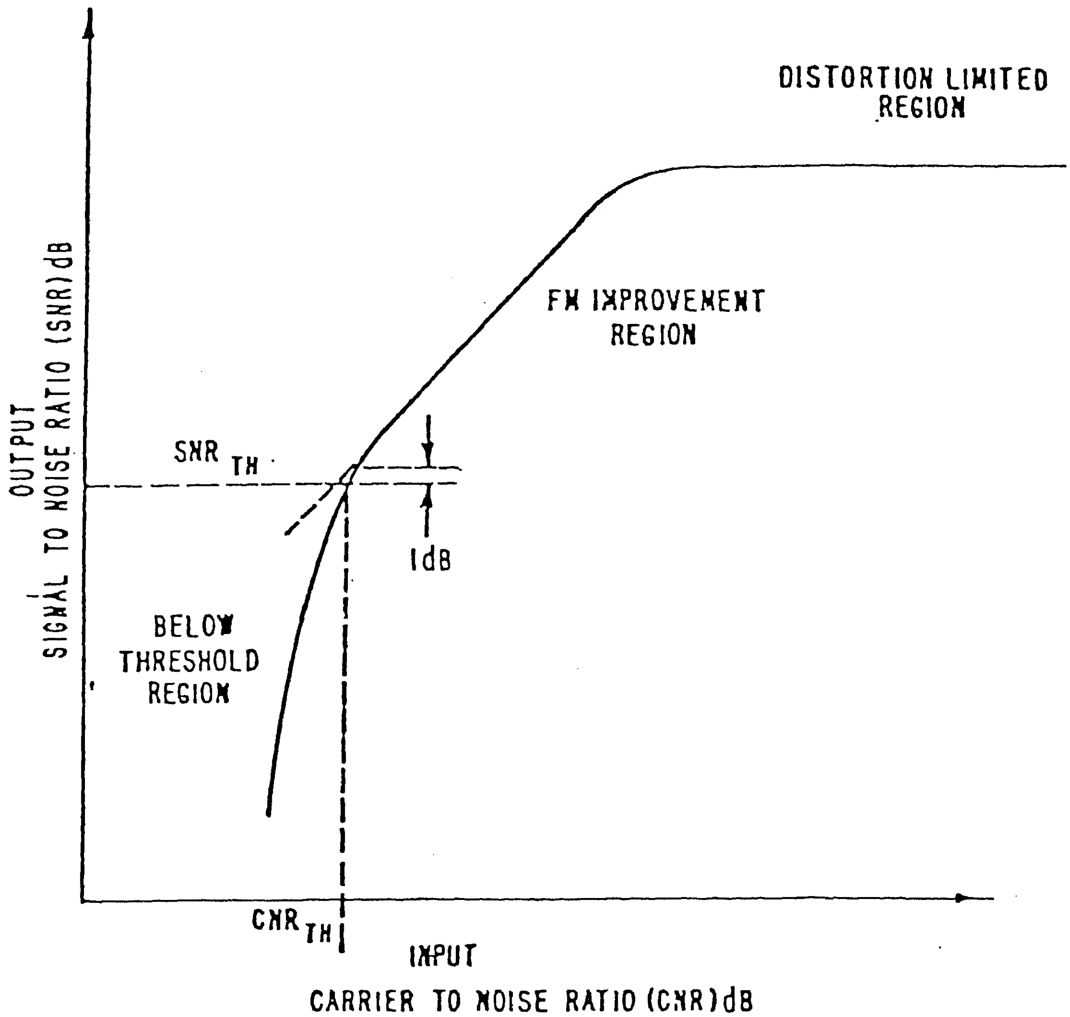

Figure 3-4. FM System Performance

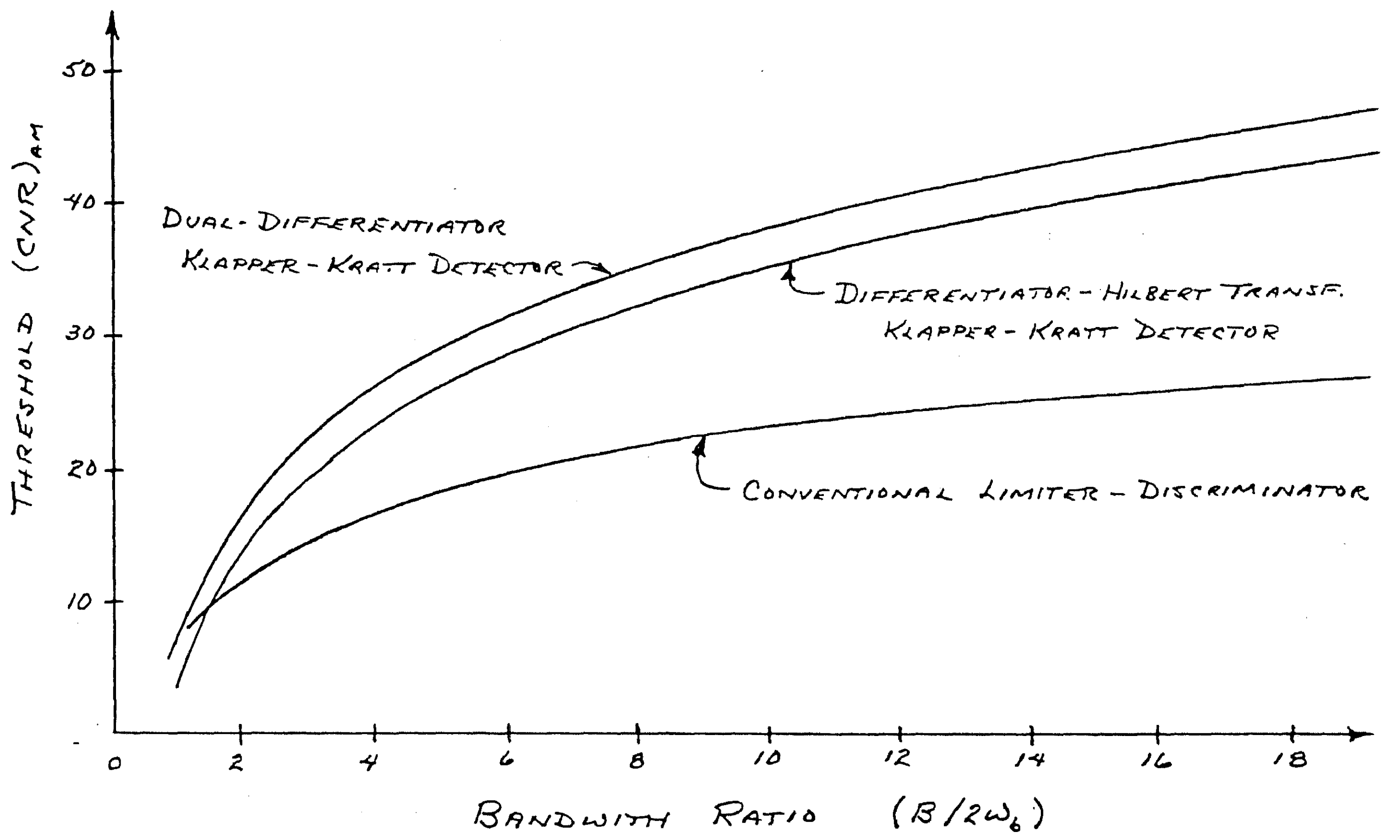

Figure 3-5. Threshold $(CNR)_{AM}$ Characteristics

REFERENCES - Chapter III

1. J. Klapper and E. Kratt, "A New Family of Low-Delay FM Detectors,", IEEE Trans. on Communications, Vol. COM-27, No. 2, Feb. 1979.

2. G. J. Kersus, "Analysis of the Klapper-Kratt FM Detector," M.S. Project, Dept. Elec. Eng., New Jersey Inst. Technol., 1976.

3. M. S. Corrington, "Frequency Modulation Caused by Common-and-Adjacent-Channel Interference," RCA Rev., Vol 7, Dec. 1946.

4. P. F. Panter, Modulation, Noise, and Spectral Analysis, Chap 14, McGraw Hill, 1965.

5. M. Schwartz, Information Transmission, Modulation, and Noise, Chapter 6, McGraw Hill, 1959.

6. A. Tarbell and J. Klapper, "Noise Performance of the Klapper-Kratt Low Delay FM Detector," NTC, Washington, D.C., Nov. 1979.

7. J. Klapper and J. T. Frankle, Phase Locked and Frequency Feedback Systems, Chapter 7, Figure 7-14, Academic Press, 1972.

CHAPTER IV

DIGITAL IMPLEMENTATION

4.1 Introduction

A direct approach to digitally implementing the detector was performed first by generating algorithms that will closely resemble the differentiator and Hilbert transformer over the frequency band of interest. The corresponding samples were also added and multiplied as required to perform the functions shown in Figure 2-1.

The differentiator and Hilbert transformer were realized using a finite impulse response (FIR), or non-recursive, design method. Such designs exhibit no phase errors, and have delays of approximately N/2 sampling periods, where N is the order of the network. They are also unconditionally stable, since they are synthesized using only zeros.

Obviously the digital system cannot still have theoretically zero delay due to the discrete time samples and the delays in generating the functional blocks. However, if actual delay is not of major importance, then the detector should offer much improved performance in other areas.

4.2 Linear-Phase Realizations

A computer program called EQFIR (Ref. 1) was used to generate the coefficients for FIR realizations of both differentiators and Hilbert transformers. The program optimizes the results over a prescribed frequency range, which was selected as 0.15 f_s to 0.35 f_s, where f_s is the sampling frequency. These values will then generate a detector that is centered at half the Nyquist frequency with a relatively wide linear bandwidth of two-fifths the Nyquist frequency.

Using these requirements, the coefficients were computed for differentiators with N= 5, 7, and 9. Only odd values of N were selected so that the delayed output of the function be an exact number of sample periods for proper configuration of the total network. The delay of the FIR block is (N-1)/2 sampling periods, which for odd values of N causes the delayed outputs to fall on exact sample times, allowing the results to be combined with other equally delayed values to perform the additional functions. Each output is generated by multiplying the N successive samples by the corresponding coefficients, and then summing the results.

The equations giving the frequency response of a general FIR configuration were derived (see Appendix IV) and used to evaluate each set of differentiator coefficients. The results are shown in Figure 4-1. Reasonable results were obtained for N=7, with N=9 giving very good results.

In a similar manner, coefficients for Hilbert transformers were computed and evaluated for N= 5, 7, 9 and 11. The results are shown in Figure 4-2. The response for N=7 and 9 are the same and provide a relatively close approximation.

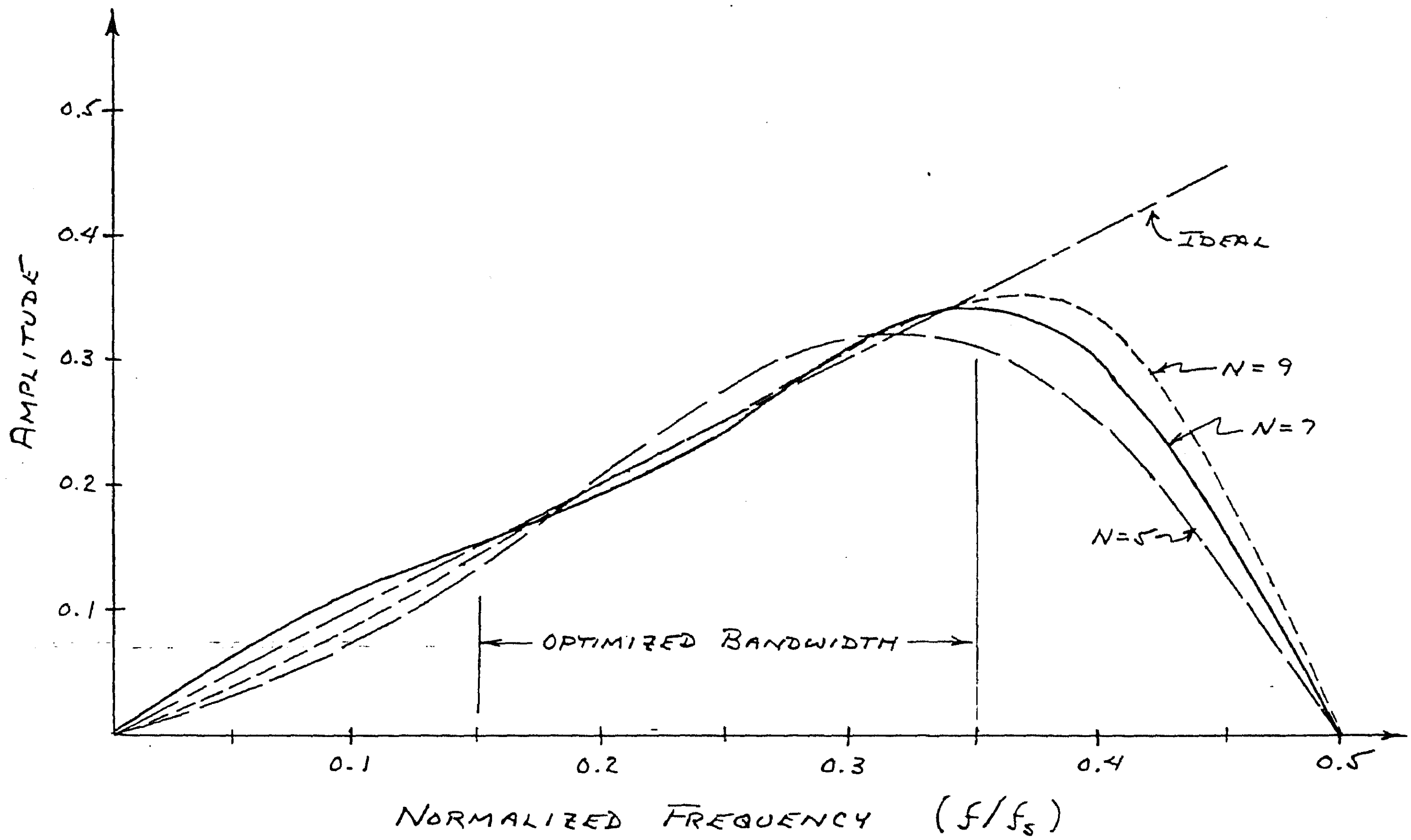

Figure 4-1. Frequency Response of Differentiators

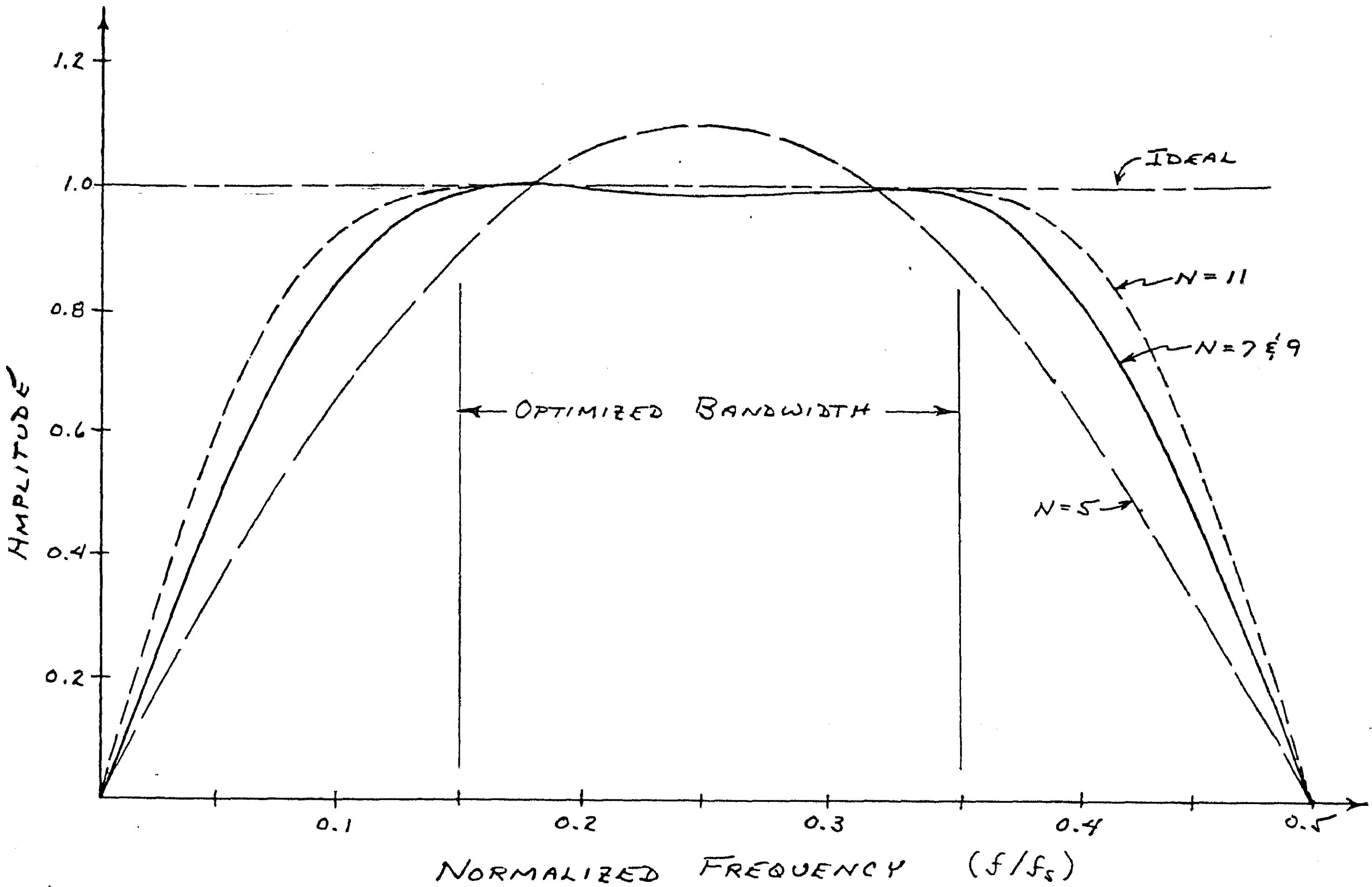

Figure 4-2. Frequency Response of Hilbert Transformers

At first, it might seem strange that two values of N give identical results. However, the frequency response equation for a FIR network is based on a Fourier structure, and any particular component that is not symmetrical with respect to the desired response has a value of zero. For example, all even harmonics of a square wave are zero. Therefore, increasing the order does not necessarily add useful terms.

Selection of a value of N was based on finding the minimum value that gave approximate results, with the assumption that later optimization of the total detector would greatly improve the response of the detector. A lower value of N also means a simpler algorithm for easier implementation and smaller values of delay. As a result, N=7 was chosen for both the differentiator and Hilbert transformer.

The equation for the frequency response of the detector was derived (see Appendix V), and is given by

$$\underline{E}_o(F) = 1/2 \sum_{m=1}^{N} \sum_{n=1}^{N} (c_{Dn} - c_{Hn})\, c_{Hm} \\ [\cos(m-n)2\pi F - \cos(N+1-n-m)2\pi F] \qquad (4\text{-}1)$$

where F is the frequency normalized to the sampling frequency, c_{Di} is the ith coefficient (or impulse response) of the differentiator and c_{Hi} is the ith coefficient of the Hilbert transformer. The detector response was then computed using the coefficients for N=7, as given in Table 4-1. The results are shown in Figure 4-3, which indicates an almost sinusoidal response with much greater linearity error than indicated by

TABLE 4-1
Original Detector Coefficients
(Impulse Response)

H(i)	DIFF. BLOCK	H. T. BLOCK
H(1) = - H(7)	0.08223	0.08510
H(2) = - H(6)	- 0.19502	0.00240
H(3) = - H(5)	0.57944	0.58080
H(4)	0	0

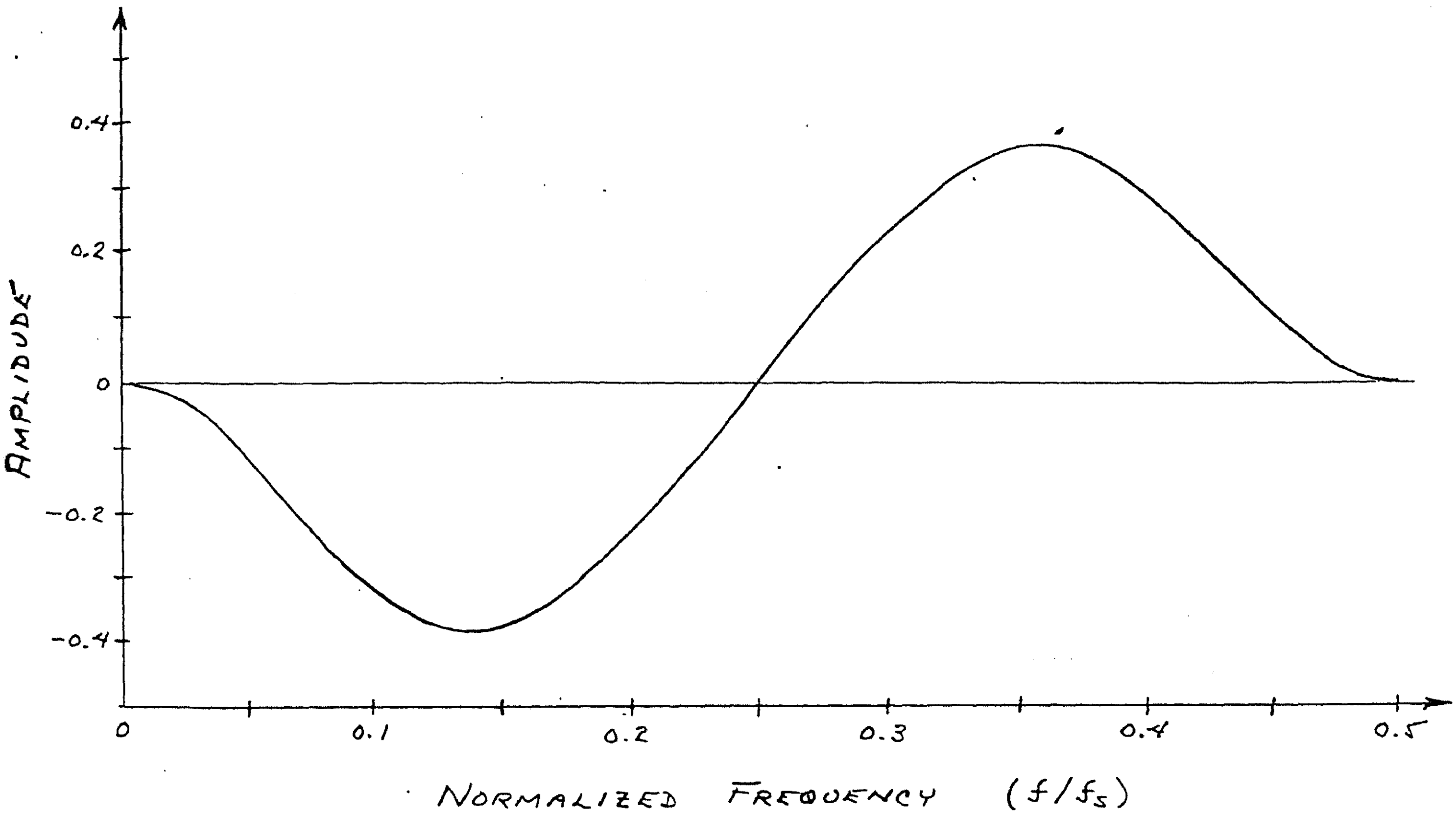

Figure 4-3. Detector Output

any of the individual components. This is because the particular errors of each block set multiplied when combined in the total detector, resulting in a much larger error.

Also observe that the detector output reduces to zero at both zero frequency and the Nyquist frequency, since the outputs of both the differentiator and Hilbert transformer go to zero at these frequencies. Therefore, the detector also provides an equivalent inherent linear phase bandpass filter characteristic. For higher order realizations, this internal bandpass property may be utilized with other bandwidths and center frequencies to eliminate undesired signals within the Nyquist band.

4.3 Linearity Optimization

Consideration was now given to optimizing the detector coefficients for linearity over the frequency range of interest ($0.15 < F < 0.35$). Constraints had to be placed on the coefficients in order to retain certain necessary properties. First, the negative symmetry of the coefficients is required to preserve the linear-phase (actually a constant 90 degree phase) characteristic of the FIR blocks. This requires that $c_i = -c_{N+1-i}$, and $c_{(N+1)/2} = 0$ since N is odd. The 90 degree phase properties of the components is required to maintain the quadrature relationships for carrier cancellation. As a result, only three values are required to define the seven general coefficients of each FIR block.

Next, the amplitude requirements need to be determined. This may be accomplished by assuming that each FIR block is multiplied by a corresponding amplitude function of frequency F, as shown in Figure 4-4. These amplitude functions represent the non-ideal amplitude variations in the realization of each function. Assuming an input $e_i(t) = \sin\omega t$, and solving in a manner similar to that used in Appendix I, the corresponding output is found to be given by

$$e_o(t) = [\,A_1(\omega) - A_2(\omega)]\,[A_2(\omega)\cos^2\omega t + A_3(\omega)\sin^2\omega t] \tag{4-2}$$

Therefore, the carrier component will cancel exactly only if $A_3(\omega) = A_2(\omega)$. This means that the coefficients of the two Hilbert transformers must be identical. Linearity of the detector is then controlled by $A_1(\omega)$ and $A_2(\omega)$, which may vary from unity and still give the desired result of $(\omega - 1)$ as long as they are related by the expression

$$A_1(\omega) = \frac{1}{\omega}\left[\frac{\omega - 1}{A_2(\omega)} + A_2(\omega)\right] \tag{4-3}$$

In the implementation, computer routines were generated (See Appendix VII) to minimize a least squares linearity error function using the Fletcher-Powell algorithm (Ref. 2). The error function was generated by summing the squares of the differences between the actual and desired detector outputs using a number of frequency points over the interval $0.15 \leq F \leq 0.35$.

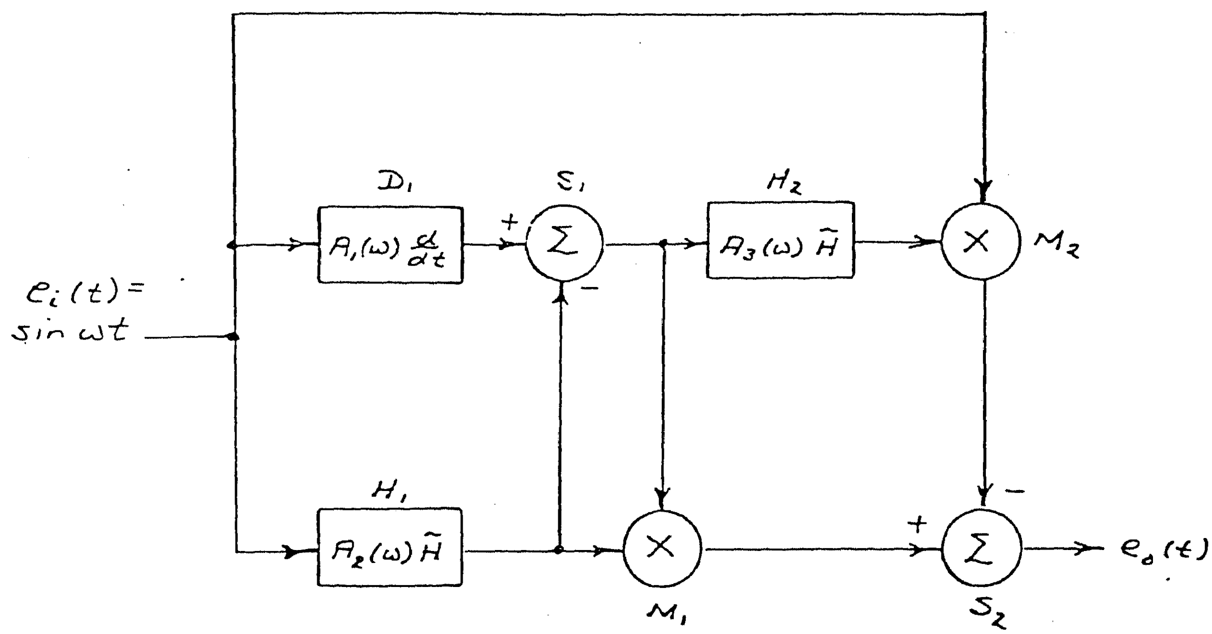

Figure 4-4. Non-Ideal Block Representations

Upon convergence, the optimized coefficients shown in Table 4-2 were obtained. The corresponding optimized detector output is shown in Figure 4-5, where it is compared with both the original detector output and the ideal output. Over the frequency range of optimization, the output is found to be extremely linear, with substantial improvement over the original response.

The internal bandpass characteristic of the detector is also improved. An equivalent gain response of the detector was generated by taking the ratio of the actual output to the ideal output of a theoretical wide-band detector. The results are shown in Figure 4-6.

REFERENCES - Chapter IV

1. J. H. McClellan, T. W. Parks and L. R. Rabiner, "FIR Linear Phase Filter Design Program," Programs for Digital Signal Processing, Chap. 5.1, IEEE Press, New York, 1979.
2. R. Fletcher and M. J. D. Powell, "A rapidly convergent descent method for minimization," Computer J., Vol. 6, No. 2, July 1963.

TABLE 4-2

Optimized Detector Coefficients
(Impulse Response)

H(i)	DIFF. BLOCK	H. T. BLOCK
H(1) = - H(7)	0.19019	0.19071
H(2) = - H(6)	- 0.21116	- 0.00157
H(3) = - H(5)	0.54117	0.54175
H(4)	0	0

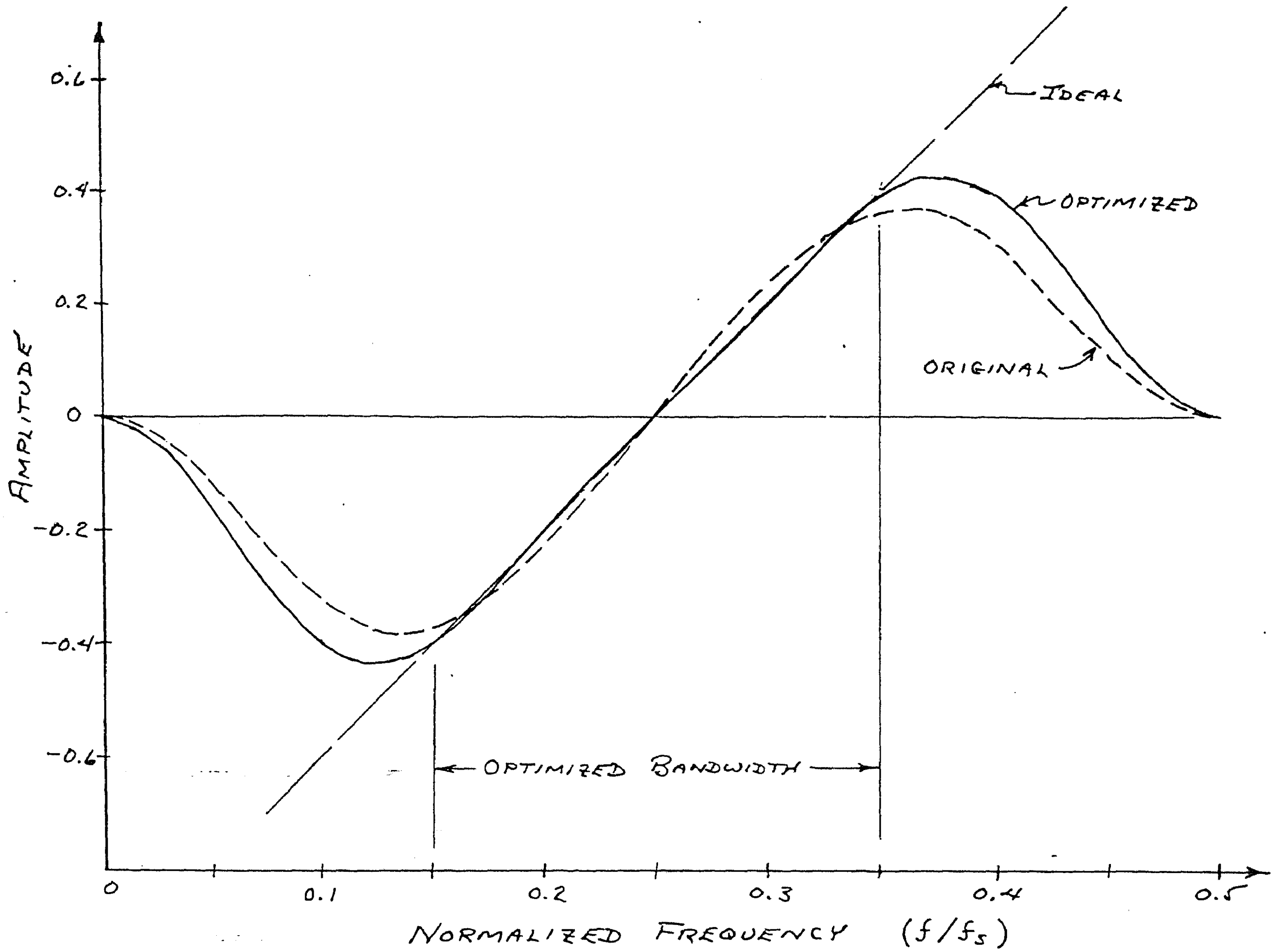

Figure 4-5. Detector Output with Linearity Optimization

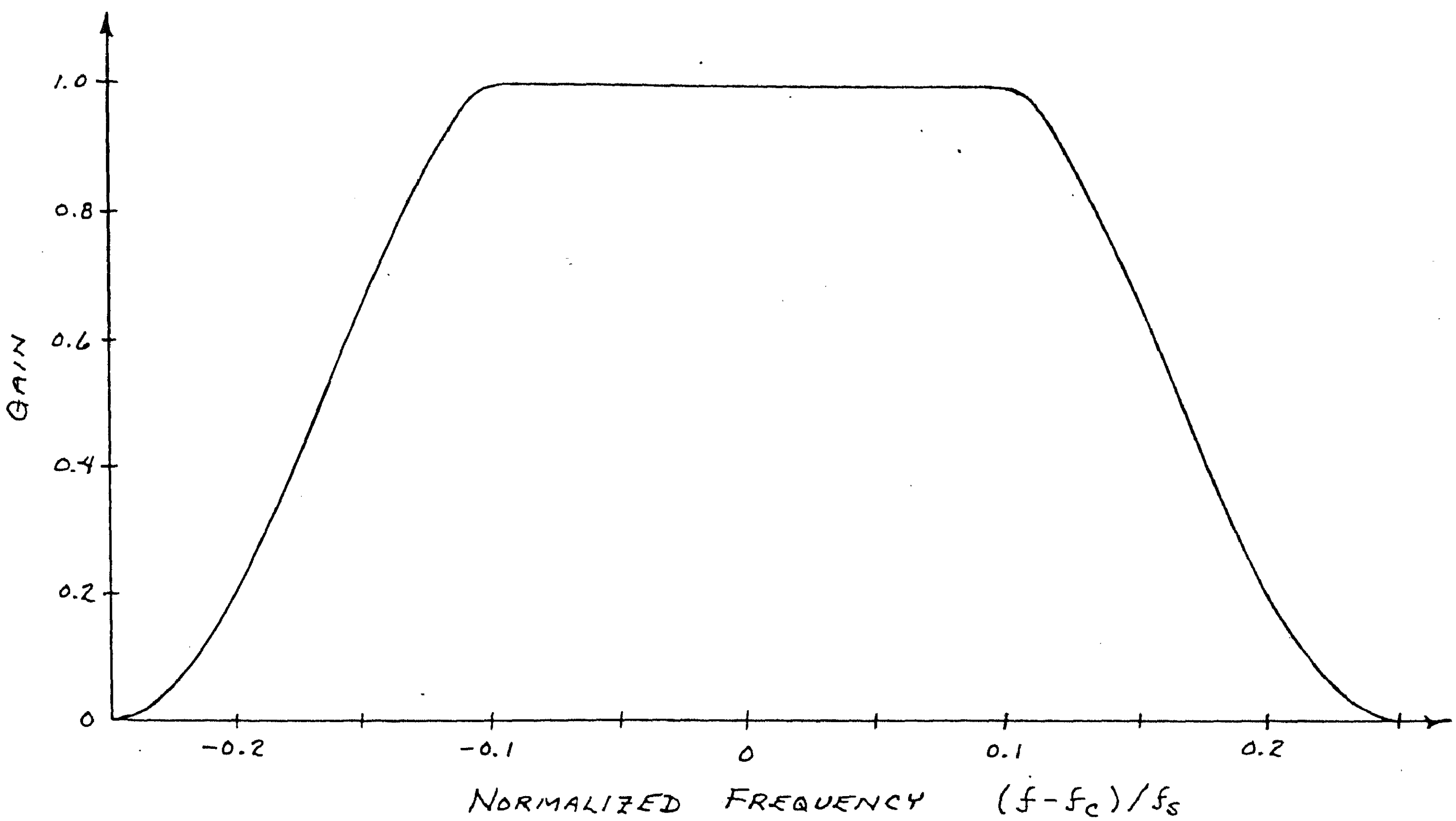

Figure 4-6. Equivalent Gain Response of the Detector

CHAPTER V

REALIZATION

5.1 Introduction

The optimized detector was realized using 11 bit A/D and D/A converters, and a DEC LSI-11 processor with an extended arithmetic chip. Even though this processor is relatively fast, it still takes approximately 60 μs for a multiplication and 8 μs for an addition or subtraction. Since a direct approach to realizing the detector of Figure 2-1 using the coefficients given in Table 4-2 would require eleven multiplications, six additions and ten subtractions, considerable time will be used in performing the functions of the algorithm alone, without even including time to perform other related functions that are necessary to input, output, or internally shift data during each cycle. The longer the computing time, the lower the maximum sampling frequency, and therefore, also the maximum operating frequency. However, by investigating the values of the coefficients and the structure of the basic detector algorithm, substantial simplifications to the algorithm were discovered, which greatly increased the maximum frequency of operation.

5.2 Algoritm Simplification

Observing the coefficients shown in Table 4-2, the coefficients for the differentiator and Hilbert transformer blocks are found to be practically identical for both the first and third values. Referring back to Figure 2-1, the outputs of D1 and H1 are subtracted in summer S1. Since multiplying an input sample by two different coefficients and then taking the difference of the results is equivalent to multiplying the input sample by the difference of the two coefficients, then the functions of D1, H1 and S1 may be replaced by a single block, as shown in Figure 5-1, with coefficients equal to $c_{Di} - c_{Hj}$. Therefore the first and third coefficients would be zero, while the second coefficient is -0.20959.

The fact that two of the coefficients of this new block are zero did not occur by accident. Recall that the output of S1 is actually the output of the discriminator before synchronous detection. The frequency response should therefore be zero at the center frequency (F = 0.25), and have odd symmetry around this point. A negative value, in this case, means a reversal of phase. Comparing this with the theoretical frequency response of a FIR block, which was derived (see Appendix IV) as

$$H(F) = j \sum_{n=1}^{\frac{N-1}{2}} 2\ c_n \sin\ (N + 1 - 2n)\pi F \qquad (5\text{-}1)$$

only the term for n = 2 produces odd symmetry about F = 0.25. The other two terms have even symmetry, and must therefore be zero.

By observing Equation 5-1 for larger values of N, alternate terms will be seen to have even symmetry and

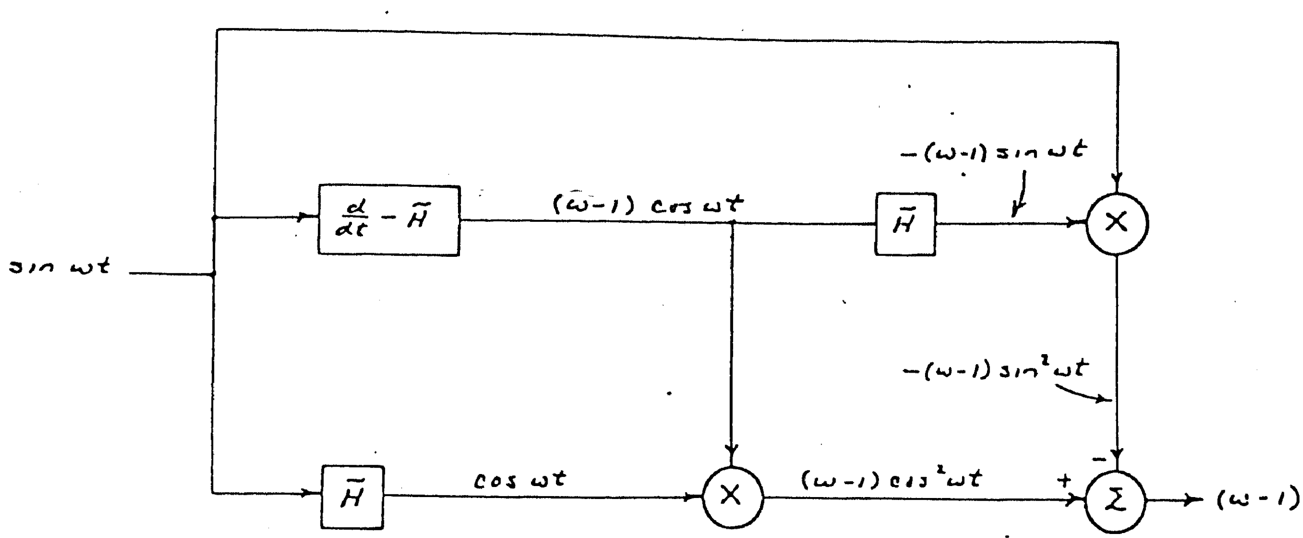

Figure 5-1. Simplified Detector Block Diagram

therefore must be equal to zero. As a result, similar simplifications may also be made for higher order detectors of different bandwidths, as long as $F_o = 0.25$. Larger bandwidths, however, will require higher values of N in order to retain good linearity. Other values of F_o do not allow such simplifications since the response is not symmetrical and therefore generally requires all terms.

Since the D-H block has only one non-zero coefficient, then only one subtraction and one multiplication is needed to realize the function. The Hilbert transformer, however, require three times as much. We would therefore like to reduce the number of Hilbert transformers, which would also reduce the computation time.

This was accomplished by taking the dual of the detector of Figure 5-1, which resulted in the configuration shown in Figure 5-2. The two detectors are equivalent in performance since the multiplier inputs are still identical. This simplified configuration, however, requires only six multiplications, one addition, and five subtractions, which is about half the complexity of the original realization.

5.3 System Configuration

The detector of Figure 5-3 was realized in a system based on an LSI-11 processor, which was used basically as a convenient laboratory tool for the experimental verification of the theoretical detector. However, the principles used

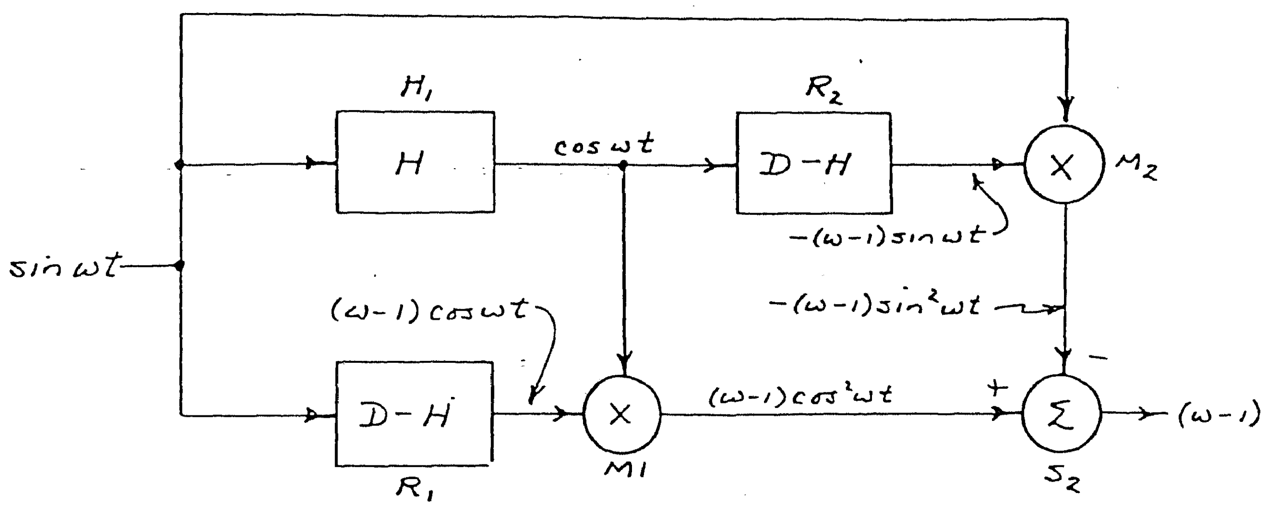

Figure 5-2. Equivalent Simplified Detector Block Diagram

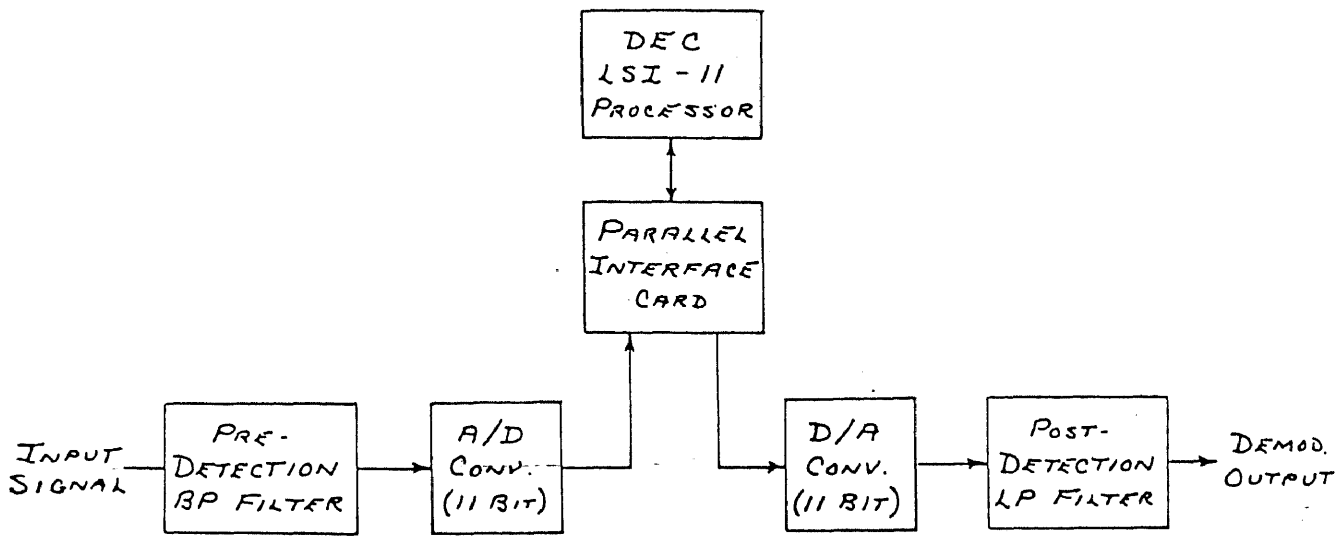

Figure 5-3. Detector System Block Diagram

here may readily be applied to other digital (or discrete-time analog) signal processing hardware being used in the industry.

As shown in Figure 5-3, sampled data to and from the processor is accomplished using a DRV-11 Parallel Interface card, which has two sixteen-bit ports, one in each direction. The input data is obtained from a 11-bit A/D converter, where one of the bits is polarity. The converter was designed to generate 1000 samples per second, with the end of conversion pulse being used to synchronize the processor. An optional BPF may be used prior to the A/D converter to remove undesired signals, or limit the noise bandwidth. A seventh order active transitional BPF, with a bandwidth of approximately 270 Hz, was used when making noise performance tests. The response of the filter is shown in Figure 5-4.

The output samples from the processor drive a 11-bit D/A converter, with one bit again being polarity. The processor outputs the previous result when it receives new input from the A/D converter. An active, 5th order Butterworth LPF using Sallen and Key sections (Ref. 1) was used to filter the output of the D/A converter. A cutoff frequency of 200 Hz was used for normal operation. The cutoff was changed to 30 Hz for noise tests.

5.4 Software Description

A flow diagram showing the algorithm for the detector in Figure 5-2 is given in Figure 5-5. Two arrays of numbers must

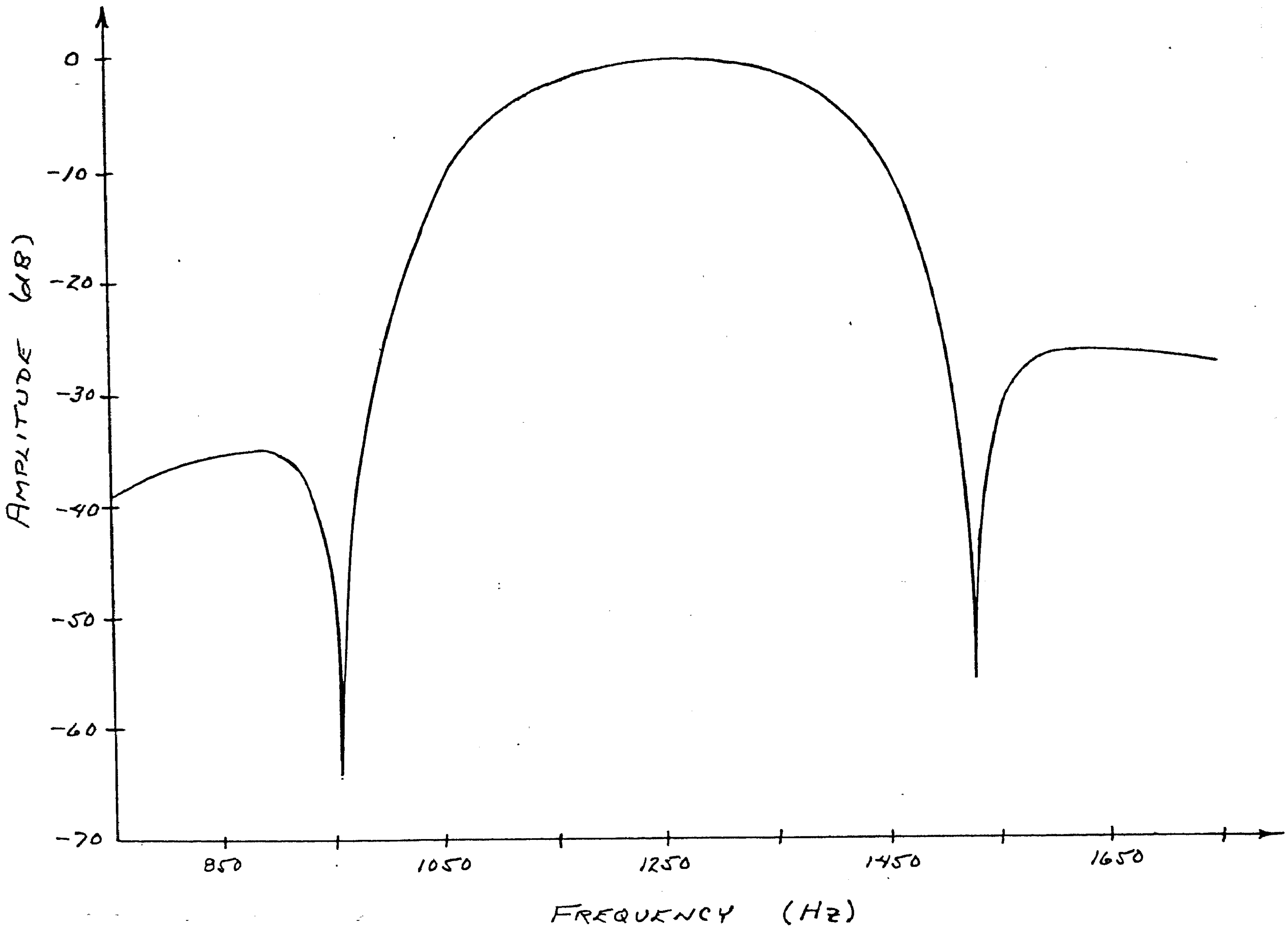

Figure 5-4. Pre-Detection BPF Frequency Response

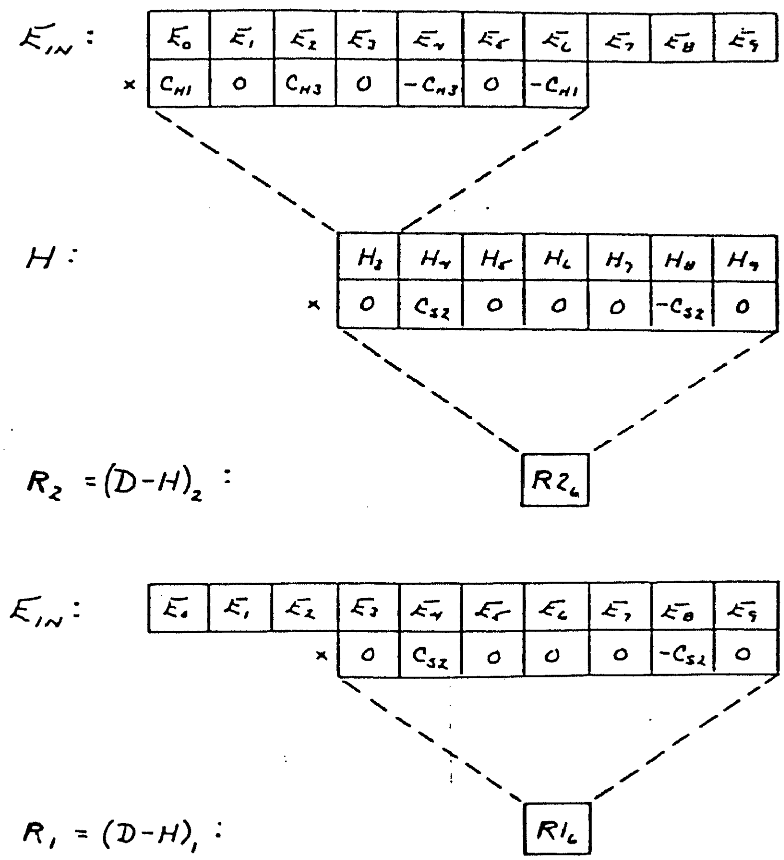

$$\text{OUTPUT} = R1_6 \cdot H_6 - R2_6 \cdot E_6$$

Figure 5-5. Detector Algorithm Flow Diagram be held in memory. One array holds ten consecutive input voltage samples, while the other contains seven outputs of the Hilbert transformer. The previous samples appear to the right.

Following the diagram, the value of H_3 is generated using

$$H_3 = (E_0 - E_6) \cdot c_{H1} + (E_2 - E_4) \cdot c_{H3} \qquad (5\text{-}2)$$

which is possible due to the symmetry of the coefficients. The output of the second D-H block, called R2, is obtained from

$$R2_6 = (H_4 - H_8) \cdot c_{S2} \qquad (5\text{-}3)$$

The delay of three sample periods for each block realization, or six for the total detector, may be seen by observing the subscripts.

In a similar manner, the output of the first D-H block is given by

$$R1_6 = (E_4 - E_8) \cdot c_{S2} \qquad (5\text{-}4)$$

and the output of the detector is found using

$$OUTPUT = R1_6 \cdot H_6 - R2_6 \cdot E_6 \qquad (5\text{-}5)$$

The values in the arrays are then shifted to the right by one, with a new sample entering at the left, and the procedure is repeated.

The above procedure has been kept general, even though the delay could have been reduced by one sampling period since the first coefficient of R2 (c_{S2}) is zero. This would allow the calculations of the D-H blocks to be shifted left one time slot, putting the output at only five delay units.

Also observe that only three different values of coefficients are required to perform the algorithm. The values of these coefficients are $c_{H1} = 0.19045$, $c_{H2} = 0.54146$ and $c_{S2} = -0.20959$.

These results were incorporated into the program RTDET.MAC, which was used to perform the algorithm in real time. The program is shown in Figure 5-6. The beginning of the program handles data I/O, which is followed by the algorithm computations. The latter portion of the program shifts the arrays in preparation for the next sample. Approximately 800 μs of computing time are required for each 1000 μs cycle.

REFERENCES - Chapter V

1. R. P. Sallen and E. L. Key, "A Practical Method of Designing RC Active Filters," IRE Trans. Circuit THeory, vol. CT-2, no. 1, March 1955.

```
        .TITLE  RTDET.MAC
LOOP:   TST     @#167770            ;TEST FOR NEW DATA
        BMI     LOOP                ;LOOP IF NONE
        MOV     @#167774,R1         ;GET NEW SAMPLE
        MOV     R0,@#167772         ;OUTPUT PREVIOUS RESULTS
        CMP     #176000,R1          ;CHECK FOR -0 INPUT
        BNE     NEXT
        CLR     R1
NEXT:   MUL     #40,R1              ;SHIFT DATA 5 BITS
        MOV     R1,ESIG             ;STORE SAMPLE
        SUB     ESIG+14,R1          ;CALC HTMP
        MOV     R1,R0
        MUL     #14141,R0           ;HTMP IN R0
        MOV     ESIG+4,R2           ;CALC HSIG(1)
        SUB     ESIG+10,R2
        MUL     #42517,R2
        ADD     R2,R0
        MOV     R0,HSIG             ;STORE RESULTS
        MOV     ESIG+10,R0          ;CALC S1SIGP*HSIG(4)
        SUB     ESIG+20,R0
        MUL     HSIG+6,R0           ;RESULT IN R0
        MOV     HSIG+2,R2           ;CALC S2SIGP*ESIG(7)
        SUB     HSIG+12,R2
        MUL     ESIG+14,R2          ;RESULT IN R2
        SUB     R2,R0               ;CALC OUTPUT
        MUL     #162455,R0          ;OUTPUT IN R0
        MOV     #10,R3              ;SHIFT ESIG DATA
        MOV     #ESIG+20,R4
        MOV     #ESIG+22,R5
LOOP1:  MOV     -(R4),-(R5)
        DEC     R3
        BGT     LOOP1
        MOV     #5,R3               ;SHIFT HSIG DATA
        MOV     #HSIG+12,R4
        MOV     #HSIG+14,R5
LOOP2:  MOV     -(R4),-(R5)
        DEC     R3
        BGT     LOOP2
        JMP     LOOP
ESIG:   .BLKW   9.                  ;ESIG(9) ARRAY
HSIG:   .BLKW   6.                  ;HSIG(6) ARRAY
        .END    1000
```

Figure 5-6. Real-Time Algorithm Computations

CHAPTER VI

ACTUAL PERFORMANCE

6.1 Introduction

The response of the detector was first measured under steady-state conditions, the results of which are shown in Figure 6-1. Compared with the theoretical response shown in Figure 4-5, the two curves are found to be almost identical. There were no noticeable carrier components on the dc output of the detector.

As predicted by the foldover theory of sampled systems, a mirror image of the detector output was found to result for frequencies immediately above the Nyquist frequency (500 to 1000 Hz), where the Nyquist frequency (or aliasing frequency) is one-half the sampling frequency (Ref. 1). At the sampling frequency of 1000 Hz, the detector repeated its baseband response. Actually the baseband response is duplicated starting at multiples of the sampling frequency, while an inverted baseband response occurs just below each of these frequencies. Therefore, as shown in Figure 6-2, a frequency translation may also be incorporated into the detector as long as the A/D converter has a good sample-and-hold circuit. Recall that the sampling frequency is based on the modulation information and not the carrier.

The performance of the detector using a modulated input was next observed under both narrow- and wide-band conditions.

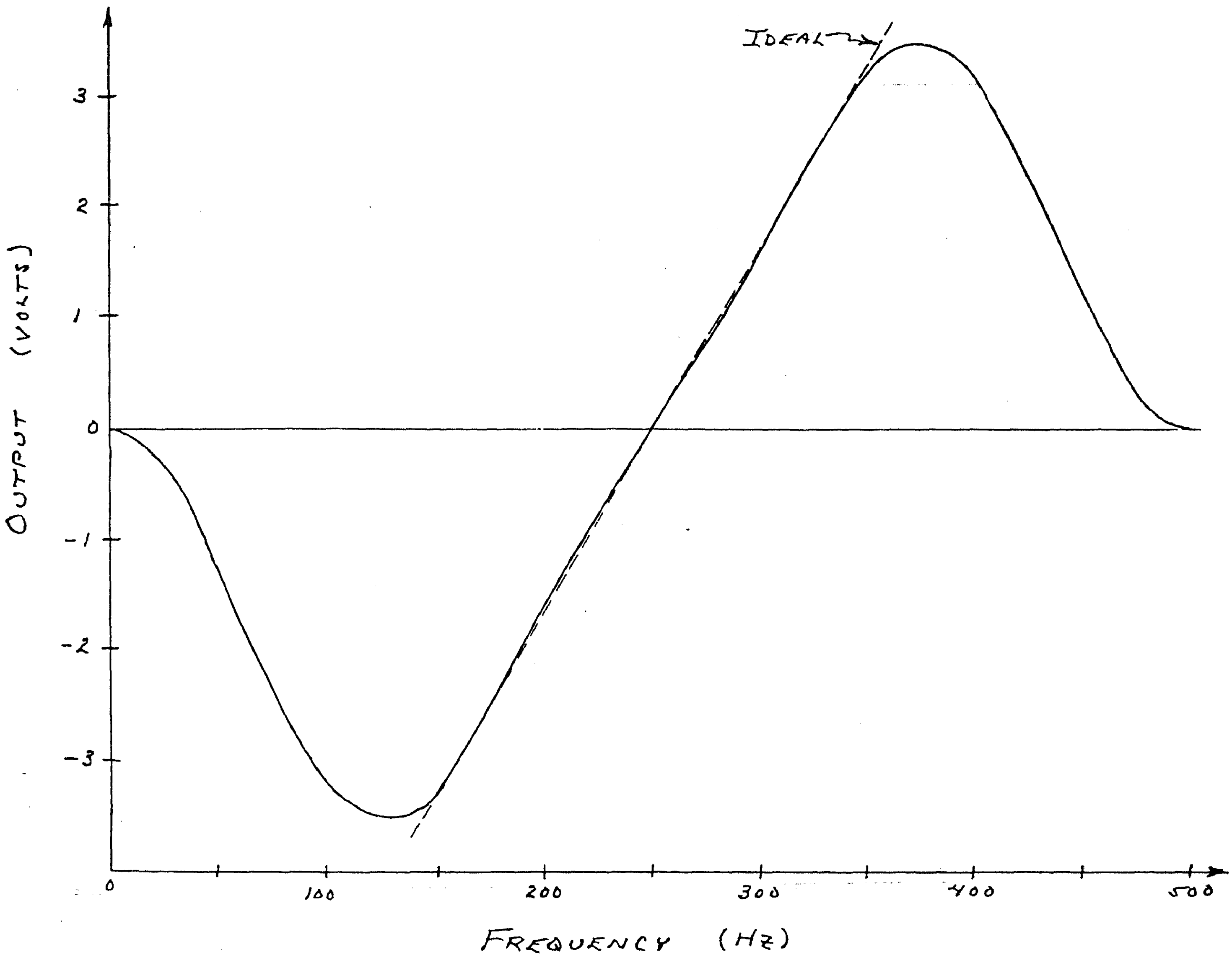

Figure 6-1. Actual Detector Response

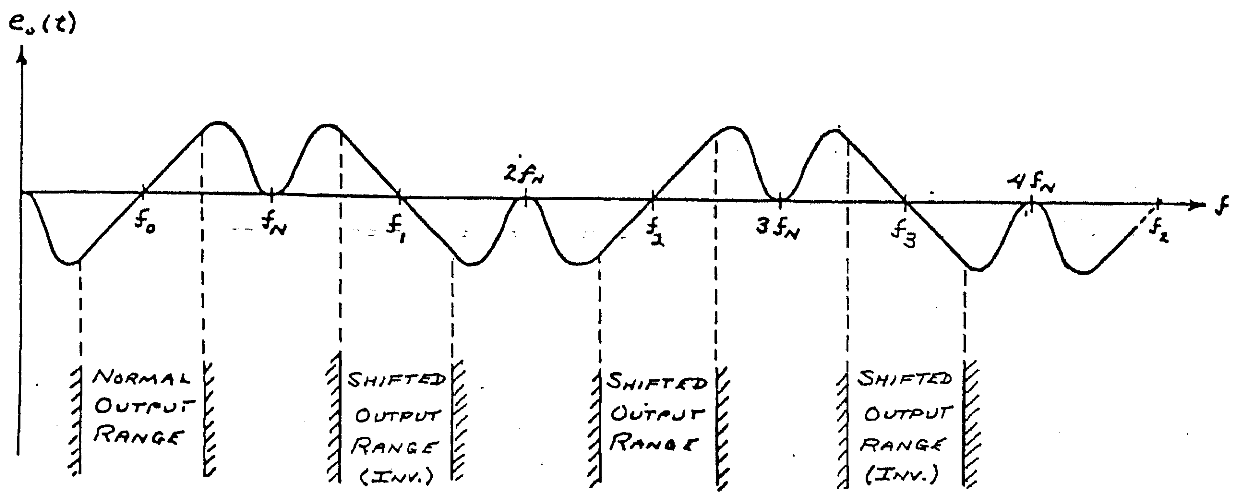

NOTE:

1. f_N = NYQUIST FREQUENCY
2. $f_s = 2 f_N$ = SAMPLING FREQUENCY

Figure 6-2. Multi-Band Detector Response

This was then followed by an evaluation of the detector under sinusoidal and noise interference conditions.

6.2 Narrow-Band Performance

The signal source was derived from a voltage controlled oscillator, which was modulated by a 50 Hz square wave output of a waveform generator. A 270 Hz bandwidth pre-detection bandpass filter was used in series with the signal source to remove higher frequency sidebands of the original wide-band signal. The source was adjusted for a center frequency of 1250 Hz (the first shifted band of the detector) and a peak shift of 50 Hz. A 200 Hz post-discriminator lowpass filter was used to remove frequencies above the Nyquist frequency (500 Hz).

Figure 6-3a presents the waveform at the input to the detector. The received carrier is square wave modulated but the narrow-band filter before the detector eliminated all sidebands beyond the first, reducing the modulation to that of a sine-wave and introducing amplitude variations on the carrier. The output of the detector prior to the filter is shown in Figure 6-3b, and after filtering in Figure 6-3c. Observe that since the algorithm completely balances out all carrier components, no ripple components appear at the detector output.

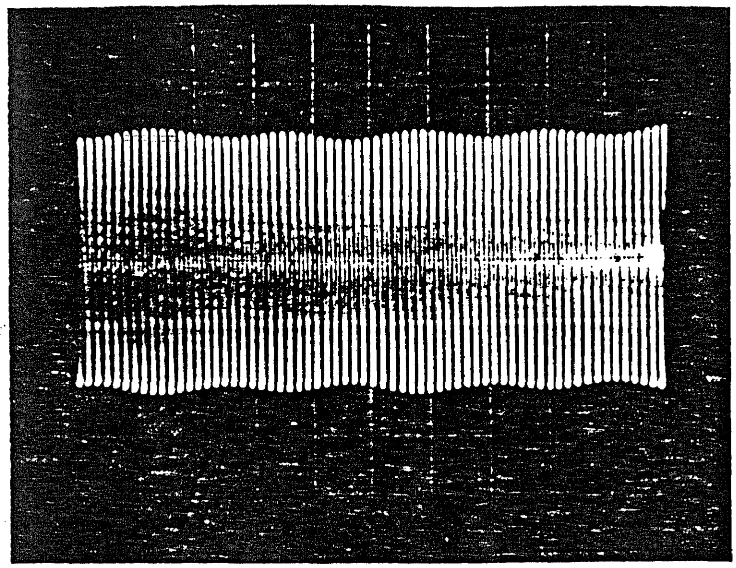

a) Modulated input signal
(vert: 200 mV/cm, horiz: 5 ms/cm)

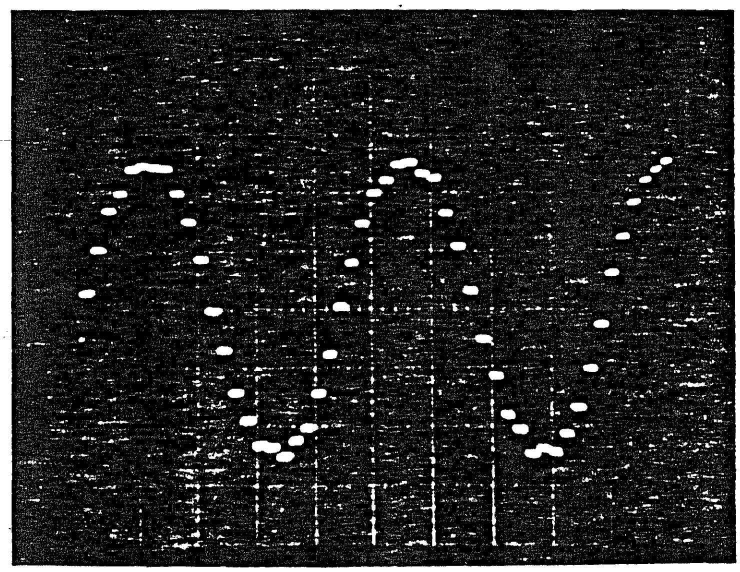

b) Detector output before filtering
(vert: 50 mV/cm, horiz: 5 ms/cm)

Figure 6-3. Narrow-Band Performance

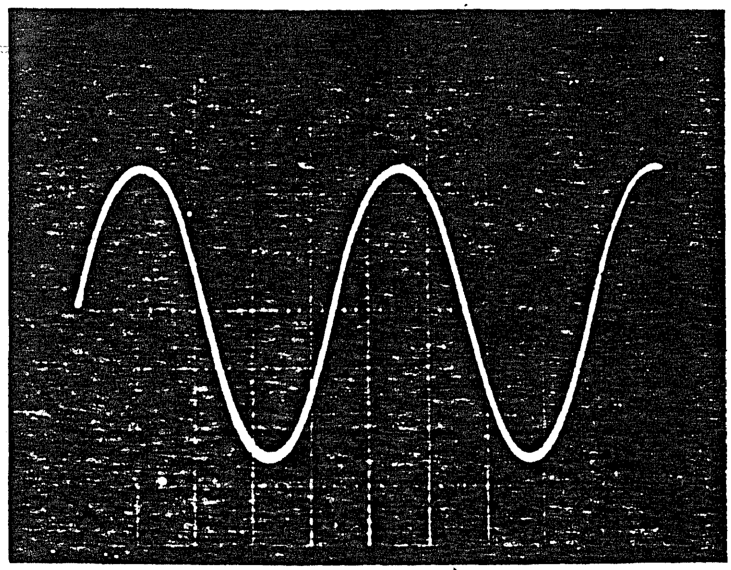

c) Detector output after filtering
(vert: 50 mV/cm, horiz: 5 ms/cm)

Figure 6-3. Narrow-Band Performance (contd)

6.3 Wide-Band Performance

In order to demonstrate the wide-band performance of the detector, the bandpass filter was removed from the test configuration. The output of the detector was then compared with the modulating signal, using four different modulating waveforms, as shown in Figure 6-4. The modulation frequency was 20 Hz for all waveforms.

Figure 6-4a compares the two waveforms for sine-wave modulation, with the outputs of the detector being the lower waveforms. The performance is essentially identical to that of the narrow-band case. By comparing the phases of the waveforms, a total delay of approximately 10.5 ms is observed. This consists of one sampling period (1 ms) delay for the A/D conversion, a six sampling period (6 ms) delay for the FIR realization, and approximately a 3.5 ms delay for the 200 Hz Butterworth lowpass filter. Figure 6-4b presents the performance using triangular modulation and is again found to be relatively ideal. However, the output of the detector when receiving a sawtooth modulating waveform shows some ringing and sloped transitions, as shown in Figure 6-4c. The ringing occurs only when there is a rapid frequency change in the input signal to the detector. A similar situation occurs when receiving a square wave modulated carrier, as shown in Figure 6-4d. The rounding of the waveforms is due to the equivalent internal bandwidth of the detector, as shown in Figure 4-6. The resulting sloped transitions of approximately 4 ms in

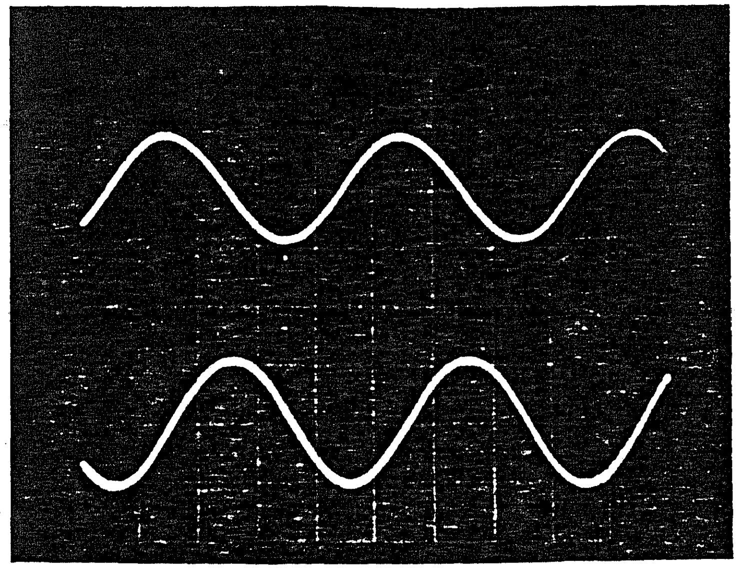

a) Sine wave modulation
(vert: 200 mV/cm, horiz: 10 ms/cm)

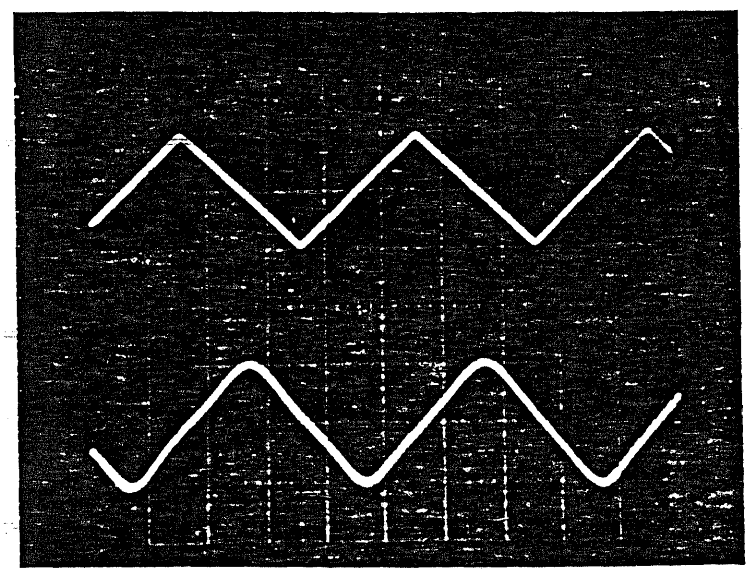

b) Triangular modulation
(vert: 200 mv/cm, horiz: 10 ms/cm)

Figure 6-4. Wide-Band Performance

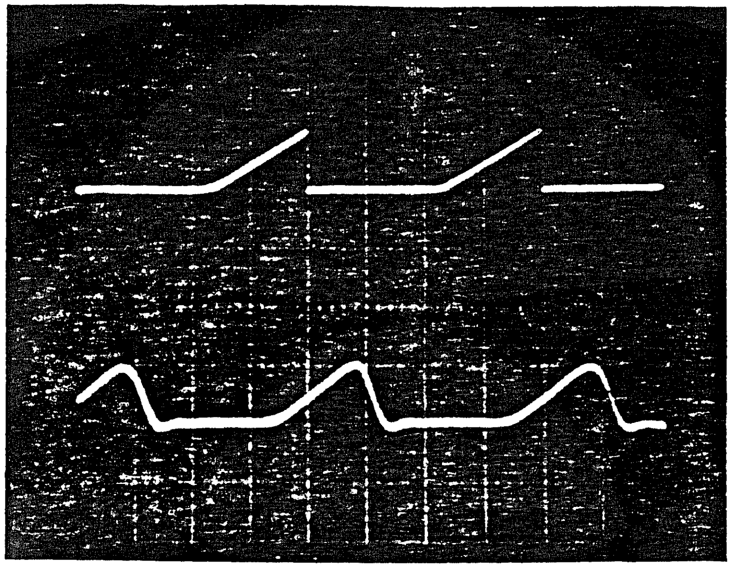

c) Saw-tooth modulation
(vert: 200 mV/cm, horiz: 10 ms/cm)

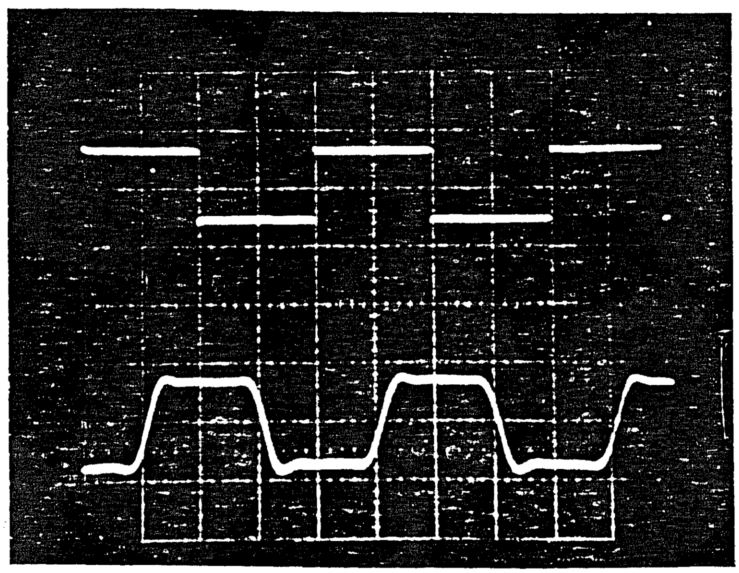

d) Square wave modulation
(vert:200 mV/cm, horiz: 10 ms/cm)

Figure 6-4. Wide-Band Performance (contd)

Figure 6-4d are equivalent to those predicted by computer simulation (see Appendix VI - Example), which shows four sampling periods (4 ms at a 1000 Hz sampling frequency) for a transition under steady state conditions. The post-discriminator filter has almost twice the bandwidth, and therefore only smoothens the output of the D/A converter without disturbing the waveform.

6.4 Sine-Wave Interference

Using the same test configuration as for the wide-band performance, an unmodulated carrier at 1250 Hz and another sine-wave of variable amplitude and frequency were used for the input to the detector. The waveform shown in Figure 6-5 is the output of the detector when the two carriers are equal in amplitude and the undesired signal is 50 Hz higher. As predicted by Equation 3-5, only a dc term and a beat frequency sine-wave appear at the output of the detector. Results for various other conditions of the interfering tone were obtained using an rms voltmeter, and are shown in Figure 6-6. Comparing these results with the theoretical results in Figure 3-1, the two are found to be almost identical.

6.5 Noise Performance

The SNR-CNR relationship was obtained by measuring the rms noise power in the absence of modulation and the signal power in the absence of noise, and then computing the resulting ratio. As with the analytical derivation, the

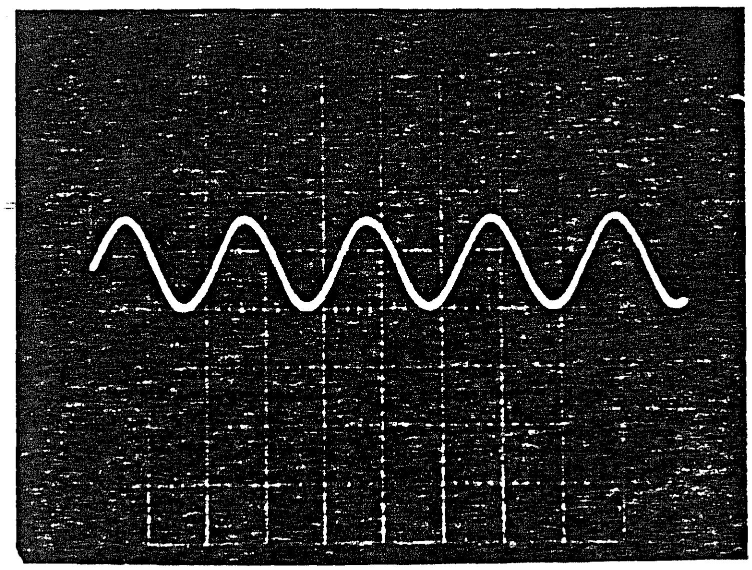

Figure 6-5. Sine Wave Interference
(vert: 50 mV/cm, horiz: 10 ms/cm)

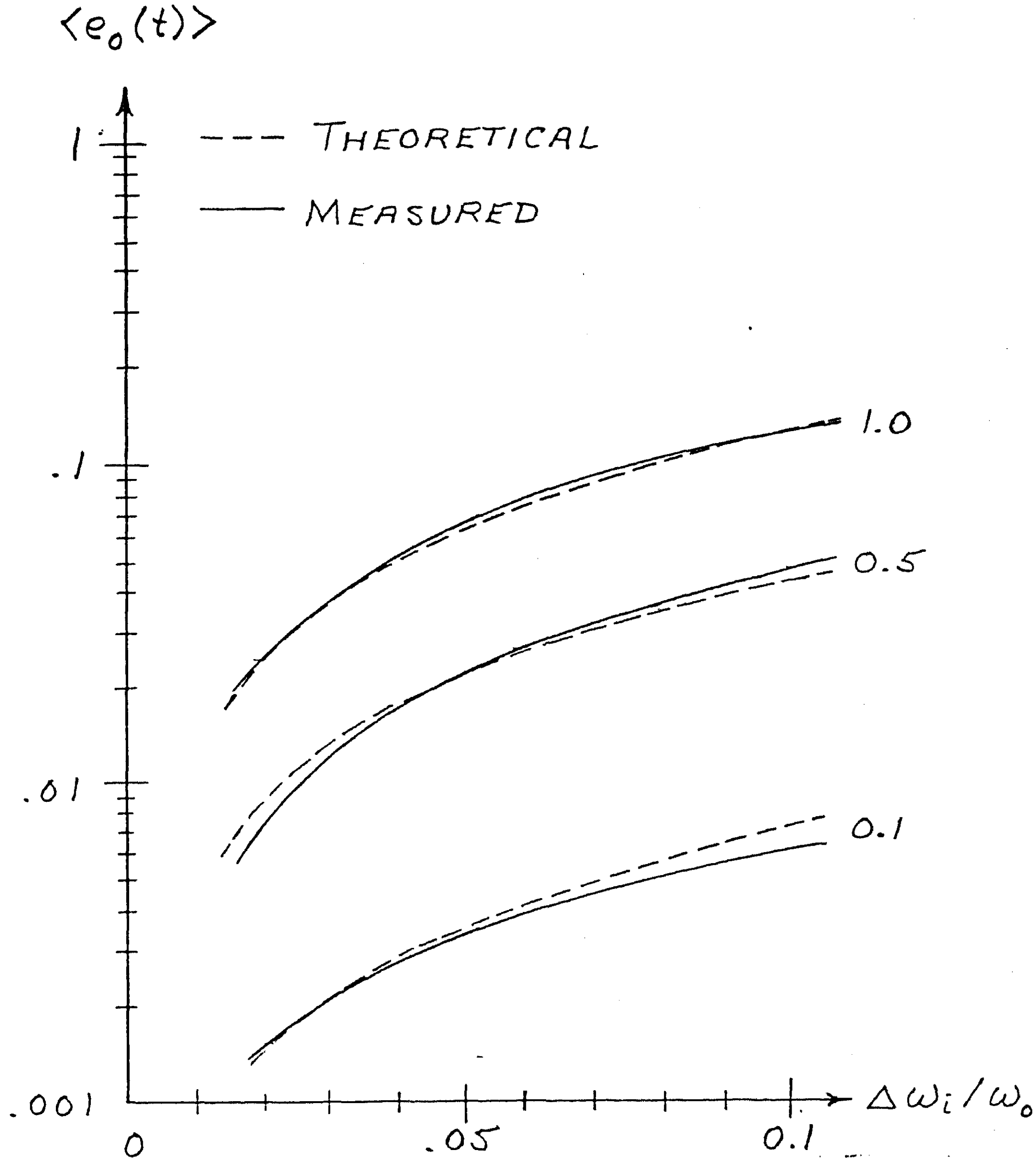

Figure 6-6. Actual $\langle e_0(t)\rangle$ vs. $\Delta\omega_i/\omega_0$ for Various B/A

effect of modulation on threshold is ignored.

Following this technique, an rms power meter was used to measure the noise output at different values of CNR (with no modulation). A reference signal output, from which the SNR calculations are made, is then obtained by removing the noise and adding tone modulation to the carrier at some specified deviation.

The measured SNR verses CNR characteristic for the detector is shown in Figure 6-7. Recall that the term $(CNR)_{AM}$ is the carrier to noise power ratio with the noise measured in a filter bandwidth of twice the base bandwidth, or

$$(CNR)_{AM} = (CNR)\ (B/2\omega_b) \tag{6-1}$$

The results show that the threshold occurs at $(CNR)_{AM} = 24.6$ dB. The SNR inprovement above threshold is 9.0 dB.

For reference, the theoretical performance of the detector, as given by Equation 3-15 is also shown in Figure 6-7. In these calculations, the following experimental parameters were used: $B = 2\pi(266)$, $\omega_b = 2\pi(28.5)$, and $\omega_a = 2\pi(50)$.

A limiter was then added between the output of the pre-detection filter and the input to the detector. The limiter also included a lowpass filter to remove the harmonics generated in the limiting process. The same procedure was then performed, with the results also shown in Figure 6-7.

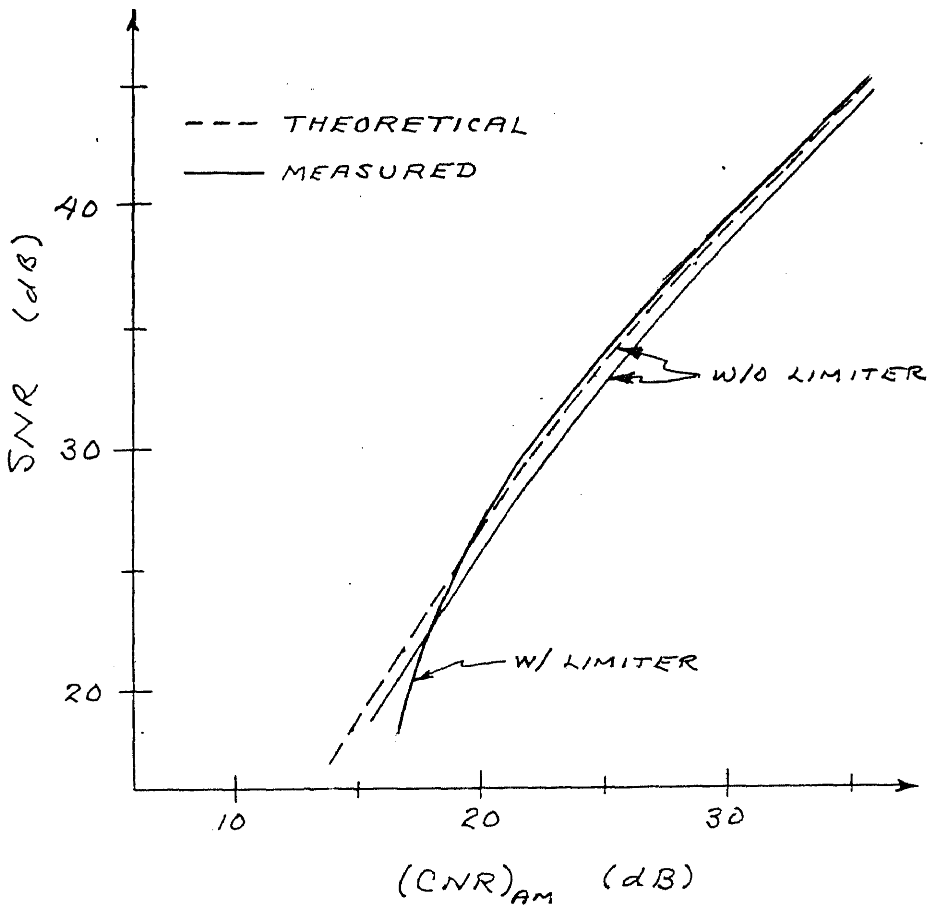

Figure 6-7. Experimental Noise Performance of the Detector

Observe that this curve has a much sharper break at threshold, which was found to occur at $(CNR)_{AM}$ = 22.0 dB. The SNR improvement above threshold is 9.5 dB. Therefore, the addition of a limiter improves threshold performancy by 2.6 dB. The linear improvement region is not sufficiently changed, with the difference being due to experimental error.

REFERENCES - Chapter VI

1. S. D. Stearns, Digital Signal Analysis, Chap. 4, Hayden, 1975.

CHAPTER VII

CONCLUSIONS

7.1 Conclusions

We have described a new extremely linear version of a family of detectors having a wide bandwidth, excellent sensitivity, and theoretically low delay. The low-delay feature is obtained in a two-fold manner: 1) through the use of networks having zero group delay, and 2) through an RF cancellation technique for the carrier. The detector exhibits excellent linearity due to its inherent structure.

The theoretical performance of the detector was analyzed for modulated input signals, unmodulated interference carriers, and narrow-band noise conditions. Theoretically, the detector has no distortion, due to the perfect linearity. For interference signal levels approaching the desired signal level, the new detector was shown to offer a considerable improvement over the limiter-discriminator. Noise performance was shown to be equal to the limiter-discriminator well above threshold, but had a higher threshold. These results were also compared with those of other forms of the detector, showing improved performance in the areas of linearity and noise threshold.

The detector of Figure 2-1 was realized using FIR digital signal processing methods, and was then optimized for linearity, resulting in substantial improvement. The digital implementation of the detector was found to exhibit a useful inherent bandpass filter characteristic with delay properties comparable to the algorithm processing delay. After several algorithm simplifications that resulted in a 35% reduction of total computing time, the detector of Figure 5-2 was implemented using laboratory digital processing hardware and used to detect a modulated carrier above the Nyquist frequency, demonstrating the bandpass characteristics resulting from frequency foldback in sampled systems. Experimental results were shown. Total system delays were associated mainly to filtering functions, and were found to be comparable with those of conventional FM detection methods.

7.2 Suggestions for Future Efforts

It is worthwhile to mention areas where future work should be performed. Several of these are given below:

(1) An investigation into the properties of the coefficients for other orders, center frequencies, and bandwidths of the detector.

(2) A general, efficient computer program to obtain the optimized coefficients of the detector using other techniques, such as a Chebychev approximation (Ref. 1), instead of a least squares approximation.

(3) Incorporation of the bandpass and lowpass filters into the same digital hardware, using a higher sampling rate for the filter functions and the frequency foldover property for the detector

portion.

(4) Detection of a series of equally spaced FM channels using the same lowpass equivalent detector algorithm and the frequency foldover characteristics, including time sharing of common hardware.

REFERENCES - Chapter VII

1. T. W. Parks and J. H. McClellan, "Chebyshev Approximation for Nonrecursive Digital Filters with Linear Phase," IEEE Trans. Circuit Theory, Vol. CT-19, No. 2, March 1972.

APPENDIX I

DETECTOR OUTPUT FOR NARROW-BAND FM WAVE

This Appendix derives the expression of the output of the detector shown in Figure 2-1 when the input is a narrow-band FM wave, comprised of a component at the center frequency and one pair of sidebands. At the same time, we present the voltage expressions at the various points of the circuit.

Reference is made to Figure 2-1. Without loss of generality, we let the gains of the summers, multipliers, and Hilbert transformers be unity and the gain of the differentiator be D. The input signal, being a small modulation index tone-modulated FM wave, is given by E1 as

$$E1 = e_i(t) = A \cos \omega t - (Ak/2) \cos (\omega_o - \omega_m)t + (Ak/2) \cos(\omega_o + \omega_m)t \qquad (A1\text{-}1)$$

where k is the modulation index. We further assume that the various blocks do not cause phase inversions. Then the output of differentiator D1 is given by

$$E2 = -AD \{ \sin \omega_o t - (k/2)[(\omega_o - \omega_m)/\omega_o] \sin(\omega_o - \omega_m)t + (k/2)[(\omega_o + \omega_m)/\omega_o] \sin (\omega_o + \omega_m)t \} \qquad (A1\text{-}2)$$

Proceeding further, we have the output of the Hilbert transformer H1 as

$$E3 = -[A \sin \omega_o t - (Ak/2) \sin (\omega_o - \omega_m)t + (Ak/2) \sin (\omega_o + \omega_m)t] \qquad (A1\text{-}3)$$

while the output of the summer S1 is

$$
\begin{aligned}
E4 &= E2 - E3 \\
&= - A \{ (1 - D\omega_0) \sin \omega_0 t \\
&\quad + (k/2)[D\omega_0(1 - \omega_m/\omega_0) - 1] \sin (\omega_0 - \omega_m)t \\
&\quad -(k/2)[D\omega_0(1 + \omega_m/\omega_0) - 1] \sin (\omega_0 + \omega_m)t \}
\end{aligned}
\qquad \text{(A1-4)}
$$

For carrier balance at center frequency ω_0, we require that

$$D\omega_0 = 1 \qquad \text{(A1-5)}$$

Due to Equation A1-5, the first term of Equation A1-4 vanishes and partial cancellation occurs in the other two terms. We may then rewrite Equation A1-4 as

$$E4 = -(AkR/2) [\sin (\omega_0 - \omega_m)t + \sin (\omega_0 + \omega_m)t] \qquad \text{(A1-6)}$$

where $R = \omega_m/\omega_0$.

Now, the output of the multiplier M1 is

$$
\begin{aligned}
E5 &= E3 \cdot E4 \\
&= BR \{ 2 \cos \omega_m t - \cos (2\omega_0 - \omega_m)t - \cos (2\omega_0 + \omega_m)t \\
&\quad + (k/2) [\cos (2\omega_0 - 2\omega_m)t - \cos (2\omega_0 + 2\omega_m)t] \}
\end{aligned}
\qquad \text{(A1-7)}
$$

where $B = A^2k/4$.

Equation A1-7 is obtained by collating terms of the same frequency after using appropriate trigonometric identities. Note that E5 is the output of the discriminator portion.

In a similar manner, we find the expressions for the RF cancellation circuit. The output of Hilbert transformer H2 is

$$E6 = -(AkR/2)\ [\ \cos\ (\omega_o - \omega_m)t + \cos\ (\omega_o + \omega_m)t\ ] \qquad \text{(A1-8)}$$

while the output of multiplier M2 is

$$\begin{aligned} E7 &= E6 \cdot E1 \\ &= -BR\ \{\ 2\ \cos\omega_m t + \cos\ (2\omega_o - \omega_m)t + \cos\ (2\omega_o + \omega_m)t \\ &\quad -(k/2)\ [\ \cos\ (2\omega_o - 2\omega_m)t - \cos\ (2\omega_o + 2\omega_m)t\ ]\ \} \end{aligned} \qquad \text{(A1-9)}$$

Finally, the output of the detector is E8 = E5 - E7:

$$E8 = e_o(t) = 2BR\ \cos\omega_m t \qquad \text{(A1-10)}$$

which is equivalent to Equation 3-2.

APPENDIX II

BASEBAND OUTPUT FOR SINE WAVE INTERFERENCE

This Appendix derives the expressions for the detector output when the input consists of a desired and an interfering carrier, with the modulation of both the desired and the interfering carriers limited to dc (frequency offset).

Proceeding as in Appendix I, and referring again to Figure 2-1, we have a desired carrier at frequency ω_d and an interfering carrier at frequency ω_i. The input to the detector is

$$E1 = A \cos \omega_d t + B \cos \omega_i t \qquad \text{(A2-1)}$$

where A and B are the amplitudes of the desired and interfering carriers, respectively. Let $\omega_d = \omega_o + \Delta\omega_d$ and $\omega_i = \omega_o + \Delta\omega_i$ where $\Delta\omega_d$ and $\Delta\omega_i$ are the deviations of the desired and interfering carriers, respectively, from the center frequency of the detector. After differentiation

$$E2 = - D [A (\omega_o + \Delta\omega_d) \sin \omega_d t + B (\omega_o + \Delta\omega_i) \sin \omega_i t] \qquad \text{(A2-2)}$$

The output of Hilbert transformer H1 is

$$E3 = - [A \sin \omega_d t + B \sin \omega_i t] \qquad \text{(A2-3)}$$

After summing and using the center frequency balance condition Equation A1-5, we get

$$E4 = E2 - E3 = - [A \frac{\Delta\omega_d}{\omega_o} \sin \omega_d t + B \frac{\Delta\omega_i}{\omega_o} \sin \omega_i t] \qquad \text{(A2-4)}$$

At the output of the discriminator portion (output of M1), we have

$$E5 = 1/2 \{ (A^2 \frac{\Delta\omega_d}{\omega_o} + B^2 \frac{\Delta\omega_i}{\omega_o})$$
$$- A^2 \frac{\Delta\omega_d}{\omega_o} \cos(2\omega_d t) - B^2 \frac{\Delta\omega_i}{\omega_o} \cos(2\omega_i t)$$
$$+ AB (\frac{\Delta\omega_d}{\omega_o} + \frac{\Delta\omega_i}{\omega_o}) [\cos(\omega_d - \omega_i)t - \cos(\omega_d + \omega_i)t] \} \tag{A2-5}$$

Finding the expressions for the RF cancellation circuit, the output of Hilbert transformer H2 is given by

$$E6 = - [A \frac{\Delta\omega_d}{\omega_o} \cos \omega_d t + B \frac{\Delta\omega_i}{\omega_o} \cos \omega_i t] \tag{A2-6}$$

while the output of M2 is

$$E7 = E6 \cdot E1$$
$$= -1/2 \{ (A^2 \frac{\Delta\omega_d}{\omega_o} + B^2 \frac{\Delta\omega_i}{\omega_o})$$
$$+ A^2 \frac{\Delta\omega_d}{\omega_o} \cos 2\omega_d t + B^2 \frac{\Delta\omega_i}{\omega_o} \cos 2\omega_i t$$
$$+ AB(\frac{\Delta\omega_d}{\omega_o} + \frac{\Delta\omega_i}{\omega_o}) [\cos(\omega_d + \omega_i)t + \cos(\omega_d - \omega_i)t] \} \tag{A2-7}$$

Finally, the output of the detector is given by

$$E8 = E5 - E7$$
$$= A^2 \frac{\Delta\omega_d}{\omega_o} + B^2 \frac{\Delta\omega_i}{\omega_o} + AB(\frac{\Delta\omega_d}{\omega_o} + \frac{\Delta\omega_i}{\omega_o}) \cos(\omega_d - \omega_i)t \tag{A2-8}$$

which is the same as Equation 3-4.

APPENDIX III

DERIVATION OF CNR - SNR RELATIONSHIP

This Appendix computes the performance of the detector in the presence of noise. The SNR is derived by finding the ratio of the detector output signal power for a sinusoidal modulated input wave and the detector output power spectral density (PSD) for an unmodulated carrier with added narrow-band noise. This result is then compared with the CNR at the input of the detector.

Proceeding as in Appendix I, and again referring to Figure 2-1, we first derive the detector output for an unmodulated carrier with added narrow-band noise as represented by Figure 3-2. The input to the detector is then given by

$$E_1 = A \sin \omega_0 t + x(t) \cos \omega_0 t - y(t) \sin \omega_0 t \qquad \text{(A3-1)}$$

After differentiating, and using the center frequency balance condition Equation A1-5, we get

$$E_2 = [A + \frac{1}{\omega_0}\dot{x}(t) - y(t)] \cos \omega_0 t - [x(t) + \frac{1}{\omega_0}\dot{y}(t)] \sin \omega_0 t \qquad \text{(A3-2)}$$

The output of Hilbert transformer H_1 is

$$E_3 = A \cos \omega_0 t - x(t) \sin \omega_0 t - y(t) \cos \omega_0 t \qquad \text{(A3-3)}$$

The summer output is then

$$E_4 = \frac{1}{\omega_0}[\dot{x}(t) \cos \omega_0 t - \dot{y}(t) \sin \omega_0 t] \tag{A3-4}$$

At the output of the discriminator portion (output of M_1), we have

$$\begin{aligned} E_5 = \frac{1}{\omega_0}\{&\dot{x}(t)[A - y(t)] \cos^2 \omega_0 t + x(t)\, \dot{y}(t) \sin^2 \omega_0 t \\ &- [A\, \dot{y}(t) + x(t)\, \dot{y}(t) - y(t)\, \dot{y}(t)] \sin \omega_0 t \cos \omega_0 t\} \end{aligned} \tag{A3-5}$$

Finding the expressions for the RF cancellation portion, the output of H_2 is given by

$$E_6 = -\frac{1}{\omega_0}[\dot{x}(t) \sin \omega_0 t + \dot{y}(t) \cos \omega_0 t] \tag{A3-6}$$

while the output of M_2 is

$$\begin{aligned} E_7 = -\frac{1}{\omega_0}\{&\dot{x}(t)[A - y(t)] \sin^2 \omega_0 t + x(t)\, \dot{y}(t) \cos^2 \omega_0 t \\ &+ [A\, \dot{y}(t) + x(t)\, \dot{x}(t) - y(t)\, \dot{y}(t)] \sin \omega_0 t \cos \omega_0 t\} \end{aligned} \tag{A3-7}$$

Finally, the output of the detector is

$$Z(t) = E_8 = \frac{1}{\omega_0}[A\, \dot{x}(t) - \dot{x}(t)\, y(t) + x(t)\, \dot{y}(t)] \tag{A3-8}$$

To determine the PSD of Z(t) we must first find $R_{zz}(\tau)$, which is the autocorrelation function of Z(t) and is defined as

$$R_{zz}(\tau) = E\{ Z(t)\, Z(t + \tau)\} \tag{A3-9}$$

Let $C = A/\omega_0$ and $D = -1/\omega_0$, then

$$Z(t) = C\, \dot{x}(t) + D\, \dot{x}(t)\, y(t) - D\, x(t)\, \dot{y}(t) \tag{A3-10}$$

Substituting into Equation A3-9 and solving by making use of the expected value identities

$$E\,[x(t)\;x(t+\tau)] = E\,[y(t)\;y(t+\tau)] \qquad \text{(A3-11)}$$

and

$$E\,[x(t)\;y(t+\tau)] = -\,E\,[x(t+\tau)\;y(t)] \qquad \text{(A3-12)}$$

we obtain

$$R_{zz}(\tau) = \frac{A^2}{\omega_o^2} R_{\dot{x}\dot{x}}(\tau) + \frac{2}{\omega_o^2} R_{yy}(\tau)\; R_{\dot{x}\dot{x}}(\tau) \qquad \text{(A3-13)}$$

after returning to the original equivalents for C and D.

The Fourier Transform of $R_{zz}(\tau)$ will produce the output power spectral density $S_{zz}(\tau)$ in watts/Hz. Therefore,

$$S_{zz}(\tau) = \frac{A^2}{\omega_o^2}\,\omega^2 S(\omega) + \frac{2}{\omega_o^2}\,\mathcal{F}\,[R_{yy}(\tau)\; R_{\dot{x}\dot{x}}(\tau)] \qquad \text{(A3-14)}$$

where the noise spectral density $S(\omega)$ is given in Figure 3-3. The second term of Equation A3-14 may be reduced by using the convolution of S_{yy} and $S_{\dot{x}\dot{x}}$, where $S_{yy} = S(\omega)$ and $S_{\dot{x}\dot{x}} = \omega^2\,S(\omega)$ over the same bandwidth $(-B/2 \leqslant \omega \leqslant B/2)$, or

$$\mathcal{F}[R_{yy}(\tau)\; R_{\dot{x}\dot{x}}(\tau)] = \frac{1}{2\pi}\,[S_{yy} * S_{\dot{x}\dot{x}}] \qquad \text{(A3-15)}$$

Op.BLANK 1 Substituting the functions, this becomes

$$\mathcal{F}\,[R_{yy}(\tau)\; R_{\dot{x}\dot{x}}(\tau)] = \frac{1}{2\pi}\int_{-\frac{B}{2}}^{t+\frac{B}{2}} \eta\,(\eta\,\omega^2)\,d\omega \qquad -B<t<0 \qquad \text{(A3-16)}$$

which after solving and changing back to the original variables, results in the expression

$$\mathcal{F}[R_{yy}(\tau)\ R_{\dot{x}\dot{x}}(\tau)] = \begin{cases} \frac{\eta^2}{6\pi}\ [(\omega + B/2)^3 + (B/2)^3] & -B\leqslant\omega<0 \\ \frac{\eta^2}{6\pi}\ [(-\omega + B/2)^3 + (B/2)^3] & 0\leqslant\omega\leqslant B \end{cases} \tag{A3-17}$$

Therefore,

$$S_{zz}(\omega) = \frac{A^2}{\omega_0^2}\,\omega^2 S(\omega) + \frac{\eta^2}{3\pi\omega_0^2} - \begin{bmatrix} (\omega + B/2)^3 + (B/2)^3 & -B\leqslant\omega<0 \\ (-\omega + B/2)^3 + (B/2)^3 & 0\leqslant\omega\leqslant B \end{bmatrix} \tag{A3-18}$$

Finally, the total noise power at the detector output is equal to the integral of $(1/2\pi)\ S_{zz}(\omega)$ over the post detection filter bandwidth, or

$$\text{Noise Power} = \frac{1}{2\pi}\int_{-\omega_b}^{\omega_b} S_{zz}(\omega)d\omega \qquad \omega_b<B/2 \tag{A3-19}$$

which is equivalent to

$$\text{Noise Power} = \frac{1}{2\pi}\left[\ \frac{A^2}{\omega_0^2}\int_{-\omega_b}^{\omega_b}\omega^2 S(\omega)d\omega \right.$$
$$\left. + \frac{2\eta^2}{3\pi\omega_0^2}\int_{-\omega_b}^{0}[(\omega + B/2)^3 + (B/2)^3]d\omega \right] \tag{A3-20}$$

The $1/2\pi$ factor is necessary when integrating over ω (radians/sec) since the units of $S_{zz}(\omega)$ are watts/Hz. Solving, the total noise power at the detector output is given by

$$\text{Noise Power} = \frac{A^2\eta\omega_b^3}{3\pi\omega_0^2}$$
$$+ \frac{\eta^2}{\pi^2\omega_0^2}\left[\ \frac{B^3\omega_b}{12} - \frac{B^2\omega_b^2}{8} + \frac{B\omega_b^3}{6} - \frac{\omega_b^4}{12}\right] \tag{A3-21}$$

The signal output power of the detector is obtained in a similar manner. Assume a modulated input signal given by

$$E_1 = A \cos(\omega_0 t + \beta \sin \omega_m t) \tag{A3-22}$$

where A is the carrier amplitude, β is the modulation index and ω_m is the frequency of the cosinusoidal modulating signal. Again referring to Figure 2-1, the output of D_1 is

$$\begin{aligned} E_2 = &-A \sin(\omega_0 t + \beta \sin \omega_m t) \\ &-A\beta \frac{\omega_m}{\omega_0} \cos \omega_m t \sin(\omega_0 t + \beta \sin \omega_m t) \end{aligned} \tag{A3-23}$$

while the output of H_1 is

$$E_3 = -A \sin(\omega_0 t + \beta \sin \omega_m t) \tag{A3-24}$$

After summing,

$$E_4 = -A\beta\left(\frac{\omega_m}{\omega_0}\right) \cos \omega_m t \sin(\omega_0 t + \beta \sin \omega_m t) \tag{A3-25}$$

The output of the discriminator portion (output of M_1) is then given by

$$E_5 = A\beta^2 \frac{\omega_m}{\omega_0} \cos \omega_m t \sin(\omega_0 t + \beta \sin \omega_m t) \tag{A3-26}$$

Obtaining the expressions for the cancellation section, the output of H_2 is

$$E_6 = -A\beta \frac{\omega_m}{\omega_0} \cos \omega_m t \cos(\omega_0 t + \beta \sin \omega_m t) \tag{A3-27}$$

while the output of M_2 is

$$E_7 = -A^2\beta \frac{\omega_m}{\omega_0} \cos \omega_m t \cos^2(\omega_0 t + \beta \sin \omega_m t) \tag{A3-28}$$

The detector output voltage is then given by

$$E_8 = A^2\beta \frac{\omega_m}{\omega_0} \cos \omega_m t \tag{A3-29}$$

which has a signal output power of

$$\text{Signal Power} = \frac{A^4 B^2 \omega_m^2}{2\omega_o^2} \tag{A3-30}$$

The SNR for the detector output may now be determined from

$$\text{SNR} = \frac{\text{Signal Power}}{\text{Noise Power}} \tag{A3-31}$$

Substituting and dividing both numerator and denominator by $A^2 \eta \omega_b^3/12\pi$, we obtain

$$\text{SNR} = \frac{\dfrac{3\pi A^2 B^2 \omega_m}{2\eta\,\omega_b^3}}{1 + \dfrac{\eta}{\pi A^2}\left[\dfrac{B^3}{4\omega_b^2} - \dfrac{3B^2}{8\omega_b} + \dfrac{B}{2} - \dfrac{\omega_b}{4}\right]} \tag{A3-32}$$

Since the CNR at the input to the detector is given by

$$\text{CNR} = \frac{A^2/2}{\eta B/2\pi} = \frac{\pi A^2}{\eta B} \tag{A3-33}$$

then the SNR may be rewritten in terms of the CNR. This results in the expression

$$\text{SNR} = \frac{\frac{3}{2}\,(\text{CNR})\left(\dfrac{\Delta\omega}{\omega_b}\right)^2 X}{1 + \dfrac{1}{(\text{CNR})}\left[\dfrac{X^2}{4} - \dfrac{3X}{8} + \dfrac{1}{2} - \dfrac{1}{4X}\right]} \tag{A3-34}$$

where $x = B/\omega_b$. This is equivalent to equation Equation 3-15.

A computer program called DETSNR.BAS was written using the results of Equation A3-34. The program lists values of SNR over a 20 dB range of CNR centered around the threshold value, which is also printed. A listing of the program and an output example for the working model of the detector are given below.

PROGRAM DETSNR.BAS

```
10 C0=10^.1
20 C1=C0-1
30 C=1/(2*C1)
40 PRINT
50 PRINT "ENTER PRE-DETECTION BW: ";
60 INPUT F1
70 PRINT "ENTER POST-DETECTOR CUTOFF FREQ.: ";
80 INPUT F2
90 PRINT "ENTER MODULATION FREQUENCY: ";
100 INPUT F3
110 PRINT "ENTER PEAK FREQ. DEVIATION: ";
120 INPUT F4
130 X=F1/F2
140 B=2*PI*F1
150 W1=2*PI*F2
160 B0=F4/F3
170 V=C*(-.25+X/2-.375*X^2+.25*X^3)
180 A0=10*LOG10(V)
190 T0=10*LOG10(V*2/X)
200 I9=10*LOG10(3*(B0*F3/F2)^2)
210 PRINT
220 PRINT "THRESHOLD CNR IS ";T0;" DB"
230 PRINT "THRESHOLD (CNR)AM IS ";A0;" DB"
240 PRINT "SNR IMPROVEMENT ABOVE (CNR)AM FOR HIGH CNR IS
 ";I9;" DB"
250 PRINT
260 T1=INT(T0-10)
270 PRINT "CNR","(CNR)AM","SNR","SNR DEGRADATION"
280 S0=1.5*B0^2*X*(F3/F2)^2
290 FOR J=0 TO 20
300 T9=T1+J
310 T=10^(T9/10)
320 A=T*X/2
330 A9=10*LOG10(A)
340 S=S0*T/(1-(.25/X-.5+3*X/8-(X^2)/4)/T)
350 S9=10*LOG10(S)
360 PRINT T9,A9,S9,S9-(A9+I9)
370 NEXT J
380 END
```

DETSNR.BAS EXAMPLE
(Working Model of the Detector)

```
DETSNR    28-JUL-82  18:30:39

ENTER PRE-DETECTION BW: ? 266
ENTER POST-DETECTOR CUTOFF FREQ.: ? 28.5
ENTER MODULATION FREQUENCY: ? 25
ENTER PEAK FREQ. DEVIATION: ? 50

THRESHOLD CNR IS  18.5985  DB
THRESHOLD (CNR)AM IS  25.2886  DB
SNR IMPROVEMENT ABOVE (CNR)AM FOR HIGH CNR IS  9.65372  DB
```

CNR	(CNR)AM	SNR	SNR DEGRADATION
8	14.6901	18.3539	-5.98991
9	15.6901	20.0796	-5.26418
10	16.6901	21.7573	-4.58653
11	17.6901	23.3828	-3.96102
12	18.6901	24.953	-3.39075
13	19.6901	26.4663	-2.87752
14	20.6901	27.9221	-2.42166
15	21.6901	29.3217	-2.02204
16	22.6901	30.6676	-1.67614
17	23.6901	31.9635	-1.38029
18	24.6901	33.2138	-1.13002
19	25.6901	34.4234	-.920399
20	26.6901	35.5974	-.746372
21	27.6901	36.7408	-.602989
22	28.6901	37.8582	-.485619
23	29.6901	38.9537	-.390083
24	30.6901	40.0311	-.312664
25	31.6901	41.0936	-.250168
26	32.6901	42.1439	-.199886
27	33.6901	43.1843	-.159515
28	34.6901	44.2166	-.127182

READY

APPENDIX IV

FREQUENCY RESPONSE OF A LINEAR-PHASE FIR NETWORK

This Appendix derives the frequency response, including both amplitude and phase, of a linear-phase FIR filter network given the coefficients (which are identical to the impulse response). The results are used to generate the responses of the differentiators and Hilbert transformers used in the detector.

The delay of a linear-phase FIR network is (N - 1)T/2, where T is the sampling interval and N is the order of the network. Assuming an input of e (t) = exp (jωt), the delayed output is then given by definition (Ref. 1) as

$$e_o(t) = e^{j\omega t} e^{j\omega(\frac{N-1}{2})T} [c_1 + c_2 e^{-j\omega T} + c_3 e^{-2j\omega T} + \ldots + c_N e^{-(N-1)j\omega T}] \qquad (A4\text{-}1)$$

where c_i is the i th coefficient, ω is the input radian frequency, and T is the sampling interval. Define a normalized frequency F (relative to the sampling frequency) given by

$$F = \frac{f}{f_s} = \frac{\omega/2\pi}{1/T} = \frac{\omega T}{2\pi} \qquad (A4\text{-}2)$$

Substituting,

$$e_o(t) = e^{j\omega t} e^{j(N-1)\pi F} [c_1 + c_2 e^{-j2\pi F} + c_3 e^{-j4\pi F} + \ldots + c_N e^{-j2(N-1)\pi F}]$$

$$= e_i(t) \{ H(F) \} \qquad (A4\text{-}3)$$

where H(F) is the transfer function, which determines the amplitude and phase of the result.

The transfer function may then be written as

$$H(F) = \sum_{n=1}^{N} c_n \, e^{j(N+1-2n)\pi F} \qquad \text{(A4-4)}$$

or, in trigometric terms,

$$H(F) = \sum_{n=1}^{N} c_n \, [\cos(N + 1 - 2n)\pi F + j \sin(N + 1 - 2n)\pi F] \qquad \text{(A4-5)}$$

Then,

$$H_{Re} = \mathrm{Re}\, [\, H(F)\,] = \sum_{n=1}^{N} c_n \cos(N + 1 - 2n)\pi F \qquad \text{(A4-6)}$$

and

$$H_{Im} = \mathrm{Im}\, [\, H(F)\,] = \sum_{n=1}^{N} c_n \sin(N + 1 - 2n)\pi F \qquad \text{(A4-7)}$$

The amplitude response is then given by

$$\text{Amplitude} = [\, H_{Re}^2 + H_{Im}^2 \,] \qquad \text{(A4-8)}$$

and the phase by

$$\text{Phase} = \tan^{-1} [\, H_{Im} / H_{Re} \,] \qquad \text{(A4-9)}$$

Now consider the special case of a linear-phase configuration with a constant 90 degree phase characteristic, as exists for differentiators and Hilbert transformers. The coefficients are then related (Ref. 1) by

$$c_n = - c_{N+1-n} \qquad \text{(A4-10)}$$

Then, is N is odd, the terms of H(F) may be taken in pairs, resulting in the expression

$$H(F) = \sum_{n=1}^{\frac{N-1}{2}} c_n \left[e^{j(N+1-2n)\pi F} - e^{-j(N+1-2n)\pi F} \right] \qquad \text{(A4-11)}$$

Since $(e^{jx} - e^{-jx}) = 2j \sin x$, then H(F) may be written as

$$H(F) = j \sum_{n=1}^{\frac{N-1}{2}} 2c_n \sin(N + 1 - 2n)\pi F \qquad \text{(A4-12)}$$

where the j indicates the 90 degree phase response. The frequency response may therefore be evaluated in a Fourier manner, consisting of a fundamental component of 2 sin 2πF and a number of harmonics, each multiplied by a corresponding coefficient. Note that the first coefficient represents the amplitude of the highest frequency component.

Coefficients with even symmetry will obviously produce similar results, except the output will be the sum of cosine terms and have a zero phase characteristic.

These results were used in a computer program called FIRTST.BAS, which was used to analyze the individual differentiators and Hilbert transformers. A program listing and output examples for the differentiator and Hilbert transformer used in the original detector are given below.

REFERENCES

1. A. Antoniou, Digital Filters: Analysis and Design, Chap. 9, McGraw-Hill, 1979.

PROGRAM FIRTST.BAS

```
10 DIM C(20)
20 PRINT "ENTER # COEFFIC "
30 INPUT N
40 PRINT "ENTER COEF  (H(1) TO H(N)) "
50 FOR I=1 TO N
60 INPUT C(I)
70 NEXT I
80 FOR J=1 TO 20
90 F=.025*J
100 H1=0
110 H2=0
120 W=PI*F
130 FOR I=1 TO N
140 W2=(N+1-2*I)*W
150 X2=(N+1-2*I)*J/40
160 X1=X2+.5
170 IF ABS(X1-INT(X1))<1.00000E-07 GO TO 190
180 H1=H1+C(I)*COS(W2)
190 IF ABS(X2-INT(X2))<1.00000E-07 GO TO 210
200 H2=H2+C(I)*SIN(W2)
210 NEXT I
220 A=SQR(H1*H1+H2*H2)
230 P=.5*PI*SGN(H2)
240 IF H1=0 GO TO 290
250 H3=H2/H1
260 P=ATN(H3)
270 IF H1<0 THEN P=P+PI
280 IF P>PI THEN P=P-2*PI
290 PRINT F,A,P
300 NEXT J
310 PRINT
320 GO TO 20
330 END
```

FIRTST.BAS EXAMPLE
(Original Differentiator)

```
FIRTST    28-JUL-82  18:32:31

ENTER # COEFFIC
? 7
ENTER COEF  (H(1) TO H(N))
? 0.08223
? -0.19502
? 0.57944
? 0
? -0.57944
? 0.19502
? -0.08223

FREQ          AMPL            PHASE
 .025          .135423         1.5708
 .05           .261905         1.5708
 .075          .373007         1.5708
 .1            .466633         1.5708
 .125          .545703         1.5708
 .15           .617424         1.5708
 .175          .691293         1.5708
 .2            .776234         1.5708
 .225          .877548         1.5708
 .25           .99442          1.5708
 .275          1.11861         1.5708
 .3            1.23475         1.5708
 .325          1.32239         1.5708
 .35           1.35932         1.5708
 .375          1.32578         1.5708
 .4            1.20853         1.5708
 .425          1.00411         1.5708
 .45           .720425         1.5708
 .475          .376482         1.5708
 .5            7.45058E-09     3.14159
```

FIRTST.BAS EXAMPLE
(Original Hilbert Transformer)

```
FIRTST    28-JUL-82  18:34:01

ENTER # COEFFIC
? 7
ENTER COEF  (H(1) TO H(N))
? 0.08510
? 0.00240
? 0.5808
? 0
? -0.58080
? -0.00240
? -0.08510

FREQ          AMPL          PHASE
 .025          .260467       1.5708
 .05           .49947        1.5708
 .075          .699343       1.5708
 .1            .849206       1.5708
 .125          .946525       1.5708
 .15           .996914       1.5708
 .175          1.01225       1.5708
 .2            1.00753       1.5708
 .225          .997133       1.5708
 .25           .9914         1.5708
 .275          .994166       1.5708
 .3            1.00188       1.5708
 .325          1.00448       1.5708
 .35           .987784       1.5708
 .375          .936925       1.5708
 .4            .840076       1.5708
 .425          .691577       1.5708
 .45           .493828       1.5708
 .475          .257501       1.5708
 .5            2.23517E-08   3.14159
```

APPENDIX V

FREQUENCY RESPONSE OF THE DETECTOR

This Appendix derives the output response of the detector from the coefficients of the differentiator and Hilbert transformer blocks, which are of a linear-phase design. As such, each block has a delay of (N - 1)T/2, where T is the sampling interval. For an input of $e_i(t) = \sin\omega t$, the output of the FIR block is then given by

$$e_o(t) = \sum_{n=1}^{N} c_n \sin\left[\omega t + \left(\frac{N+1}{2} - n\right)\omega T\right] \qquad \text{(A5-1)}$$

where c_n is the n th coefficient and N is the order of the block.

Referring to Figure 2-1, the output of the differentiator is given by

$$E_2 = \sum_{n=1}^{N} c_{Dn} \sin\left[\omega t + \left(\frac{N+1}{2} - n\right)\omega T\right], \qquad \text{(A5-2)}$$

while the output of Hilbert transformer H1 is

$$E_3 = \sum_{n=1}^{N} c_{Hn} \sin\left[\omega t + \left(\frac{N+1}{2} - n\right)\omega T\right] \qquad \text{(A5-3)}$$

The output of summer S1 is then

$$\begin{aligned} E_4 &= E_2 - E_3 \\ &= \sum_{n=1}^{N} (c_{Dn} - c_{Hn}) \sin\left[\omega t + \left(\frac{N+1}{2} - n\right)\omega T\right] \end{aligned} \qquad \text{(A5-4)}$$

Then the output of multiplier M1 is given by

$$E_5 = E_3 \cdot E_4$$
$$= 1/2 \sum_{m=1}^{N} \sum_{n=1}^{N} (c_{Dn} - c_{Hn})\, c_{Hm} \{ \cos(m - n)\omega T$$
$$- \cos [2\omega t + (N + 1 - n - m)\omega T] \} \quad \text{(A5-5)}$$

Determining the equations for the RF cancellation circuit, the output of H2 is

$$E_6 = \sum_{m=1}^{N} \sum_{n=1}^{N} (c_{Dn} - c_{Hn})\, c_{Hm} \sin [\omega t + (N + 1 - n - m)\omega T] \quad \text{(A5-6)}$$

while the output of multiplier M2 is

$$E_7 = 1/2 \sum_{m=1}^{N} \sum_{m=1}^{N} (c_{Dn} - c_{Hn})\, c_{Hm} \{ \cos (N + 1 - n - m)\omega T$$
$$- \cos [2\omega t + (N + 1 - n - m)\omega T] \} \quad \text{(A5-7)}$$

The output of the detector is therefore given by

$$E_8 = E_5 - E_7$$
$$= 1/2 \sum_{m=1}^{N} \sum_{n=1}^{N} (c_{Dn} - c_{Hn})\, c_{Hm} [\cos(m - n)\omega T$$
$$- \cos(N + 1 - n - m)\omega T] \quad \text{(A5-8)}$$

In terms of the normalized frequency F (relative to the sampling frequency), which is defined by $F = \omega T/2\pi$, the detector output may be written as

$$e_o(t) = 1/2 \sum_{m=1}^{N} \sum_{n=1}^{N} (c_{Dn} - c_{Hn})\, c_{Hm} [\cos(m - n)2\pi F$$
$$- \cos(N + 1 - n - m)2\pi F] \quad \text{(A5-9)}$$

which is the same as Equation 4-1.

This result was incorporated into a computer program called GENDET.BAS, which calculates the complete frequency response of the linear-phase FIR detector network from the coefficients. A listing of the program and output examples for the original and optimized detector are given below.

PROGRAM GENDET.BAS

```
10 A=TTYSET(255%,133%)
20 DIM C1(9),C2(9),C3(9),E0(20),F(20)
30 PRINT "INPUT C1(1) TO C1(3):"
40 FOR I=1 TO 3 \ INPUT C1(I) \ NEXT I
50 PRINT "INPUT C2(1) TO C2(3):"
60 FOR I=1 TO 3 \ INPUT C2(I) \ NEXT I
70 PRINT  \ PRINT " #             FREQ           OUTPUT"
80 C1(4)=0
90 C2(4)=0
100 C3(4)=0
110 F0=.25
120 FOR I=1 TO 3
130 C3(I)=C2(I)
140 C1(8-I)=-C1(I)
150 C2(8-I)=-C2(I)
160 C3(8-I)=-C3(I)
170 NEXT I
180 FOR I=1 TO 19
190 F(I)=.025*I
200 W=2*PI*F(I)
210 E0(I)=0
220 FOR M=1 TO 7
230 FOR N=1 TO 7
240 X=COS((M-N)*W)-COS((8-N-M)*W)
250 E0(I)=E0(I)+.5*(C1(N)-C2(N))*C3(M)*X
260 NEXT N
270 NEXT M
280 GO TO 310
290 M1=M1+(F(I)-F0)*E0(I)
300 M2=M2+(F(I)-F0)^2
310 PRINT I,F(I),E0(I)
320 NEXT I
330 STOP
340 E=0
350 M0=M1/M2
360 FOR I=1 TO 9
370 E=E+(E0(I)-M0*(F(I)-F0))^2
380 NEXT I
390 PRINT E
400 END
```

GENDET.BAS EXAMPLE
(Original Detector)

```
GENDET     28-JUL-82   18:35:47

INPUT C1(1) TO C1(3):
? 0.08223
? -0.19502
? 0.57944
INPUT C2(1) TO C2(3):
? 0.08510
? 0.00240
? 0.58080

 #              FREQ            OUTPUT
 1              .025           -.0325697
 2              .05            -.118657
 3              .075           -.228221
 4              .1             -.324883
 5              .125           -.379388
 6              .15            -.378318
 7              .175           -.32489
 8              .2             -.233035
 9              .225           -.119242
 10             .25             2.99392E-03
 11             .275            .123714
 12             .3              .233307
 13             .325            .319332
 14             .35             .367002
 15             .375            .364331
 16             .4              .309532
 17             .425            .216137
 18             .45             .1119
 19             .475            .0306378

STOP AT LINE 330

READY
```

GENDET.BAS EXAMPLE
(Optimized Detector)

```
GENDET     28-JUL-82  18:37:38

INPUT C1(1) TO C1(3):
? 0.19019
? -0.21116
? 0.54117
INPUT C2(1) TO C2(3):
? 0.19071
? -0.00157
? 0.54175
```

#	FREQ	OUTPUT
1	.025	-.0444834
2	.05	-.15884
3	.075	-.295055
4	.1	-.398986
5	.125	-.4345
6	.15	-.396504
7	.175	-.307082
8	.2	-.198598
9	.225	-.0946343
10	.25	-8.43114E-05
11	.275	.0945655
12	.3	.198714
13	.325	.307228
14	.35	.396379
15	.375	.433909
16	.4	.398027
17	.425	.294079
18	.45	.158205
19	.475	.0442871

```
STOP AT LINE 330

READY
```

APPENDIX VI

TIME RESPONSE OF THE DETECTOR

The purpose of this Appendix is to develop the requirements for simulating the detector in the time domain, including the generation of both sine wave and square wave modulated FM signals as sources for the detector.

In generating a computer model of a source generator, consider a general FM wave defined by

$$e_{FM}(t) = A_c \cos [w_c t + m_f \int_0^t g(\tau)\, d\tau] \qquad (A6-1)$$

where $g(\tau)$ is the modulation signal and m_f is the modulation magnitude.

For sinusoidal modulation, assume that

$$g(t) = \cos \omega_m t \qquad (A6-2)$$

Then, the output is given by

$$e_{FM}(t) = A_c \cos [\omega_c t + \beta (\sin \omega_m t)] \qquad (A6-3)$$

where β is the modulation index (maximum frequency deviation divided by the modulation frequency).

For square wave modulation (FSK), the modulation signal may be written as

$$g(t) = SGN (\cos \omega_m t) \qquad (A6-4)$$

and

$$\int_0^t g(\tau)\ d\tau = \sin^{-1}(\sin \omega_m t) \qquad (A6-5)$$

where the inverse sine is limited by $\pm\pi/2$. The generator output is then given by

$$e_{FM}(t) = A_c \cos [\omega_c t + \beta \sin^{-1}(\sin \omega_m t)] \qquad (A6-6)$$

where $\sin^{-1}(\sin \omega_m t)$ is limited to $\pm\pi/2$.

Simulation of the detector follows implementing the algorithms previously described.

A computer program called GENSIM.BAS was written using the above results. For each sample time, the program shows the outputs at each point in the detector. A listing of the program and a typical example of an FSK signal are given below.

PROGRAM GENSIM.BAS

```
10 DIM C1(10),C2(10),C3(10)
20 DIM V1(20),D1(20),H1(20),S1(20),M1(20)
30 A9=TTYSET(255%,133%)
40 PRINT "ENTER ORDER OF SECTIONS (N ODD):";
50 INPUT N
60 PRINT "ENTER COEFFIC (SLOPE=1/F0) FOR DIFFERENTIATOR
 ((N-1)/2):"
70 M=(N-1)/2
80 FOR I=1 TO M
90 INPUT C1(I)
100 NEXT I
110 PRINT "ENTER COEFFIC (AMPL=1) FOR HILBERT TRANSF.
 ((N-1)/2):"
120 FOR I=1 TO M
130 INPUT C2(I)
140 NEXT I
150 PRINT "ENTER COEFFIC (AMPL=1) FOR HILBERT TRANSF. #2
 ((N-1)/2):"
160 FOR I=1 TO M
170 INPUT C3(I)
180 NEXT I
190 PRINT " ENTER DETECTOR CENTER FREQ. (0-.5):";
200 INPUT F0
210 PRINT "ENTER DESIRED CARRIER FREQ. (0-.5) & AMPL:";
220 INPUT F,A
230 PRINT "ENTER DESIRED MODULATION FREQ (0-.5):";
240 INPUT F1
250 PRINT "ENTER MAX CARRIER FREQ SHIFT FROM FC:";
260 INPUT F2
270 IF F1=0 THEN K=0  GO TO 310
280 K=F2/F1
290 PRINT "ENTER MODULATION TYPE (0=SINE,1=FSK):";
300 INPUT M9
310 W=2*PI*F
320 PRINT "ENTER   OUTPUT LINES: ";
330 INPUT L1
340 T=-N
350 FOR I=0 TO N
360 T9=T-I  I9=I
370 GOSUB 810
380 NEXT I
390 PRINT
400 PRINT "TIME";TAB(10);"*    INPUT    *    OUTPUT    *";
 TAB(66);"OUTPUTS OF INTERNAL BLOCKS";TAB(125);"*"
410 PRINT
420 PRINT " T","V1(0)","V2(N-1)","D1(M)","H1(M)",
 "S1(M)","M1(M)","H2(N-1)","M2(N-1)"
430 PRINT
440 REM CALCULATE BLOCKS
450 D1(M)=0
460 H1(M)=0
```

```
470 FOR I=1 TO M
480 D1(M)=D1(M)+C1(I)*(V1(I-1)-V1(N-I))
490 H1(M)=H1(M)+C2(I)*(V1(I-1)-V1(N-I))
500 NEXT I
510 S1(M)=H1(M)-D1(M)
520 M1(M)=S1(M)*H1(M)
530 H2=0
540 FOR I=1 TO M
550 H2=H2+C3(I)*(S1(I+M-1)-S1(N+M-I))
560 NEXT I
570 M2=H2*V1(N-1)
580 S2=M2-M1(N-1)
590 V2=S2
600 REM V2 DELAYED N-1 SAMPLES
610 IF T<0 GO TO 630
620 PRINT T,V1(0),V2,D1(M),H1(M),S1(M),M1(M),H2,M2
630 T=T+1
640 FOR I=1 TO N-1
650 J=N-I
660 V1(J)=V1(J-1)
670 NEXT I
680 FOR I=M+1 TO N+M-1
690 J=2*N-I-1
700 D1(J)=D1(J-1)
710 H1(J)=H1(J-1)
720 S1(J)=S1(J-1)
730 M1(J)=M1(J-1)
740 NEXT I
750 T9=T
760 I9=0
770 GOSUB 810
780 IF T<L1 GO TO 440
790 PRINT
800 GO TO 210
810 REM INPUT SIGNAL SUBROUTINE
820 S9=0
830 X=2*F1*T9
840 IF ABS(X-INT(X))<1.00000E-06 GO TO 860
850 S9=SIN(PI*X)
860 S8=S9
870 IF M9=0 GO TO 910
880 IF ABS(S9)=1 THEN S8=PI*S9/2  GO TO 910
890 Y=SQR(1-S9*S9)
900 S8=ATN(S9/Y)
910 X=W*T9+K*S8
920 X1=X/PI
930 IF ABS(X1-INT(X1))<1.00000E-06 THEN V1(I9)=0  GO TO 950
940 V1(I9)=A*SIN(X)
950 RETURN
```

GENSIM.BAS EXAMPLE
(Detector Response to an FSK Input Signal)

```
GENSIM    05-SEP-82  23:01:15

ENTER ORDER OF SECTIONS (N ODD):? 7
ENTER COEFFIC (SLOPE=1/FO) FOR DIFFERENTIATOR ((N-1)/2):
? 0.19019
? -0.21116
? 0.54117
ENTER COEFFIC (AMPL=1) FOR HILBERT TRANSF. ((N-1)/2):
? 0.19071
? -0.00157
? 0.54175
ENTER COEFFIC (AMPL=1) FOR HILBERT TRANSF. #2 ((N-1)/2):
? 0.19071
? -0.00157
? 0.54175
 ENTER DETECTOR CENTER FREQ. (0-.5):? 0.25
ENTER DESIRED CARRIER FREQ. (0-.5) & AMPL:? 0.25,1.0
ENTER DESIRED MODULATION FREQ (0-.5):? 0.030
ENTER MAX CARRIER FREQ SHIFT FROM FC:? 0.075
ENTER MODULATION TYPE (0=SINE,1=FSK):? 1
ENTER # OUTPUT LINES: ? 80
```

TIME *	INPUT *	OUTPUT *	OUTPUTS OF INTERNAL BLOCKS					
T	V1(O)	V2(N-1)	D1(M)	H1(M)	S1(M)	M1(M)	H2(N-1)	M2(N-1)
0	0	.279291	1.23118	.897096	-.334088	-.299709	.0907246	.0280355
1	.891007	.335416	-.732693	-.533873	.19882	-.106145	.257107	.181802
2	-.809017	.290521	-.565913	-.41235	.153564	-.0633219	-.274624	.261183
3	-.156435	.307235	1.24653	.908279	-.338253	-.307228	.0481044	7.52520E-03
4	.951057	.307228	-.565913	-.41235	.153564	-.0633219	.248552	.201083
5	-.707106	.307228	-.732693	-.533873	.19882	-.106145	-.273742	.243906
6	-.309017	.307228	1.23118	.897096	-.334088	-.299709	0	0
7	.987688	.307228	-.385199	-.280673	.104526	-.0293376	.273742	.243906
8	-.587782	.307228	-.881431	-.64225	.239181	-.153614	-.248552	.201083
9	-.891007	.307235	1.10241	.780481	-.321924	-.251256	-.0481044	7.52520E-03
10	0	.290521	-.292908	-.332108	-.0392	.0130186	.274624	.261183
11	.891006	.335416	-.778001	-.713492	.0645083	-.0460262	-.257107	.181802
12	.809016	.279291	.551144	.531803	-.0193413	-.0102858	-.0907246	.0280355
13	-.156434	.229693	.451824	.745017	.293194	.218434	.245737	.242711
14	-.951056	.0497918	.213612	.367851	.15424	.0567372	-6.40645E-03	3.76560E-03
15	-.707108	-.120575	-.331042	-.530886	-.199844	.106094	.146869	-.130861
16	.309015	-.218434	-.556269	-.892078	-.335809	.299568	.0378862	0
17	.987688	-.323099	-.17404	-.279105	-.105064	.0293239	-.298945	-.266362
18	.587787	-.280292	.398244	.638657	.240412	.153541	-.215321	-.174198
19	-.453989	-.308479	.535639	.858993	.323354	.277759	.0569634	-8.91098E-03
20	-1	-.307103	.0881059	.141293	.0531873	7.51501E-03	.292075	-.277779
21	-.453992	-.307083	-.455641	-.730702	-.275061	.200988	.21714	-.153542
22	.587782	-.307083	-.501819	-.804757	-.302938	.243791	-.0948933	-.0293235
23	.987688	-.307083	-4.15927E-07	-1.42936E-06	-1.01343E-06	1.44856E-12	-.303302	-.299568
24	.309015	-.307083	.501816	.804753	.302937	.24379	-.180499	-.106095
25	-.707105	-.307082	.455642	.730704	.275061	.200988	.139412	-.0632914
26	-.309021	-.307146	.0340042	-.0188481	-.0528522	9.96162E-04	.307146	-.307146
27	.987689	-.318784	-.453609	-.641803	-.188194	.120784	.165189	-.0749943
28	-.587782	-.280259	-.558043	-.559013	-9.69648E-04	5.42046E-04	-.134865	-.0792714
29	-.453995	-.283764	.832346	.644619	-.187727	-.121012	-.286293	-.282768
30	1	-.126588	-.0728856	-.0196387	.0532469	-1.04570E-03	-.0187845	-5.80469E-03
31	-.453984	-4.13604E-04	-1.00847	-.734815	.273653	-.201084	-1.81646E-04	1.28443E-04
32	-.58779	.126806	1.11066	.809281	-.301384	-.243904	-.0187508	5.79440E-03
33	.987688	.283835	7.06352E-06	5.55745E-06	-1.50607E-06	-8.36992E-12	.286314	.28279
34	-.309012	.28029	-1.11067	-.809284	.301386	-.243907	-.134754	.079206

GENSIM.BAS EXAMPLE (contd)

35	-.707111	.318827	1.00846	.734809	-.273651	-.201082	-.165029	.0749222
36	.951054	.307164	.195007	.142091	-.0529166	-7.51895E-03	.307164	.307164
37	-.156426	.307228	-1.18552	-.863826	.321698	-.277891	-.139477	.0633205
38	-.809023	.307228	.881425	.642246	-.239179	-.153612	-.180585	.106146
39	.891004	.307228	.385208	.28068	-.104528	-.0293389	.303445	.299709
40	0	.307228	-1.23119	-.897099	.334089	-.299711	-.0949365	.0293366
41	-.891007	.307228	.732687	.533868	-.19882	-.106143	-.217244	.153616
42	.587782	.307207	.523842	.370162	-.15368	-.0568866	.292168	.277868
43	.98769	.308599	-1.04172	-.749403	.292318	-.219064	-.0568198	8.88810E-03
44	.309018	.280259	.510314	.531501	.0211865	.0112607	-.215218	.174116
45	-.707103	.323208	.647498	.712524	.0650257	.0463324	.2989	.266322
46	-.951058	.219064	-.370574	-.332686	.0378883	-.0126049	.0378315	0
47	-.156438	.119845	-.452521	-.775648	-.323127	.250632	-.147143	.131105
48	.809019	-.0501685	-.398244	-.638658	-.240414	.153542	-6.52642E-03	-3.83612E-03
49	.891007	-.229954	.174035	.279099	.105064	.0293234	-.245582	-.242559
50	0	-.278701	.556272	.89208	.335808	.299568	-.0908314	-.0280686
51	-.891004	-.33542	.331044	.530888	.199844	.106095	.257216	-.181878
52	-.809019	-.290564	-.255691	-.410045	-.154353	.0632917	.274685	-.261241
53	.156438	-.307076	-.5632	-.903196	-.339996	.307083	.0479948	-7.50821E-03
54	.951054	-.307082	-.255692	-.410045	-.154354	.063292	-.248434	-.200987
55	.707111	-.307083	.331045	.530888	.199843	.106094	-.273613	-.243791
56	-.309012	-.307083	.55627	.892079	.335809	.299568	-7.81554E-08	0
57	-.987688	-.307082	.174038	.279104	.105066	.0293242	.273613	-.24379
58	-.587782	-.307083	-.39824	-.638653	-.240413	.15354	.248434	-.200988
59	.891004	-.307076	-.452526	-.775652	-.323126	.250633	-.0479936	-7.50802E-03
60	1.19842E-05	-.290565	-.370572	-.332686	.037886	-.0126041	-.274685	-.261241
61	-.89101	-.335421	.647492	.712519	.0650271	.046333	-.257216	-.18188
62	.809009	-.278701	.510319	.531504	.021185	.0112599	.0908294	-.0280674
63	.156444	-.229954	-1.04172	-.749402	.292315	-.219061	.245581	-.242558
64	-.95106	-.0501698	.523823	.370146	-.153676	-.0568827	6.52762E-03	-3.83682E-03
65	.707098	.119842	.732702	.533879	-.198823	-.106147	.14714	.131102
66	.309024	.219061	-1.23118	-.897094	.334087	-.299708	-.0378283	-4.53343E-07
67	-.987691	.323206	.385187	.280664	-.104523	-.0293358	-.2989	.266323
68	.587778	.280257	.881439	.642256	-.239183	-.153617	.215214	.17411
69	.453995	.308598	-1.18552	-.863822	.321697	-.277889	.0568249	8.88992E-03
70	-1	.307207	.194991	.142079	-.0529117	-7.51763E-03	-.29217	.277871
71	.453984	.307228	1.00847	.734817	-.273654	-.201085	.217241	.153611
72	.587797	.307228	-1.11066	-.809277	.301385	-.243904	.0949414	.0293392
73	-.987687	.307228	-9.15497E-06	-5.09911E-06	4.05585E-06	-2.06813E-11	-.303445	.29971
74	.309001	.307228	1.11067	.809287	-.301386	-.243908	.180582	.106142
75	.707115	.307227	-1.00846	-.734808	.273649	-.201079	.139481	.0633237
76	-.309012	.307161	-.0729082	-.0196568	.0532514	-1.04675E-03	-.307164	.307164
77	-.987687	.318826	.832355	.644626	-.187729	-.121015	.165023	.074918
78	-.587787	.280289	-.558035	-.559004	-9.69768E-04	5.42104E-04	.134758	.0792101
79	.453984	.283835	-.453619	-.64181	-.188191	.120783	-.286314	.282788

ENTER DESIRED CARRIER FREQ. (0-.5) & AMPL!? ^C

STOP AT LINE 220

READY

APPENDIX VII

LINEARITY OPTIMIZATION OF THE DETECTOR

The parameters of the detector were optimized using the subroutine FMFP.FOR, which is now included in most Fortran scientific subroutine packages. It is based on an algorithm developed by Fletcher and Powell to minimize a function of a number of variables by varying the value of the variables. The subroutine must be given an initial set of values, which it then modifies by successive approximations in order to reduce the value of the function. To accomplish this, the routine requires that the value of the function and the gradient vector of the function with respect to each variable be calculated for each new approximation.

Therefore, in order to optimize the linearity of the detector in Figure 2-1 using the Fletcher-Powell algorithm, we must first generate the expressions for both the error function to be minimized and the corresponding gradient vector.

As shown in Equation A5-9, the output of the detector for the normalized frequency F is given by

$$e_o(F) = 1/2 \sum_{m=1}^{N} \sum_{n=1}^{N} \{ (c_{Dn} - c_{Hn})\, c_{Hm} \cdot [\cos(m - n)2\pi F - \cos(N + 1 - n - m)2\pi F] \} \qquad (A7\text{-}1)$$

Using the least squares method, with the constraint that the ideal detector output be zero at F_o and have a slope of M, the error function is then given by

$$\text{Error} = \sum_{i=1}^{P} [\, e_o(F_i) - M\,(F_i - F_o)\,]^2 \qquad \text{(A7-2)}$$

where P is the number of frequency points used to represent the function and M is the slope of the detector output. Due to the structure of the ideal detector, the slope M is a constant given by

$$M = 1 \,/\, F \qquad \text{(A7-3)}$$

The gradient vector is defined as

$$\text{GRAD} = \frac{\partial(\text{Error})}{\partial c_1}, \frac{\partial(\text{Error})}{\partial c_2}, \ldots\ldots, \frac{\partial(\text{Error})}{\partial c_n} \qquad \text{(A7-4)}$$

where

$$\frac{\partial(\text{Error})}{\partial c_j} = 2 \sum_{i=1}^{P} [\, e_o(F_i) - M\,(F_i - F_o)\,] \; \frac{\partial e_o(F)}{\partial c_j} \qquad \text{(A7-5)}$$

The expression for the partial derivatives of the output with respect to the coefficient c_j depends on which block the coefficient is associated. For the coefficients of the differentiator D1, we have $c_j = c_{Dn}$, and the partial derivative may be written as

$$\frac{\partial e_o(F_i)}{\partial c_{Dn}} = 1/2 \sum_{m=1}^{N} \sum_{n=1}^{N} (1 - C_{Hn})\, C_{Hm}\, X(F_i) \qquad \text{(A7-6)}$$

where

$$X(F_i) = \cos(m - n)2\pi F_i - \cos(N + 1 - n - m)2\pi F_i \qquad \text{(A7-7)}$$

Then for Hilbert transformer H1, we have $c_j = c_{Hn}$ and

$$\frac{\partial e_o(F_i)}{\partial c_{Hn}} = 1/2 \sum_{m=1}^{N} \sum_{n=1}^{N} (c_{Dn} - 1)\ c_{Hm}\ X(F_i) \qquad \text{(A7-8)}$$

And finally, for H2 we have $c_j = c_{Hm}$ and

$$\frac{\partial e_o(F_i)}{\partial C_{Hm}} = 1/2 \sum_{m=1}^{N} \sum_{n=1}^{N} (c_{Dn} - c_{Hn})\ X(F_i) \qquad \text{(A7-9)}$$

These results were then incorporated into subroutine FUNCT.FOR, which is called by the Fletcher-Powell routine. The main program DETLN.FOR is needed to handle the input and output data for the subroutines.

Listings of these computer programs are given below.

PROGRAM DETLIN.FOR

```
      PROGRAM DETLIN
      DIMENSION X(21),G(21),H(378),ARG(21),GRAD(21)
      BYTE ANS
      EXTERNAL FUNCT
      WRITE(7,10)
   10 FORMAT('$ENTER ORDER (ODD # <16):')
      READ(5,*) NC
      NC2=(NC-1)/2
      N=2*NC2
      M=NC2
      F0=0.25
      WRITE(7,15)
   15 FORMAT('$DIFF COEF NORMALIZED? ')
      READ(7,16) ANS
   16 FORMAT(A1)
      WRITE(7,20)
   20 FORMAT(' ENTER DIFF COEF ((N-1)/2):')
      READ(5,*) (X(I),I=1,M)
      IF(ANS.EQ.'N') GO TO 26
      DO 25 I=1,M
      X(I)=X(I)/F0
   25 CONTINUE
   26 WRITE(7,30)
   30 FORMAT(' ENTER HILB. TRANS. COEF ((N-1)/2):')
      MS=NC2+1
      MF=2*NC2
      READ(5,*) (X(I),I=MS,MF)
      EST=0.01
      EPS=1.E-6
      LIMIT=100
      WRITE(7,46)
   46 FORMAT(' ENTER EST, EPS & LIMIT FOR FMFP.FOR: ')
      READ(5,*) EST,EPS,LIMIT
      CALL FMFP(FUNCT,N,X,F,G,EST,EPS,LIMIT,IER,H)
      CALL RCTRLO
      WRITE(7,50) F,IER
   50 FORMAT(/5X,'VALUE=',F12.5,10X,'IER=',I3/)
      WRITE(7,60)
   60 FORMAT(5X,'COEF OF D,H & GRAD OF COEF:')
      DO 80 I=1,NC2
      I2=I+NC2
      WRITE(7,70) I,X(I),X(I2),G(I),G(I2),
   70 FORMAT(5X,I2,4F15.5)
   80 CONTINUE
      CALL EXIT
      END
```

PROGRAM FUNCT.FOR

```
C   SUBROUTINE FOR 'FMFP.FOR' THAT CALCULATES A LINEARITY
C     ERROR FUNCTION FOR A DETECTOR WITH ZERO OUTPUT AT CENTER
C     FREQ. USING LINEAR PHASE COEFFIC. UP TO 15TH ORDER, AND
C     COMMON HILB. TRANS. COEFFIC. FOR ZERO CARRIER RIPPLE.
C
      SUBROUTINE FUNCT (N,ARG,VAL,GRAD)
      DIMENSION ARG(1),GRAD(1)
      DIMENSION EO(21),DM(3,7),DEO(3,7,9)
      DIMENSION CD(15),CH(15)
      DIMENSION ES(15)
      PI=3.1415926
C       DEFINE FREQ. POINTS  (FUNCTION)
      FREQ(I)=0.125+0.025*I
      FO=0.25
      NFREQ=9
C       CALCULATE ORDER OF SECTIONS = NC
      NC=N+1
      NC2=N/2
C       OBTAIN COMPLETE SET OF COEFFIC  (NC ODD)
      DO 10 I=1,NC2
      CD(I)=ARG(I)
      CH(I)=ARG(I+NC2)
      CD(NC-I+1)=-CD(I)
      CH(NC-I+1)=-CH(I)
   10 CONTINUE
      NCM=NC2+1
      CD(NCM)=0.
      CH(NCM)=0.
      S1=0.
      S2=0.
C       CALCULATE ERROR
      DO 30 K=1,NFREQ
      F=FREQ(K)
      W=2.*PI*F
      E=0.
      DO 25 I=1,NC
      DO 20 J=1,NC
      X=COS((I-J)*W)-COS((NC+1-I-J)*W)
      EADD=((CD(J)-CH(J))*CH(I))*X
      E=E+EADD
      ES(J)=EADD
   20 CONTINUE
   25 CONTINUE
      EO(K)=0.5*E
      FD=F-FO
      S1=S1+FD*EO(K)
      S2=S2+FD*FD
   30 CONTINUE
      VM=S1/S2
      VMD=1./FO
      VAL=0.
```

```
      DO 40 K=1,NFREQ
      F=FREQ(K)
      VAL=VAL+(EO(K)-VMD*(F-FO))**2
   40 CONTINUE
C       ITERATION FOR GRADIENT CALC
      DO 50 I=1,N
      GRAD(I)=0.
   50 CONTINUE
      DO 70 I=1,NC2
      DO 70 M=1,2
      DO 60 K=1,NFREQ
      DEO(M,I,K)=0.
   60 CONTINUE
      DM(M,I)=0.
   70 CONTINUE
      D=S2
C       COMPUTE PARTIAL DERIVATIVES
      DO 100 K=1,NFREQ
      F=FREQ(K)
      W=2.*PI*F
      DO 90 I=1,NC
      DO 90 J=1,NC
      X=COS((I-J)*W)-COS((NC+1-I-J)*W)
      DO 80 L=1,NC2
      IF(J.EQ.L) GO TO 72
      IF(J.EQ.NC+1-L) GO TO 72
      GO TO 74
   72 P5=0.5*CH(I)*X
      IF(J.GT.NCM) P5=-P5
      DEO(1,L,K)=DEO(1,L,K)+P5
   74 VCM=1.
      IF(I.EQ.L) GO TO 75
      IF(I.EQ.NC+1-L) GO TO 75
      GO TO 76
   75 IF(I.EQ.J) VCM=2.
      P5=0.5*(CD(J)-VCM*CH(J))*X
      IF(I.GT.NCM) P5=-P5
      GO TO 79
   76 IF(J.EQ.L) GO TO 77
      IF(J.EQ.NC+1-L) GO TO 77
      GO TO 80
   77 P5=-0.5*CH(I)*X
      IF(J.GT.NCM) P5=-P5
   79 DEO(2,L,K)=DEO(2,L,K)+P5
   80 CONTINUE
   90 CONTINUE
      DO 95 L=1,NC2
      DO 95 M=1,2
      DM(M,L)=DM(M,L)+(F-FO)*DEO(M,L,K)/D
   95 CONTINUE
  100 CONTINUE
C       COMPUTE GRADIENT VECTORS
      DO 120 K=1,NFREQ
      F=FREQ(K)
      W=2.*PI*F
```

```
      DO 110 M=1,2
      DO 110 L=1,NC2
      I=3*(M-1)+L
      DM(M,L)=0.
      GRAD(I)=GRAD(I)+2.*(EO(K)-VMD*(F-FO))*(DEO(M,L,K)
     1-DM(M,L)*(F-FO))
  110 CONTINUE
  120 CONTINUE
      WRITE(7,150) VAL
  150 FORMAT(/E15.8)
      DO 170 J=1,2
      WRITE(7,160)(ARG(3*(J-1)+I),I=1,3),(GRAD(3*(J-1)+I),
     1I=1,3)
  160 FORMAT(15X,3E17.8,6X,3E17.8)
  170 CONTINUE
      RETURN
      END
```

PROGRAM FMFP.FOR

```
C
C
 ***************************************************************
C
C        SUBROUTINE FMFP
C
C         PURPOSE
C           TO FIND A LOCAL MINIMUM OF A FUNCTION OF SEVERAL
C           VARIABLES BY THE METHOD OF FLETCHER AND POWELL
C
C        USAGE
C           CALL FMFP(FUNCT,N,X,F,G,EST,EPS,LIMIT,IER,H)
C
C        DESCRIPTION OF PARAMETERS
C           FUNCT - USER-WRITTEN SUBROUTINE CONCERNING THE
C                   FUNCTION TO BE MINIMIZED. IT MUST BE OF
C                   THE FORM SUBROUTINE FUNCT(N,ARG,VAL,GRAD)
C                   AND MUST SERVE THE FOLLOWING PURPOSE
C                   FOR EACH N-DIMENSIONAL ARGUMENT VECTOR
C                   ARG, FUNCTION VALUE AND GRADIENT VECTOR
C                   MUST BE COMPUTED AND, ON RETURN, STORED
C                   IN VAL AND GRAD RESPECTIVLY
C           N     - NUMBER OF VARIABLES
C           X     - VECTOR OF DIMENSION N CONTAINING THE
C                   INITIAL ARGUMENT WHERE THE ITERATION
C                   STARTS. ON RETURN, X HOLDS THE ARGUMENT
C                   CORRESPONDING TO THE COMPUTED MINIMUM
C                   FUNCTION VALUE
C           F     - SINGLE VARIABLE CONTAINING THE MINIMUM
C                   FUNCTION VALUE ON RETURN, I.E. F=F(X).
C           G     - VECTOR OF DIMENSION N CONTAINING THE
C                   GRADIENT VECTOR CORRESPONDING TO THE
C                   MINIMUM ON RETURN, I.E. G=G(X).
C           EST   - IS AN ESTIMATE OF THE MINIMUM FUNCTION
C                   VALUE.
C           EPS   - TESTVALUE REPRESENTING THE EXPECTED
C                   ABSOLUTE ERROR.  A REASONABLE CHOICE IS
C                   10**(-6), I.E. SOMEWHAT GREATER THAN
C                   10**(-D), WHERE D IS THE NUMBER OF
C                   SIGNIFICANT DIGITS IN FLOATING POINT
C                   REPRESENTATION.
C           LIMIT - MAXIMUM NUMBER OF ITERATIONS.
C           IER   - ERROR PARAMETER
C                   IER = 0 MEANS CONVERGENCE WAS OBTAINED
C                   IER = 1 MEANS NO CONVERGENCE IN LIMIT
C                           ITERATIONS
C                   IER =-1 MEANS ERRORS IN GRADIENT
C                           CALCULATION
C                   IER = 2 MEANS LINEAR SEARCH TECHNIQUE
C                           INDICATES IT IS LIKELY THAT THERE
C                           EXISTS NO MINIMUM.
```

```
C           H      - WORKING STORAGE OF DEMENSION N*(N+7)/2.
C
C        REMARKS
C            I) THE SUBROUTINE NAME REPLACING THE DUMMY
C               ARGUMENT FUNCT MUST BE DECLARED AS EXTERNAL IN
C               THE CALLING PROGRAM.
C           II) IER IS SET TO 2 IF , STEPPING IN ONE OF THE
C               COMPUTED DIRECTIONS, THE FUNCTION WILL NEVER
C               INCREASE WITHIN A TOLERABLE RANGE OF ARGUMENT.
C               IER = 2 MAY OCCUR ALSO IF THE INTERVAL WHERE F
C               INCREASES IS SMALL AND THE INITIAL ARGUMENT
C               WAS RELATIVELY FAR AWAY FROM THE MINIMUM SUCH
C               THAT THE MINIMUM WAS OVERLEAPED.  THIS IS DUE
C               TO THE SEARCH TECHNIQUE WHICH DOUBLES THE
C               STEPSIZE UNTIL A POINT IS FOUND WHERE THE
C               FUNCTION INCREASES.
C
C        SUBROUTINES AND FUNCTION SUBPROGRAMS REQUIRED
C           FUNCT
C
C        METHOD
C           THE METHOD IS DESCRIBED IN THE FOLLOWING ARTICLE
C           R. FLETCHER AND M.J.D. POWELL, A RAPID DESCENT
C           METHOD FOR MINIMIZATION.
C           COMPUTER JOURNAL VOL.6, ISS. 2, 1963, PP.163-168.
C
C
 ............................................................
C
      SUBROUTINE FMFP(FUNCT,N,X,F,G,EST,EPS,LIMIT,IER,H)
C
C        DIMENSIONED DUMMY VARIABLES
      DIMENSION H(1),X(1),G(1)
C
C        COMPUTE FUNCTION VALUE AND GRADIENT VECTOR FOR
C        INITIAL ARGUMENT
      CALL FUNCT(N,X,F,G)
C
C        RESET ITERATION COUNTER AND GENERATE IDENTITY MATRIX
      IER=0
      KOUNT=0
      N2=N+N
      N3=N2+N
      N31=N3+1
    1 K=N31
      DO 4 J=1,N
      H(K)=1.
      NJ=N-J
      IF(NJ)5,5,2
    2 DO 3 L=1,NJ
      KL=K+L
    3 H(KL)=0.
    4 K=KL+1
C
C        START ITERATION LOOP
```

```
    5 KOUNT=KOUNT+1
C
C        SAVE FUNCTION VALUE, ARGUMENT VECTOR AND GRADIENT
C        VECTOR
      OLDF=F
      DO 9 J=1,N
      K=N+J
      H(K)=G(J)
      K=K+N
      H(K)=X(J)
C
C        DETERMINE DIRECTION VECTOR H
      K=J+N3
      T=0.
      DO 8 L=1,N
      T=T-G(L)*H(K)
      IF(L-J)6,7,7
    6 K=K+N-L
      GO TO 8
    7 K=K+1
    8 CONTINUE
    9 H(J)=T
C
C        CHECK WHETHER FUNCTION WILL DECREASE STEPPING
C        ALONG H.
      DY=0.
      HNRM=0.
      GNRM=0.
C
C        CALCULATE DIRECTIONAL DERIVATIVE AND TESTVALUES FOR
C        DIRECTION VECTOR H AND GRADIENT VECTOR G.
      DO 10 J=1,N
      HNRM=HNRM+ABS(H(J))
      GNRM=GNRM+ABS(G(J))
   10 DY=DY+H(J)*G(J)
C
C        REPEAT SEARCH IN DIRECTION OF STEEPEST DESCENT IF
C        DIRECTIONAL DEREIVATIVE APPEARS TO BE POSITIVE OR
C        ZERO.
      IF(DY)11,51,51
C
C        REPEAT SEARCH IN DIRECTION OF STEEPEST DECENT IF
C        DIRECTION VECTOR H IS SMALL COMPARED TO GRADIENT
C        VECTOR G.
   11 IF(HNRM/GNRM-EPS)51,51,12
C
C        SEARCH MINIMUM ALONG H
C
C        SEARCH ALONG H FOR POSITIVE DIRECTIONAL DERIVATIVE
   12 FY=F
      ALFA=2.*(EST-F)/DY
      AMEDA=1.
C
C        USE ESTIMATE FOR STEPSIZE ONLY IF IT IS POSITIVE AND
C        LESS THAN 1. OTHERWISE TAKE 1. AS STEPSIZE
```

```
      IF(ALFA)15,15,13
   13 IF(ALFA-AMEDA)14,15,15
   14 AMEDA=ALFA
   15 ALFA=0.
C
C         SAVE FUNCTION AND DERIVATIVE VALUES FOR OLD ARGUMENT
   16 FX=FY
      DX=DY
C
C         STEP ARGUMENT ALONG H
      DO 17 I=1,N
   17 X(I)=X(I)+AMEDA*H(I)
C
C         COMPUTE FUNCTION VALUE AND GRADIENT FOR NEW ARGUMENT
      CALL FUNCT(N,X,F,G)
      FY=F
C
C         COMPUTE DIRECTIONAL DERIVATIVE DY FOR NEW ARGUMENT.
C         TERMINATE SEARCH, IF DY IS POSITIVE. IF DY IS ZERO
C         THE MINIMUM IF FOUND
      DY=0.
      DO 18 I=1,N
   18 DY=DY+G(I)*H(I)
      IF(DY)19,36,22
C
C          TERMINATE SEARCH ALSO IF THE FUNCTION VALUE
C          INDICATES THAT A MINIMUM HAS BEEN PASSED
   19 IF(FY-FX)20,22,22
C
C          REPEAT SEARCH AND DOUBLE STEPSIZE FOR FURTHER
C          SEARCHES
   20 AMEDA=AMEDA+ALFA
      ALFA=AMEDA
C         END OF SEARCH LOOP
C
C         TERMINATE IF THE CHANGE IN ARGUMENT GETS VERY LARGE
      IF(HNRM*AMEDA-1.E10)16,16,21
C
C         LINIAR SEARCH TECHNIQUE INDICATES THAT NO MINIMUM
C         EXISTS
   21 IER=2
      RETURN
C
C         INTERPOLATE CUBICALLY IN THE INTERVAL DEFINED BY THE
C         SEARCH ABOVE AND COMPUTE THE ARGUMENT X FOR WHICH THE
C         INTERPOLATION POLYNOMIAL IS MINIMIZED.
   22 T=0.
   23 IF(AMEDA)24,36,24
   24 Z=3.*(FX-FY)/AMEDA+DX+DY
      ALFA=AMAX1(ABS(Z),ABS(DX),ABS(DY))
      DALFA=Z/ALFA
      DALFA=DALFA*DALFA-DX/ALFA*DY/ALFA
      IF(DALFA)51,25,25
   25 W=ALFA*SQRT(DALFA)
      ALFA=DY-DX+W+W
```

```
      IF(ALFA)250,251,250
  250 ALFA=(DY-Z+W)/ALFA
      GO TO 252
  251 ALFA=(Z+DY-W)/(Z+DX+Z+DY)
  252 ALFA=ALFA*AMEDA
      DO 26 I=1,N
   26 X(I)=X(I)+(T-ALFA)*H(I)
C
C        TERMINATE, IF THE VALUE OF THE ACTUAL FUNCTION AT X
C        IS LESS THAN THE FUNCTION VALUES AT THE INTERVAL
C        ENDS.  OTHERWISE REDUCE THE INTERVAL BY CHOOSING ONE
C        END-POINT EQUAL TO X AND REPEAT THE INTERPOLATION.
C        WHICH END-POINT IS CHOOSEN DEPENDS ON THE VALUE OF
C        THE FUNCTION AND ITS GRADIENT AT X.
C
      CALL FUNCT(N,X,F,G)
      IF(F-FX)27,27,28
   27 IF(F-FY)36,36,28
   28 DALFA=0.
      DO 29 I=1,N
   29 DALFA=DALFA+G(I)*H(I)
      IF(DALFA)30,33,33
   30 IF(F-FX)32,31,33
   31 IF(DX-DALFA)32,36,32
   32 FX=F
      DX=DALFA
      T=ALFA
      AMEDA=ALFA
      GO TO 23
   33 IF(FY-F)35,34,35
   34 IF(DY-DALFA)35,36,35
   35 FY=F
      DY=DALFA
      AMEDA=AMEDA-ALFA
      GO TO 22
C
C        TERMINATE, IF FUNCTION HAS NOT DECREASED DURING LAST
C        ITERATION
   36 IF(OLDF-F+EPS)51,38,38
C
C        COMPUTE DIFFERENCE VECTORS OF ARGUMENT AND GRADIENT
C        FROM TWO CONSECUTIVE ITERATIONS
   38 DO 37 J=1,N
      K=N+J
      H(K)=G(J)-H(K)
      K=N+K
   37 H(K)=X(J)-H(K)
C
C        TEST LENGTH OF ARGUMENT DIFFERENCE VECTOR AND
C        DIRECTION VECTOR IF AT LEAST N ITERATIONS HAVE BEEN
C        EXECUTED. TERMINATE, IF BOTH ARE LESS THAN EPS.
      IER=0
      IF(KOUNT-N)42,39,39
   39 T=0.
      Z=0.
```

```
      DO 40 J=1,N
      K=N+J
      W=H(K)
      K=K+N
      T=T+ABS(H(K))
   40 Z=Z+W*H(K)
      IF(HNRM-EPS)41,41,42
   41 IF(T-EPS)56,56,42
C
C        TERMINATE, IF NUMBER OF ITERATIONS WOULD EXCEED LIMIT
   42 IF(KOUNT-LIMIT)43,50,50
C
C        PREPARE UPDATING OF MATRIX H
   43 ALFA=0.
      DO 47 J=1,N
      K=J+N3
      W=0.
      DO 46 L=1,N
      KL=K+L
      W=W+H(KL)*H(K)
      IF(L-J)44,45,45
   44 K=K+N-L
      GO TO 46
   45 K=K+1
   46 CONTINUE
      K=N+J
      ALFA=ALFA+W*H(K)
   47 H(J)=W
C
C        REPEAT SEARCH IN DIRECTION OF STEEPEST DESCENT IF
C        RESULTS ARE NOT SATISFACTORY
      IF(Z*ALFA)48,1,48
C
C        UPDATE MATRIX H
   48 K=K31
      DO 49 L=1,N
      KL=N2+L
      DO 49 J=L,N
      NJ=N2+J
      H(K)=H(K)+H(KL)*H(NJ)/Z-H(L)*H(J)/ALFA
   49 K=K+1
      GO TO 5
C        END OF ITERATION LOOP
C
C        NO CONVERGENCE AFTER LIMIT ITERATIONS
   50 ERR=1
      RETURN
C
C        RESTORE OLD VALUES OF FUNCTION AND ARGUMENTS
   51 DO 52 J=1,N
      K=N2+J
   52 X(J)=H(K)
      CALL FUNCT(N,X,F,G)
C
C        REPEAT SEARCH IN DIRECTION OF STEEPEST DECENT IF
```

```
C         DERIVATIVE FAILS TO BE SUFFICIENTLY SMALL
      IF(GNRM-EPS)55,55,53
C
C         TEST REPEATED FAILURE OF ITERATION
   53 IF(IER)56,54,54
   54 IER=-1
      GO TO 1
   55 IER=0
   56 RETURN
      END
```

APPENDIX VIII

SYSTEM SCHEMATIC DIAGRAMS

This Appendix gives the schematic diagrams for those system components used in the experimental evaluation of the detector that had to be designed and constructed. The following schematics are included:

1) A/D Converter
2) D/A Converter
3) Pre-detection BPF
4) Limiter with LPF
5) 30 Hz Post-discriminator LPF
6) 200 Hz Post-discriminator LPF

A/D CONVERTER

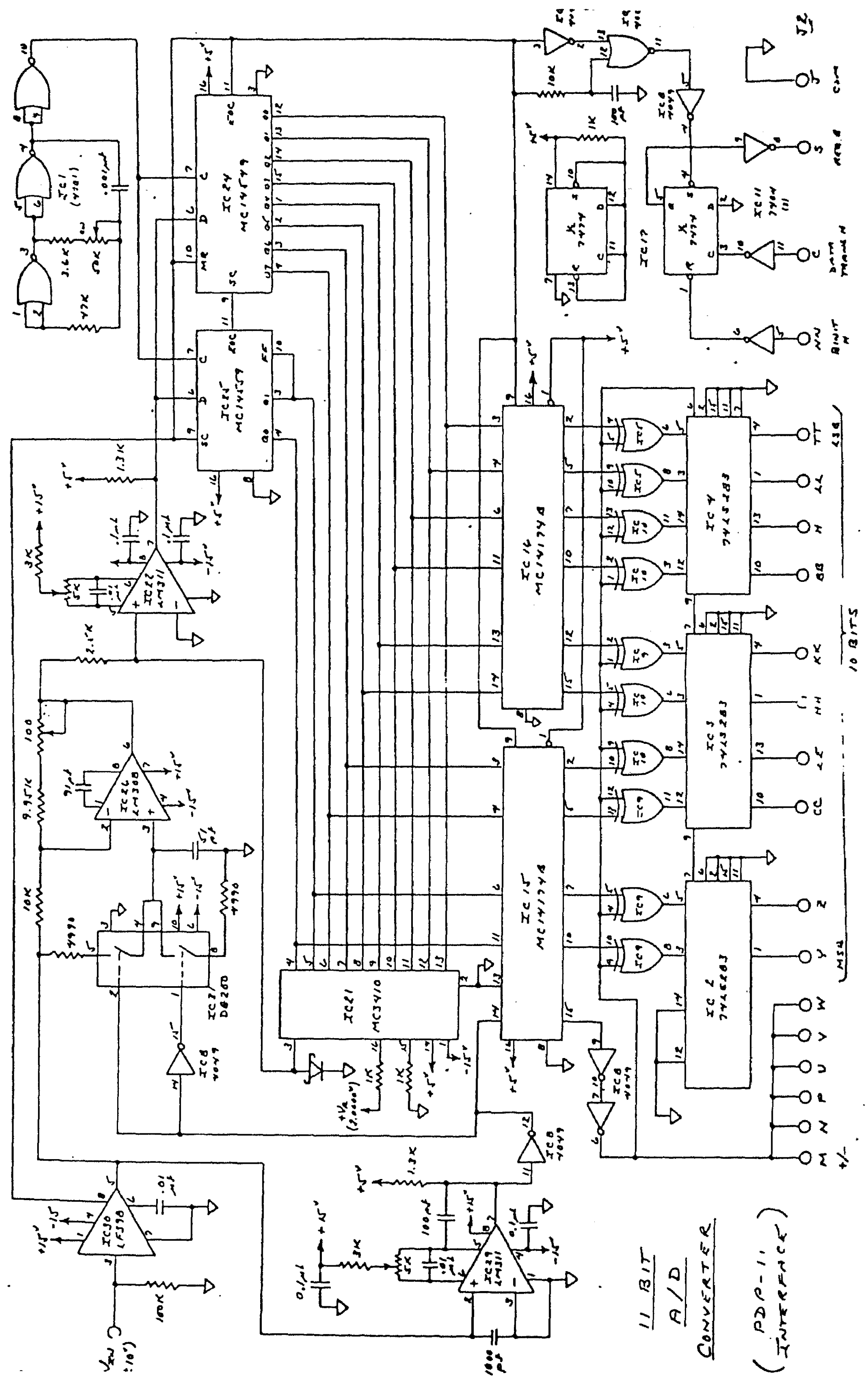

D/A CONVERTER

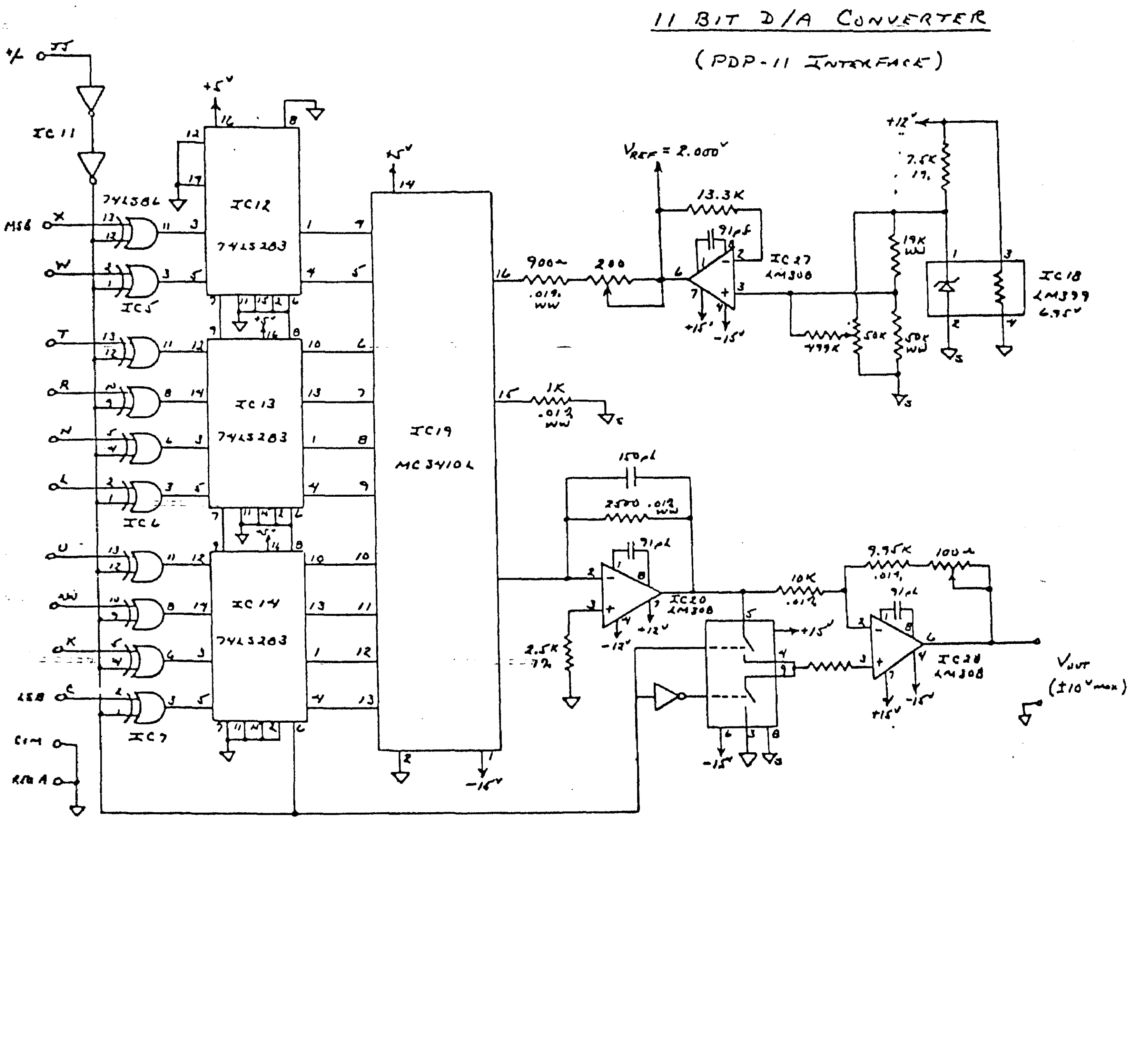

PRE-DETECTION BPF

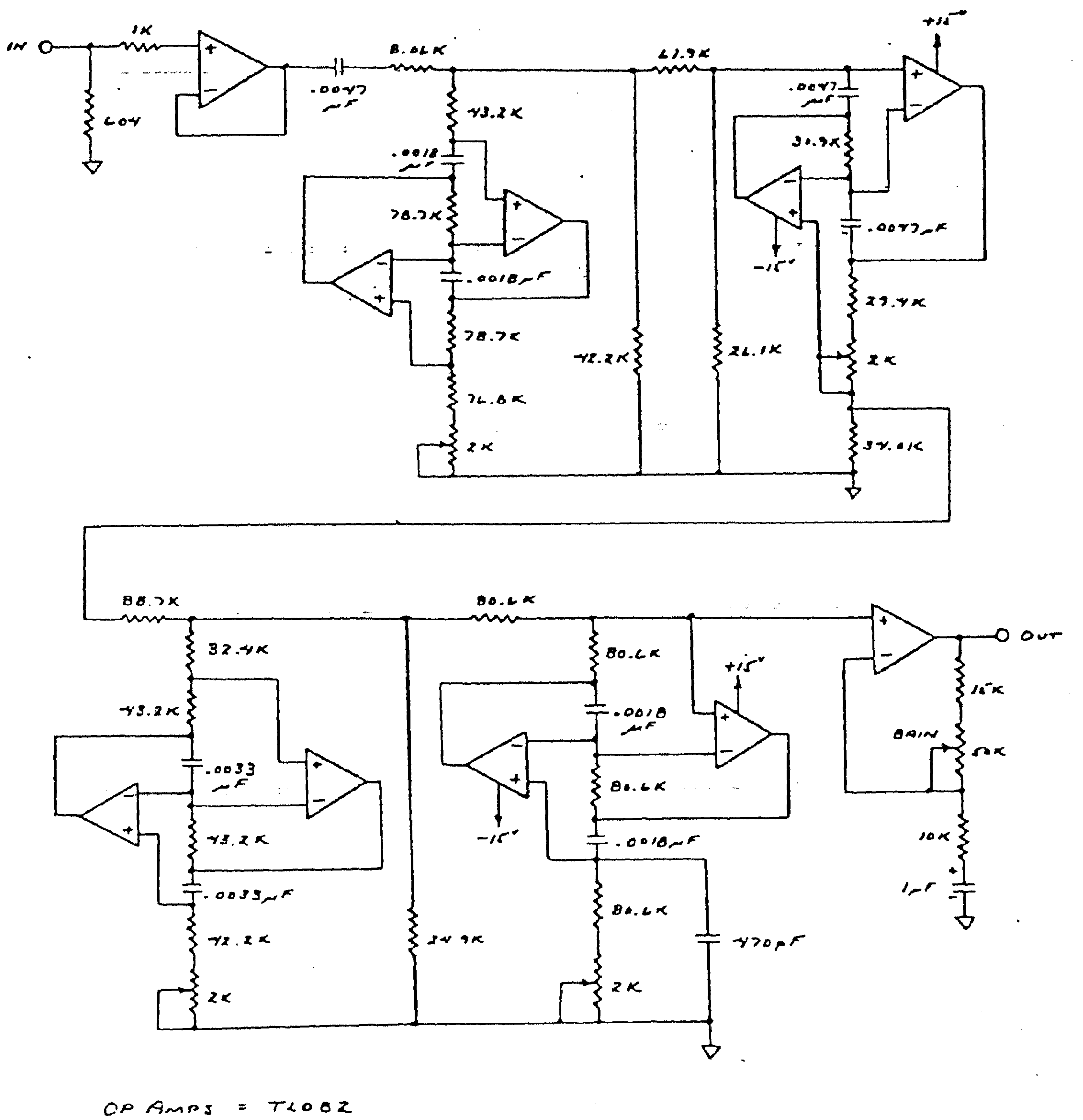

LIMITER WITH LPF

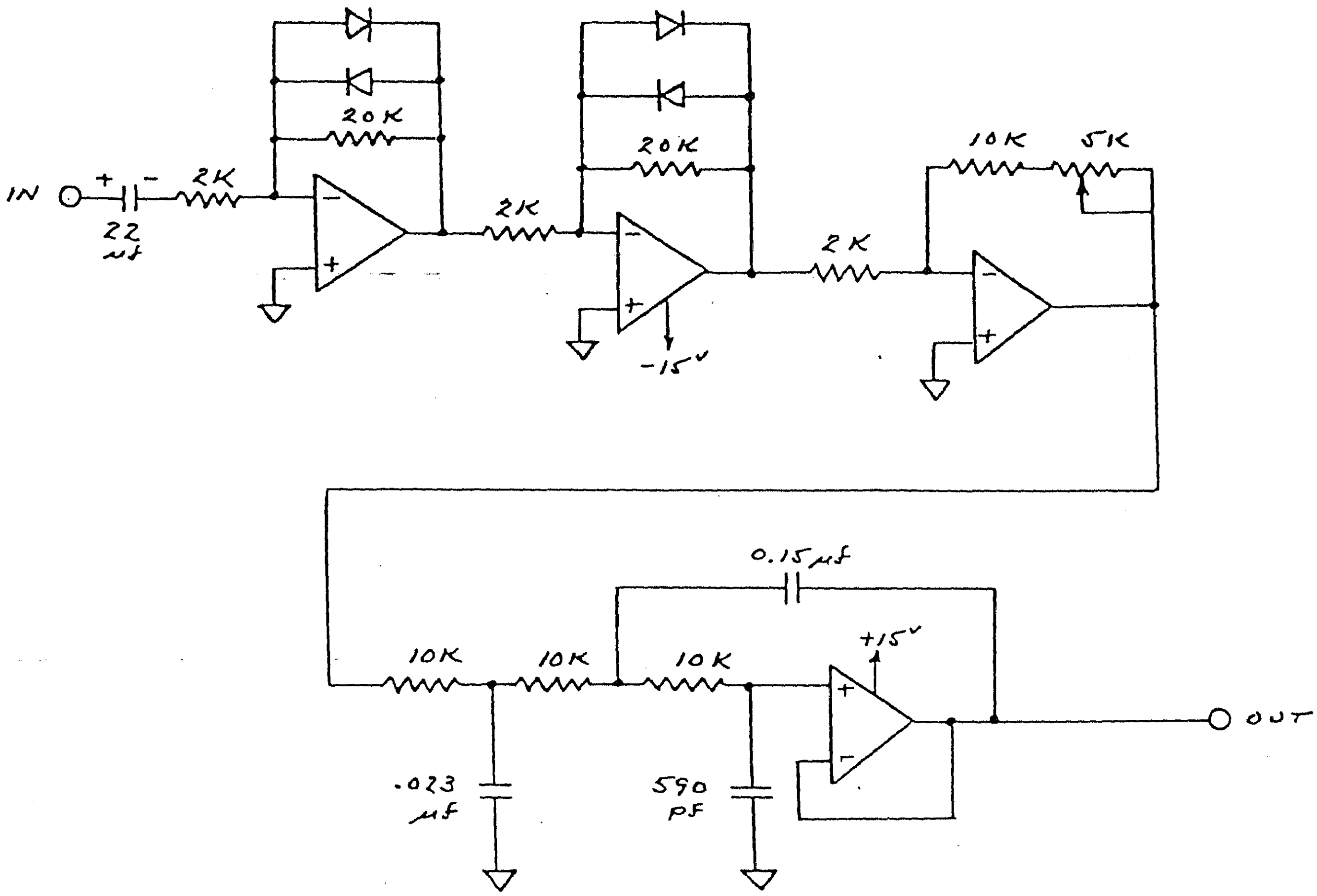

OP-AMPS = TL084
DIODES = 1N914B

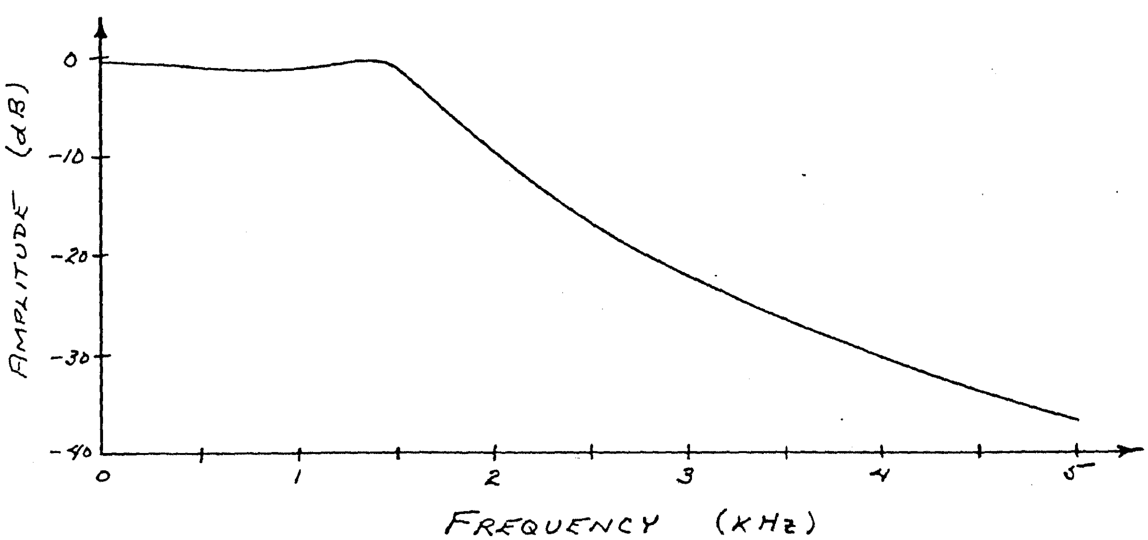

30 HZ POST-DISCRIMINATOR LPF

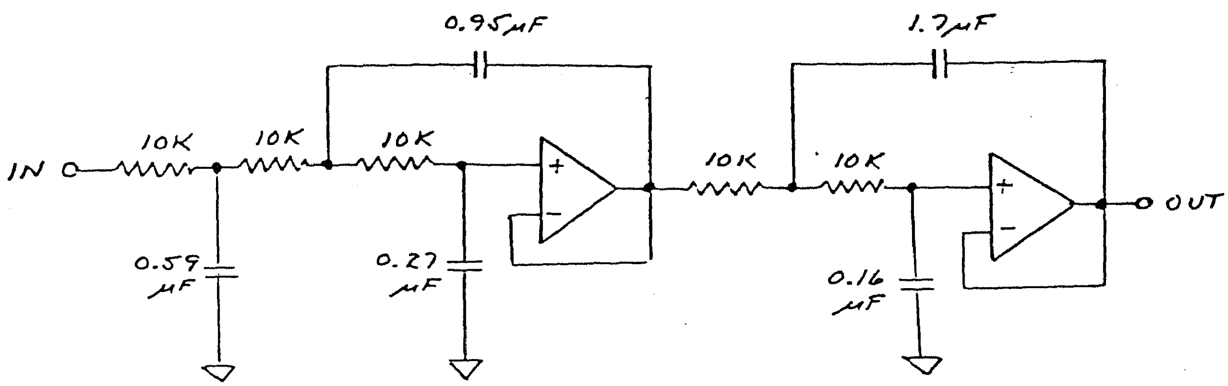

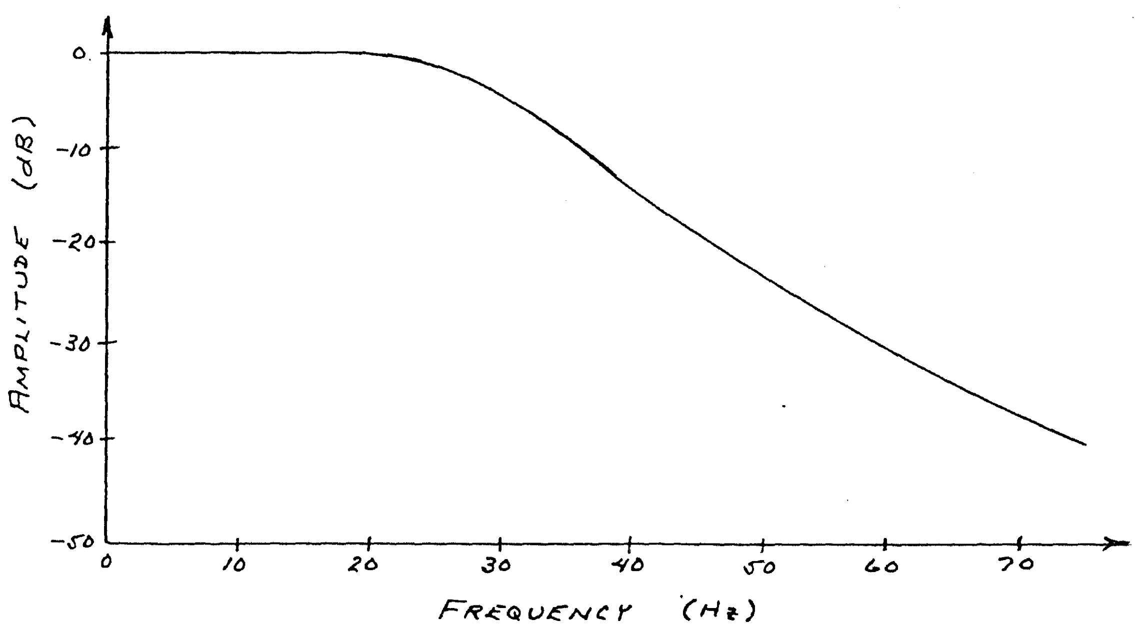

200 HZ POST-DISCRIMINATOR LPF

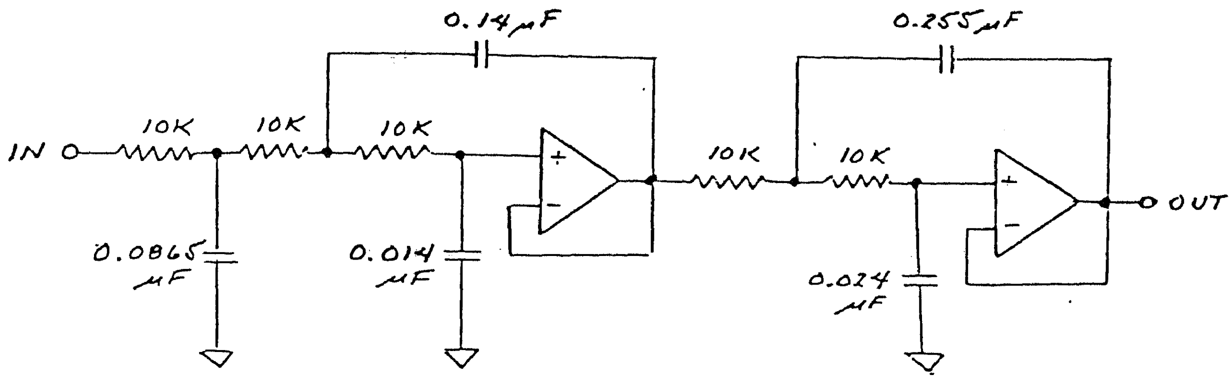

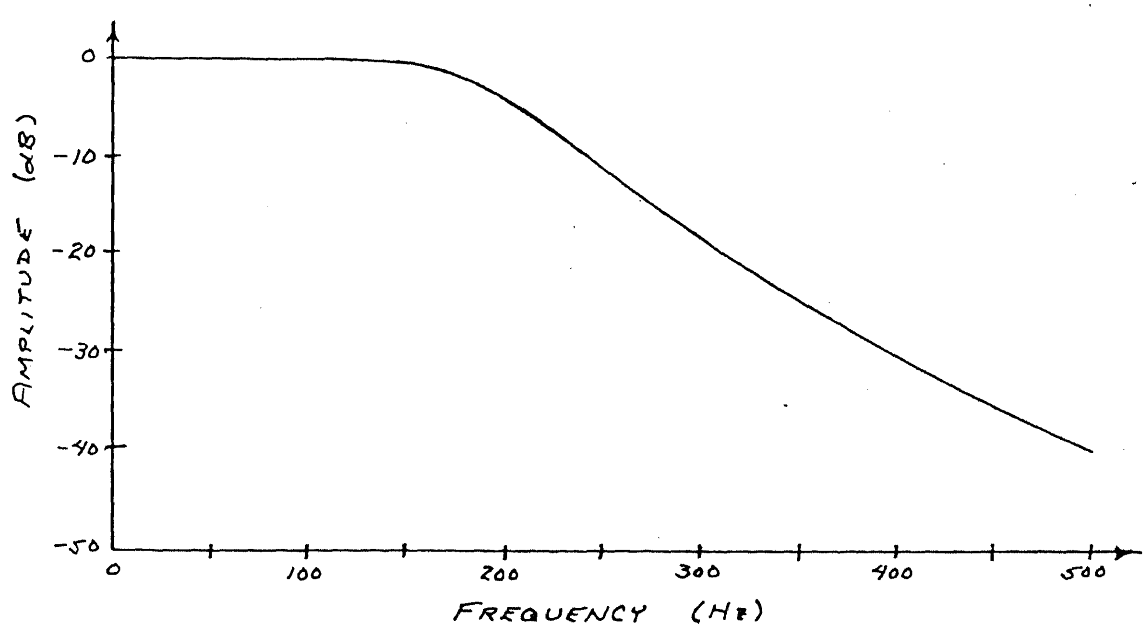

BIBLIOGRAPHY

BOOKS

1. K. K. Clarke and D. T. Hess, Communications Circuits: Analysis and Design, Addison-Wesley, 1971.
2. P. F. Panter, Modulation, Noise, and Spectral Analysis, Chapter 14, McGraw Hill, 1965.
3. M. Schwartz, Information Transmission, Modulation, and Noise, Chapter 6, McGraw Hill, 1959.
4. J. Klapper and J. T. Frankle, Phase Locked and Frequency Feedback Systems, Chapter 7, Figure 7-14, Academic Press, 1972.
5. S. D. Stearns, Digital Signal Analysis, Chapter 4, Hayden, 1975.
6. A. Antoniou, Digital Filters: Analysis and Design, Chapter 9, McGraw-Hill, 1979.

PAPERS

1. J. Klapper and E. Kratt, "A New Family of Low-Delay FM Detectors," IEEE Transactions on Communications, Vol. COM-27, No. 2, Feb. 1979.
2. J. Park, "An FM Detector for Low S/N,". IEEE Transactions on Communication Technology, Vol. COM-18, No. 2, April 1970.
3. E. T. Patronis, "A Frequency Modulation Detector using Operational Amplifiers," Audio Mag., Feb. 1970.

4. G. J. Kersus, "Analysis of the Klapper-Kratt FM Detector," M.S. project, Dept. Elec. Eng., New Jersey Inst. Technol., 1976.

5. M. S. Corrington, "Frequency Modulation Caused by Common-and-Adjacent-Channel Interference," RCA Rev., Vol 7, Dec. 1946.

6. A. Tarbell and J. Klapper, "Noise Performance of the Klapper-Kratt Low Delay FM Detector," NTC, Washington, D.C., Nov. 1979.

7. J. H. McClellan, T. W. Parks and L. R. Rabiner, "FIR Linear Phase Filter Design Program," Programs for Digital Signal Processing, Chap. 5.1, IEEE Press, New York, 1979.

8. R. Fletcher and M. J. D. Powell, "A rapidly convergent descent method for minimization," Computer J., Vol. 6, No. 2, July 1963.

9. T. W. Parks and J. H. McClellan, "Chebyshev Approximation for Nonrecursive Digital Filters with Linear Phase," IEEE Trans. on Circuit Theory, Vol. CT-19, No. 2, March 1972.

10. R. P. Sallen and E. L. Key, "A Practical Method of Designing RC Active Filters," IRE Trans. Circuit Theory, Vol. CT-2, No. 1, March 1955.